NASA
CR
3688
c.1

LOAN COPY: RE
AFWL TECHNICA
KIRTLAND AFB,
0062407
TECH LIBRARY KAFB, NM

NASA Contractor Report 3688

Computer Programs for Generation and Evaluation of Near-Optimum Vertical Flight Profiles

John A. Sorensen, Mark H. Waters,
and Leda C. Patmore

CONTRACT NAS1-15497
MAY 1983

25th Anniversary
1958-1983

NASA

TECH LIBRARY KAFB, NM

0062407

NASA Contractor Report 3688

Computer Programs for Generation and Evaluation of Near-Optimum Vertical Flight Profiles

John A. Sorensen, Mark H. Waters,
and Leda C. Patmore
Analytical Mechanics Associates, Inc.
Mountain View, California

Prepared for
Langley Research Center
under Contract NAS1-15497

National Aeronautics
and Space Administration

Scientific and Technical
Information Branch

1983

FOREWORD

This continuing effort for development of concepts for generating near-optimum vertical flight profiles that minimize fuel or direct operating costs was supported under NASA Contract No. NAS1-15497, by Langley Research Center, Hampton, VA. The project Technical Monitor at Langley Research Center was Kathy H. Samms. Technical discussion and suggestions from Ms. Samms, Charles E. Knox, and Samuel A. Morello of Langley Research Center are gratefully acknowledged.

COMPUTER PROGRAMS FOR GENERATION AND EVALUATION OF NEAR-OPTIMUM VERTICAL FLIGHT PROFILES

John A. Sorensen, Mark H. Waters, and Leda C. Patmore

Analytical Mechanics Associates, Inc.
Mountain View, California 94043

SUMMARY

The objectives of this continuing effort are to develop and evaluate algorithms and flight management concepts for the minimization of fuel or direct operating costs. These concepts are to be used for on-board computation and steering of turbojet transport aircraft in the vertical plane between fixed origin and destination airports along a given horizontal path. The algorithms developed may be used either for flight planning purposes or incorporated in an on-board flight management system.

As part of these objectives, two extensive computer programs have been developed. The first, called OPTIM, generates a reference near-optimum vertical profile, and it contains control options so that the effects of various flight constraints on cost performance can be examined. The second, called TRAGEN, is used to simulate an aircraft flying along an optimum or any other vertical reference profile. TRAGEN is used to verify OPTIM's output, examine the effects of uncertainty in the values of parameters (such as prevailing wind) which govern the optimum profile, or compare the cost performance of profiles generated by different techniques.

This report presents a general description of these programs, the efforts to add special features to them, and sample results of their usage. OPTIM and TRAGEN are available from Computer Software Management Information Center, Barrow Hall, University of Georgia, Athens, Georgia 30601.

TABLE OF CONTENTS

		Page
I.	INTRODUCTION	1
II.	OPTIM	
	OPTIMIZATION OF VERTICAL FLIGHT PROFILES	5
	Program Capability	6
	Fixed Time of Arrival	8
	Optimum Step Climb	23
	Cabin Pressurization Constraint on Descent	26
	Variable Wind Profiles	35
	Example Results	38
	Related Issues	67
	Program Modification for Airborne Implementation	78
III.	TRAGEN	
	GENERATION OF OPTIMUM AND REFERENCE FLIGHT TRAJECTORIES	83
	TRAGEN Characteristics	84
	TRAGEN Results	88
IV.	SUMMARY, CONCLUSIONS, AND RECOMMENDATIONS	99
	Summary and Conclusions	99
	Recommendations	102
APPENDIX A		
	EFFECT OF CONSTRAINED DESCENT ON FLIGHT PERFORMANCE	107
APPENDIX B		
	TAKE-OFF PERFORMANCE ANALYSIS	119
REFERENCES		133

LIST OF FIGURES

Page

1. Effect of Fuel Prices on Direct Operating Cost for U.S. Trunk Airlines 2

2. Recent Price Growth for Jet Fuel 2

3. Coefficient of Drag C_D as a Function of Lift Coefficient C_L and Mach Number 9

4. Normalized Thrust as a Function of Mach Number and EPR 10

5. Cruise Cost as a Function of Airspeed at 9.75 km (32000 ft) for Cost-of-Time of $300./hr.. 12

6. Trip Time and Fuel Burned as Functions of Cost-of-Time. Cruise Altitude Fixed at 10 km (33,000 ft) 14

7. Portion of Minimax Fit with Lift Coefficient C_L = .05 15

8. Cruise Cost and C_D as a Function of Airspeed at 9.75 km (32000 ft) for Cost-of-Time = $600./hr, Aircraft Weight = 38.6 tonne (85000 lb) and Cost-of-Fuel = $0.33/kg ($.15/lb) 16

9. Comparison of Cruise Cost as a Function of Cruise Weight for Minimax and Least Squares Polynomials 18

10. Drag Coefficient Surface Fit Accuracy Between Data Points at M = 0.6, 0.68, and 0.74 with C_L Given 20

11. Kink Problem at M = 0.6 with Modified Surface Fit and its Solution with Cubic Adjustment Between M = 0.6 and 0.68 22

12. Sketch of Altitude vs Range Profile for Step Climb Computations. . 25

13. Air Pressure and Rate of Change of Pressure as Functions of Altitude 27

14. Rate of Change of Cabin Pressure with Time for Different Equivalent Cabin Descent Rates 28

15. Variations of h_{cab} Proportional to $h_{a/c}$ 29

16. 737 Operations Manual Profile of Cabin Altitude as a Function of Airplane Altitude 32

17. Sketch of Modified Optimum Profile Due to Cabin Pressurization Constraint on Descent 34

18. Horizontal Route Choices from Orlando to Chicago 36

LIST OF FIGURES (Cont.)

19a. State Variables for Optimum Climb Profiles of the Twin-Jet Aircraft Traveling 1000 nmi 39

19b. State Variables for Optimum Descent Profiles of the Twin-Jet Aircraft Traveling 1000 nmi 40

19c. Altitude vs True Airspeed for the Optimum Profile of the Twin-Jet with Cruise Altitude Free and Optimized with V_a Only 41

20a. State Variables for Optimum Climb Profiles of the Tri-Jet Aircraft Traveling 1000 nmi 42

20b. State Variables for Optimum Descent Profiles of the Tri-Jet Aircraft Traveling 1000 nmi 43

21a. Optimum Climb Profile for Twin-Jet Showing Effects of Temperature Variation 45

21b. Optimum Descent Profile for Twin-Jet Showing Effects of Temperature Variation 46

21c. Altitude vs True Airspeed for Optimum Twin-Jet Profiles as a Function of Temperature Variation 47

22a. Comparison of Minimum Fuel and Minimum Cost Climb Profile 49

22b. Comparison of Minimum Fuel and Minimum Cost Descent Profiles . . . 50

22c. Altitude vs True Airspeed for Twin-Jet Minimum Fuel and Minimum Cost Profiles 51

23. Minimum Speed Constraint V_{min} for Twin-Jet 52

24. Chart Showing Acceptable Speed/Altitude Operating Region for a 38.6 tonne Twin-Jet Aircraft. Maximum Climb Flight Path Angle Shown as Parameter 54

25. Variable Wind Analysis Comparitive Vertical Profiles 55

26. Typical Chicago - Phoenix Flight Plan Route Structure with Alternate Waypoints 58

27. Comparison of Minimum Cost and Fuel for Step Climb and Constant Cruise Altitude Cases of Twin-Jet Over 1000 nmi Range 61

28. Minimum Cost and Fuel as Function of Range to Begin Step Climb Tri-Jet Traveling 1000 nmi 62

29. Comparison of Optimum and Constrained Descent Profiles (Tri-Jet Model 63

LIST OF FIGURES (Cont.)

30. Comparison of Optimum and Constrained Descent Profiles (Twin-Jet) . . 64

31. Sketch of Profile with Holding Pattern (Option 1) 66

32. Fuel Saved Using Time-of-Arrival Option as Function of Time Delay and Range. (Two-Part Profile; Twin Jet Aircraft) 68

33. Percentage Fuel Saved Using Time-of-Arrival Option as Function of Time Delay and Range. (Two-Part Profile; Twin-Jet Aircraft) 69

34. Location of Three Locations Where Engine Air is Bled from the Twin-Jet Model. 71

35. Effect of Powerplane Losses on Cruise Cost and Required EPR 74

36. Typical Take-off Profile for a Twin-Jet Aircraft 77

37. Comparison of Optimum and Simplified (IAS/Mach Schedule) Climb and Descent Profiles 95

A.1. Baseline Descent Profile for Study of Cabin Pressurization Constraint Effects 108

A.2. Descent Profile Variations as a Function of Rate of Descent. 111

A.3. Variation in Descent Range, Time, and Fuel Burned as Functions of Rate of Descent Limits 112

A.4. Descent Profile Variations as a Function of Cabin Overpressure Constraints 113

A.5. Variation in Descent Range, Time, and Fuel Burned as Functions of Cabin Overpressure Constraints 114

A.6. Variation in Descent Profiles for Changes in the Constant Indicated Airspeed Segment 115

A.7. Variations in Descent Range, Time, and Fuel Burned for Changes in the Constant Indicated Airspeed Segment. 116

B.1. Twin-Jet Take-off; Flaps 10 or 15 Schedule 120

B.2. Twin-Jet Take-off; Flaps 2 or 5 Schedule 121

B.3. Twin-Jet Take-off; Flaps 1 Schedule. 122

B.4. Bar Chart Showing Performance Measures for Different Flap Schedules. 125

B.5. Performance as a Function of Beginning Rotation Speed V_R 126

LIST OF FIGURES (Cont.)

B.6. Performance as a Function of Rotation Rate 127

B.7. Performance as a Function of Maximum Rotation Load Factor. 128

B.8. Performance as a Function of Airport Altitude. 130

B.9. Performance as a Function of Change in Ambient Temperature 131

B.10. Performance as a Function of Departure Heading Change. 132

LIST OF TABLES

		Page
1.	Comparison of Run Time, in CPU Seconds, for Two Typical OPTIM Runs Using Three Methods of Determining C_D and T_h/δ.	19
2.	Altitude Separation Rules for IFR Flight.	24
3.	Variable Wind Analysis.	56
4.	Comparison of Time and Fuel for Variations of Chicago - Phoenix Flight Plan with a Tri-Jet Aircraft (Time: $600./hr; Fuel: $.15/lb.).	59
5.	Effect of Engine Losses on Thrust and Fuel Flow	73
6.	Effect of Changing Take-off Parameters of Fuel Usage to 210 kt Airspeed.	78
7.	OPTIM Program Size Reduction Results	79
8.	OPTIM Run Time Comparisons for 1000 nmi Flight	80
9.	Comparison of Six Twin-Jet Profiles as Generated by OPTIM and Simulated by TRAGEN. 1000 nmi Range.	89
10.	Effect of Weight Inaccuracy on Flight Performance	91
11.	Effect of Wind Inaccuracy on Flight Performance	92
12.	Typical Aircraft Characteristics as Specified in Manufacturer's Handbook [15]	94
13.	Comparison of "Optimum" Profile and Similar Profile Approximated with Constant Mach/IAS Schedule for Climb and Descent	97
B.1.	Recommended Take-off Setting for EPR, Flaps, and Airspeed as Functions of Weight, Temperature, and Other Parameters for Twin-Jet Model	123

SYMBOLS

A_{bl}	-	bleed air from engine (kg/sec)
A_t	-	total engine airflow (kg/sec)
a_{ij}, $b_{k\ell}$	-	coefficients in polynomial curve fits
$a_1 - a_3$	-	coefficients of C_D curve fit
C_D	-	total drag coefficient
C_f	-	cost of fuel ($/kg or $/lb)
C_L	-	total lift coefficient
C_t	-	cost of time ($/hr)
$C_1 - C_3$	-	constants specifying engine thrust and fuel losses
c	-	a constant
D, D_c	-	drag (N)
EPR	-	engine pressure ratio
g	-	acceleration due to gravity (m/s^2)
H, H_c	-	Hamiltonian used for optimization ($/m)
H_p	-	horsepower
$h_{a/c}$, h	-	ambient pressure altitude of aircraft (m)
h_c	-	cruise altitude (m)
h_{cab}	-	aircraft cabin altitude (m)
h_p	-	altitude where cabin pressure equals landing pressure (m)
h_{TO}	-	aircraft takeoff or landing altitude (m)
KIAS	-	indicated airspeed (kt)
L	-	lift (N)
M	-	Mach number
m	-	aircraft mass (kg)
p	-	air pressure (N/m^2)
q	-	pitch rate (°/s)
R_F	-	Breguet range factor (m/kg)
R_{f1}, R_{f2}	-	range points at end of cruise (m)

SYMBOLS (Cont')

S_{FC}	-	specific fuel consumption (kg/hr)/N
T, T_h	-	thrust (N)
TOA	-	time-of-arrival (s)
t	-	time
t_o, t_f	-	initial and final times of trajectory (s)
V, V_a, V_c	-	airspeed, command airspeed (kt)
V_g	-	ground speed (kt)
V_R	-	rotation speed at take-off (kt)
V_w	-	longitudinal component of wind velocity (kt)
V_1, V_2	-	take-off phase definition speeds (kt)
W, W_i, W_f	-	mass of the aircraft; initial and final mass (kg)
$\dot{w}$	-	fuel flow (kg/hr)
x	-	range traveled (nmi)

GREEK SYMBOLS

α	-	angle-of-attack (°)
γ, γ_c	-	flight path angle with respect to airmass; command value (°)
Δp	-	incremental pressure (N/m^2)
δ, δ_{amb}	-	ambient pressure ratio
δ_T	-	throttle setting (%)
λ, λ_{min}	-	cruise cost per unit distance ($/nmi); also, adjoint variable or costate used for optimization
π	-	thrust control setting (throttle, EPR, or RPM)
ϕ	-	roll angle (°)
Θ_{amb}	-	ambient temperature ratio

SUBSCRIPTS AND NOTATION

a/c	-	aircraft
amb	-	ambient
c	-	value during cruise or command value
cab	-	cabin value
END	-	end value
f	-	final value
i	-	initial value
idle	-	value during idle thrust
max	-	maximum value
min	-	minimum value
TO	-	takeoff value
$(\dot{\ })$	-	first derivative with respect to time
$(\ddot{\ })$	-	second derivative with respect to time
$\partial(\ )$	-	partial of indicated variable
$\Delta(\ )$	-	change in value

UNITS

In this report, the common British units used by U.S. aircraft manufacturers are given in parentheses after a numerical value is first presented in mks units. Note that pounds mass and pounds force are both used rather than using slugs as a measure of mass. Here, the common definition of one pound mass equals (1/32.2) times one slug mass (1 slug = 32.2 lb sec^2/ft) is used.

I

INTRODUCTION

Jet fuel prices continue to escalate, and the impact on airline direct operating costs is now quite significant. This is illustrated by the two charts reproduced here as Figs. 1 and 2; this condition reflects the diminishing supply of world petroleum resources. Until a practical, alternate fuel source is developed, fuel conservation is a problem that requires continued attention in the aviation community.

Two partial solutions are to build more fuel efficient aircraft, and to utilize optimization techniques to minimize the quantity of fuel required to transport a given amount of cargo and passengers. This report focuses on a particular element of the latter case, and it continues with the efforts reported in Refs. (1) and (2).

To minimize utilization of jet fuel and to maintain the same level of jet transportation service we now enjoy requires a unified approach to the research efforts of government and industry. This research would evolve advanced fuel conservation techniques, flight planning methods, and flight management equipment for the air transportation industry. Four primary areas of research and development are involved:

(1) The optimization of enroute flight paths,

(2) The optimization of terminal area flight paths,

(3) The incorporation of these optimization techniques into upgraded, automated air traffic control, and

(4) Upgrading the ability to predict and model weather factors into the flight planning process.

Important to the development effort is the appropriate testing of the new approaches in realistic airline environments.

This effort addresses one aspect of item (1) above - namely, the on-board generation of near-optimum vertical profiles for enroute travel. Here, it is assumed that the horizontal path that the aircraft follows is pre-determined,

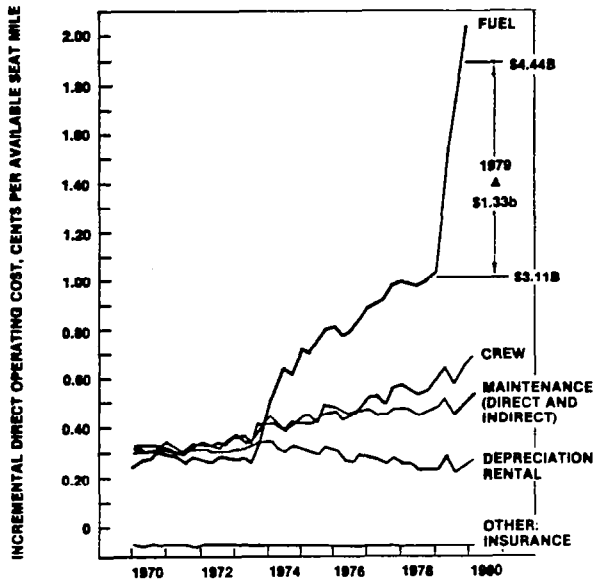

Figure 1. Effect of Fuel Prices on Direct Operating Cost for U.S. Trunk Airlines (Dec. 1980 Astronautics and Aeronautics magazine)

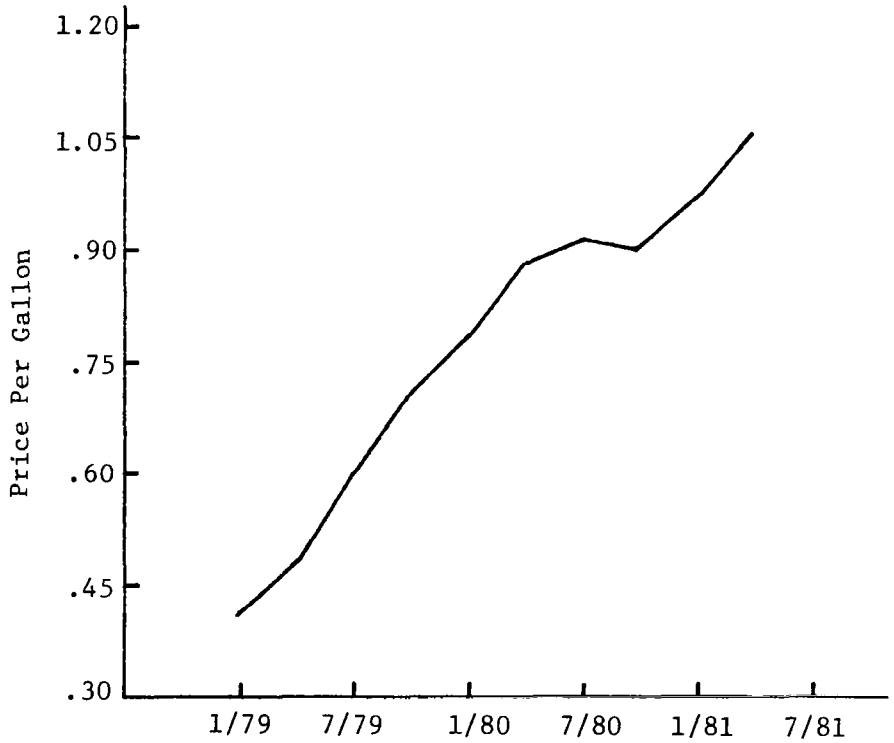

Figure 2. Recent Price Growth for Jet Fuel (Sept. 1981 Air Line Pilot magazine.)

based on some flight planning method, and it consists of a sequence of way-points between the origin and destination airports. Over this horizontal field, wind and temperature profiles are also pre-determined as functions of altitude and range. The goal, then, is to devise an on-board computer-based system to determine the best vertical profile that follows this horizontal path, and that takes into account the wind and temperature conditions. The "best" profile is one which tends to minimize either the direct operating cost of the flight or the total fuel consumed during the flight. Various ATC, time-of-arrival, and passenger comfort constraints may be placed on the derived profile.

The ability to generate a near-optimum vertical profile can be used as part of an airline's flight planning activity, it can be incorporated as an algorithm into an on-board flight management system, or it can be incorporated into the software of an automated enroute air traffic control system. The effort over the past four years was initially directed at establishing a general concept for this vertical optimization task. As part of this effort, two computer programs, oriented primarily for off-line analytical studies, were developed:

1) OPTIM - generates a near-optimum vertical profile that minimizes fuel or direct operating cost over a fixed range of flight.

2) TRAGEN - simulates an aircraft flying along an optimum vertical profile or some other reference trajectory to determine comparitive savings.

In Ref. 2, it was recommended that modifications and extensions be made to these programs to improve their accuracy and utility. These recommended changes have been made, and they are described in this report.

In addition, the primary effort this past year has been to streamline a version of the OPTIM program so that it is suitable for on-board operation as part of an advanced flight management system. This was done on a mini-computer (PDP 11-70) compatible with the NASA Advanced Transport Operating System (ATOPS) airborne computers. The results of this development are summarized in this report.

Chapter III describes the capability of the OPTIM program, documents the development and studies conducted to incorporate modifications and new options, and presents examples of the utility of the new system. Related areas of study, including the effects of various engine losses and the aircraft takeoff procedure on the mission fuel requirements, are described. Finally, the increase in program efficiency accomplished this past year along with requirements to implement the OPTIM algorithm in an experimental flight management system are presented.

Chapter III describes the capability of the TRAGEN program including the provision for including multiple cruise segments in the flight simulation. Examples are presented which simulate the aircraft following profiles generated by OPTIM and pilot handbook reference profiles. Also, sensitivity runs are made to show the effect of wind model and takeoff weight errors.

Chapter IV summarizes this effort, derives conclusions based on the fuel optimization examples presented in Chapters II and III, and makes recommendations concerning further work. Appendices A and B document parametric studies of fuel requirements for the constrained descent due to cabin pressurization and the takeoff phase of flight.

II

OPTIM

OPTIMIZATION OF VERTICAL FLIGHT PROFILES

OPTIM is a versatile computer program which has been developed for the purpose of generating a near-optimum vertical profile for a turbojet aircraft flying over a fixed range. This program is an outgrowth and extension of work begun by Dr. Hienz Erzberger and his associates at NASA Ames Research Center [3-5].

The key aspect of the program is the minimization of a Hamiltonian function,

$$H = \frac{C_f \dot{w} + C_t + \lambda V_g}{V_a (T-D)/mg} , \tag{1}$$

at successive energy states during the climb and descent portions of the profile. Here,

C_f - cost of fuel ($/kg)

C_t - cost of time ($/hr)

$\dot{w}$ - fuel rate (kg/hr)

λ - adjoint variable or co-state ($/nmi)

V_g - ground speed (kt)

V_a - airspeed (kt)

T - thrust (N)

D - drag (N)

mg - aircraft weight (N)

The objective is to choose the best values of airspeed V_a and thrust T at each specific energy state during climb and descent to minimize Eq. (1). The physical meaning of the costate λ is the negative value of the minimum cost

per unit distance traveled during cruise for a specific cruise weight, or

$$- \lambda = \min_{V_a} \left[\frac{C_f \dot{w} + C_t}{V_g} \right] \tag{2}$$

Ground speed V_g is determined from the horizontal projection of the vector sum of the aircraft velocity $\overline{V}_a$ with respect to the air mass and the wind velocity $\overline{V}_w$. The appropriate value of λ in Eq. (1) during climb is that value obtained from Eq. (2) for the aircraft weight at the top of climb. Similarly, λ for descent is based on weight at the top of descent.

Details of the Eq. (1) derivation and the basic structure of OPTIM are found in Refs. 2 and 6. This program has been released to the aviation industry through NASA Langley Research Center, and it currently is being utilized by several airlines, aircraft, engine, and avionics manufacturers, and government agencies.

In this chapter, the existing capability of the OPTIM program is described, and the research and extensions added during the past eighteen months are outlined. Examples of studies which can be made with the program are presented. The related issues of take-off analysis and engine installation loss modeling are discussed. Finally, development of a version of the program as the basis for an advanced flight management system is summarized.

Program Capability

The original computer program developed by Erzberger and Lee [5] was based on aerodynamic and engine models of a medium range tri-jet transport aircraft. It had the following options;

1. fixed or free thrust during climb and descent (fixed thrust consisted of maximum thrust during climb and idle thrust during descent);
2. airspeed free or constrained to less than 250 kt below 3.048 km (10,000 ft) altitude;
3. no wind or a fixed wind profile over the entire flight range. (The wind profile is a function of altitude only.); and

4. variations in flight cost by variation of the input constants C_f and C_t. (A minimum fuel profile is achieved by setting C_t to zero.)

This program served as the basis for development of at least one commerical flight management system [7].

Since that time, the following options and features have been added to the basic OPTIM program.

1. the ability to begin flight profile generation in cruise. (This assumes the climb portion of the flight has been completed.);

2. fixed or free cruise altitude;

3. fixed or free time-of-arrival. Fixed time-of-arrival implies that the fuel used is minimized while achieving the desired arrival time;

4. optimum step climb from one fixed cruise altitude to another. (Currently, the step is assumed to be 1219 m (4000 ft)). The step is optimized in the sense of determining where in cruise it should begin;

5. different wind profiles for climb, cruise, and descent;

6. free or constrained rate-of-descent to account for cabin pressurization constraints;

7. choice of either a tri-jet or a twin-jet transport aircraft model. The program has also been modified so that it is convenient to add additional aircraft models; and

8. addition of output plotting capability.

In addition, considerable reduction in the size and running time of the program has been accomplished. Reference 6 is an edited Users' Guide which describes how to utilize the new features of OPTIM.

The version of OPTIM which has been configured for airborne implementation has the added capability of simulating up to twenty consecutive horizontal segments. Separate wind and temperature profiles can be defined for each of these segments.

OPTIM has the following applications:

1. It can determine how much fuel consumption and operating costs can be saved by flying a near-optimum path rather than a reference trajectory specified in the pilot's handbook.

2. It serves as a benchmark for evaluating alternate sub-optimum algorithms.
3. It can be incorporated into an airline's flight planning system.
4. It can be incorporated into advanced automatic air traffic control software.
5. It serves as the basis for the design of an advanced flight management system.
6. It can be used to study performance effects of new engines or aerodynamic characteristics by manfacturers.

The following sections first discuss the research that was conducted to provide the OPTIM program's options, features, and applications as listed above. This represents a continuation of the research reported in Refs. 1 and 2. Then examples of some of these options are presented.

Fixed Time of Arrival

As described in Refs. 2 and 6, the cost of fuel C_f can be fixed, and the cost of time C_t can be varied to control the time-of-arrival (TOA) while minimizing fuel for a fixed range flight path. There are several advantages to using this technique as an alternative to using the holding pattern for arrival time control. It was demonstrated in Refs. 2 and 8 that using the fixed TOA optimization capability could save an appreciable amount of fuel.

For certain flight conditions, however, the OPTIM computer program was unable to converge to the desired TOA [2]. This problem was traced to the fact that both the drag coefficient C_D and normalized thrust T/δ were determined from using table lookup and linear interpolation between tabular points. Also, the tables given for the twin-jet and tri-jet drag and thrust models had some points which were in obvious numerical error.

The solution to the numerical computation problems associated with table lookup and linear interpolation of data was to use polynomial curve fits to represent the data. This also required having access to the original smooth data for each aircraft. For example, Figs. 3 and 4 represent smooth drag and thrust data for the twin-jet aircraft.

An important fact that remained to be determined, however, was the type of polynomial curve fitting to be used on the data. Several different successive types of polynomials were tried, concluded to be adequate, and

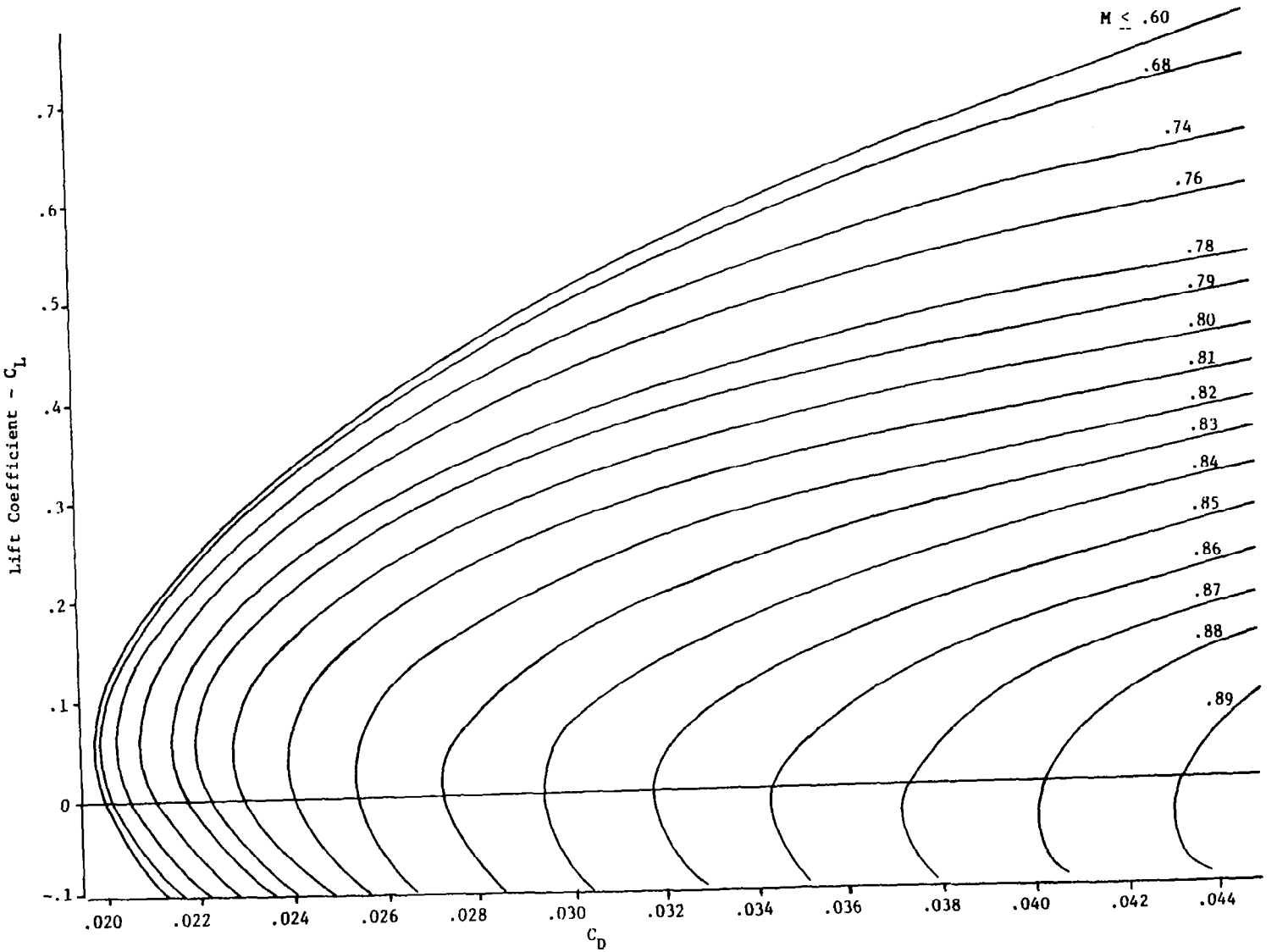

Figure 3. Coefficient of Drag C_D as a Function of Lift Coefficient C_L and Mach Number.

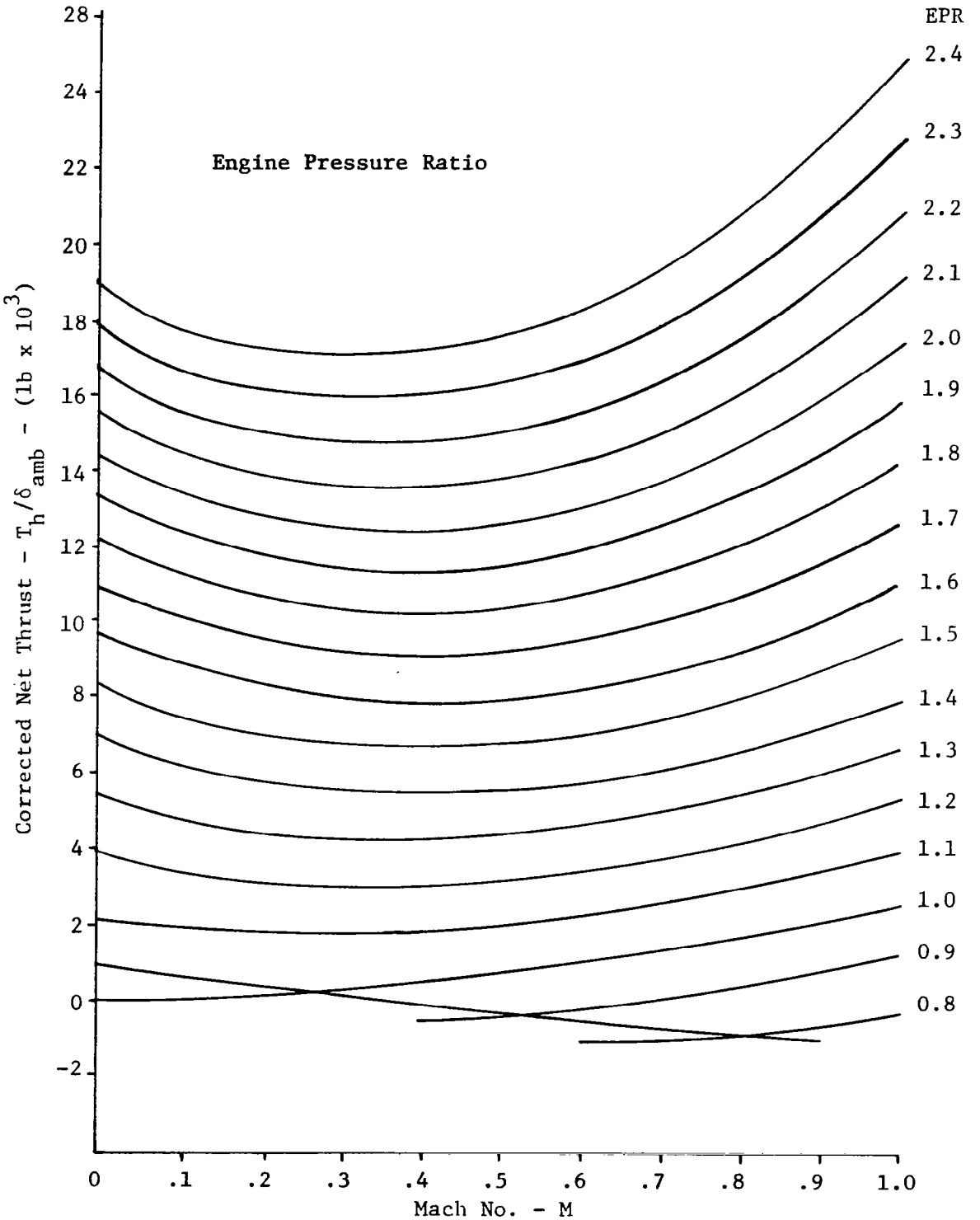

Figure 4. Normalized Thrust as a Function of Mach Number and EPR

then later determined to have problems before a final solution was found. It is instructive to examine this process, for much was learned, and the same problems could be encountered in modeling of other aircraft types.

Minimax Solution An initial computational technique was found which could be used to fit a smooth surface through points which represent one variable as a function of two others (e.g., C_D vs C_L, M and T/δ vs EPR, M). This surface was represented by a ratio of two polynomials, or

$$z = f(x,y) ,$$
$$= \frac{a_{00} + a_{10}x + a_{20}x^2 + \ldots + a_{m0}x^m + a_{01}y + \ldots + a_m x^m y^n}{b_{00} + b_{10}x + b_{20}x^2 + \ldots + b_{p0}x^p + b_{01}y + \ldots + b_{pq}x^p y^q} \quad (3)$$

Here, the numerator has parameters x and y raised to the powers m and n. The denominator has the same parameters raised to the powers p and q. Such a polynomial expression has (m+1)(n+1) + (p+1)(q+1) coefficients a_{ij} and $b_{k\ell}$ such that the resulting mathematical expression Eq. (3) was within some tolerance of the input data points z_i for every input pair (x_i,y_i). This required adjusting the orders m, n, p, and q, and the density of the input data points until an acceptable fit was reached. This method was referred to as the minimax solution.

For the twin-jet model, input data points were selected from Figs. 3 and 4 for the surface fit routine. For simplicity, m, n, p, and q were set equal. It was found that surface fits which were within 1% of the data points could be obtained with fifth order polynomials for the drag coefficient (72 coefficients a and b). For thrust, third order polynomials were sufficient (32 coefficients). These coefficients were used to update the appropriate subroutines in the OPTIM program. The emphasis in the curve fitting process was to obtain continuous polynomial expressions for C_D and T/δ with sufficient accuracy to test the TOA convergence concept.

To test the new polynomial surface fits, a program was developed to compute cruise costs for the twin-jet model at various altitudes and airspeeds. Figure 5 shows the results of typical cost computations for the aircraft having a mass of 40.824 tonne (90,000 lb), flying at an altitude of 9.7536 km

(32,000 ft) with cost of fuel set at \$.33/kg (\$.15/lb), and the cost of time set at \$300./hr.

The upper solid line in Fig. 5 shows the computed cruise cost as a function of true airspeed before curve fitting (that is, using the tabular values of C_D and T/δ). Note that there is a local minimum cost at 390 kt (M = 0.68), a local maximum at 407 kt (M = 0.7), and a sharp kink at 430 kt (M = 0.74). Clearly, no optimization is possible with such a representation.

The upper dashed line in Fig. 5 shows the computed cost after the drag coefficient C_D has been surface fit as a function of C_L and M. This line is much smoother than before. However, the local maximum still exists at 407 kt and two local minima exist at 400 kt and 420 kt. The bottom dot-dash line shows the computed cost after both the drag coefficient and the normalized thrust coefficient T/δ were surface fit. This line is smooth and has a single minimum point at 418 kt. This is the desired form of the cost function which allows optimization.

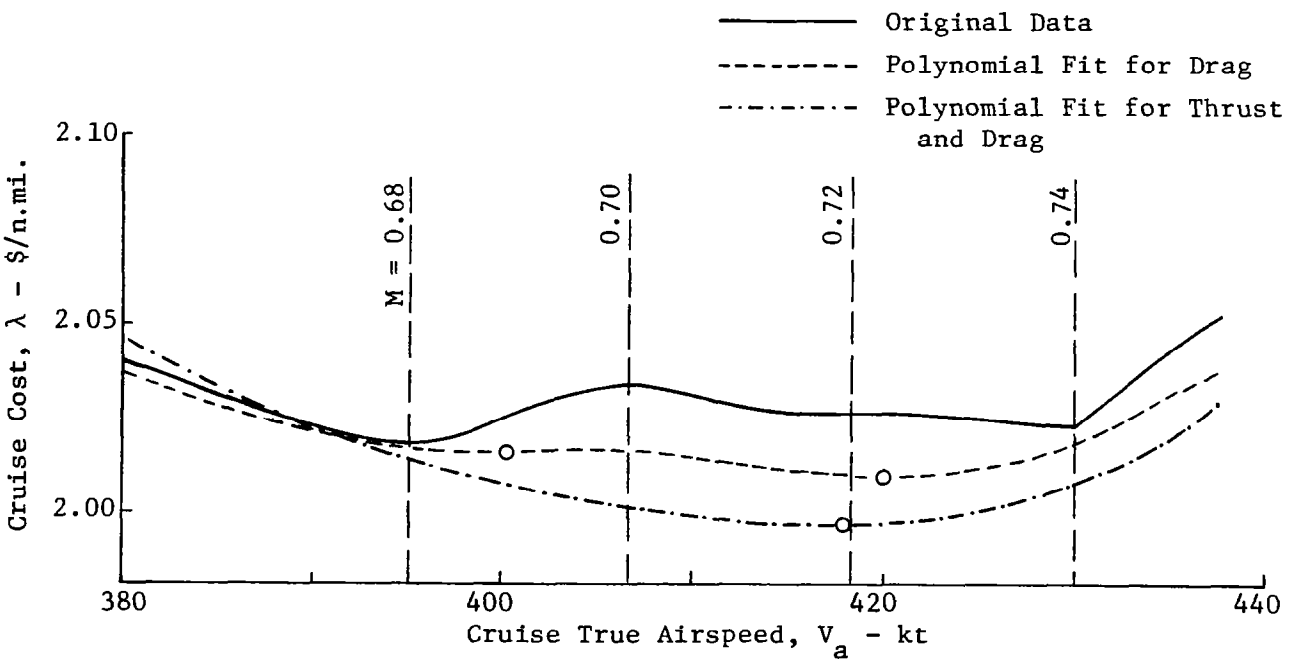

Figure 5. Cruise Cost as a Function of Airspeed at 9.75 km (32000 ft) for Cost-of-Time of \$300./hr.

The fixed time-of-arrival option of the OPTIM program was exercised with the new drag and thrust subroutines being used. First, five different runs were made with range set at 1000 nmi., cruise altitude fixed at 10 km (33,000 ft), and cost-of-fuel C_f set at \$.33/kg (\$.15/lb). Desired arrival times were set at 8700, 9000, 9300, 9600, and 9900 sec (145, 150, 155, 160, and 165 min). In each case, the program converged to the desired arrival time (± 10 sec) within four iterations beginning with cost-of-time C_t set to zero.

Figure 6 shows the results of these runs in terms of fuel burned and trip time as functions of cost-of-time. As can be seen, the minimum fuel point exists at C_t of zero. Also, the trip time is a smooth, continuous function of the variable cost C_t. Being able to vary C_t from \$900/hr to -\$300/hr allows the pilot to adjust his time-of-arrival (TOA) by more than 1200 sec (20 min).

Figure 6 was based on flying with a fixed cruise altitude. Another run was made with the cruise altitude constraint removed and the desired TOA set at 9900 sec. The run converged with C_t of -\$293./hr. For this condition, the cruise altitude began at 9.913 km (32525 ft) and ended at 10.343 km (33935 ft). Fuel burned was 5348 kg (11790 lb) which is 26 kg (58 lb) less (.5%) than for the fixed altitude case.

These cases looked very promising but were by no means exhaustive. Other runs that were tried showed that other convergence problems existed at certain weight and altitude combinations. The minimax polynomial, although it fit the data overall to within 1%, was not a smooth fit. Its 72 coefficients described a surface which had certain peaks and valleys (due to the high order feature of the fit) between the given data points. This means that a value of the drag coefficient C_D calculated from the minimax polynomial may only be slightly in error at any given data point. However, that error may grow substantially (away from the desired surface) in going to the adjoining point as illustrated in Fig. 7. Note that although the fit is generally good, the polynomial value of C_D evaluated for M of .79 is not between the polynomial values for M of .78 and .80.

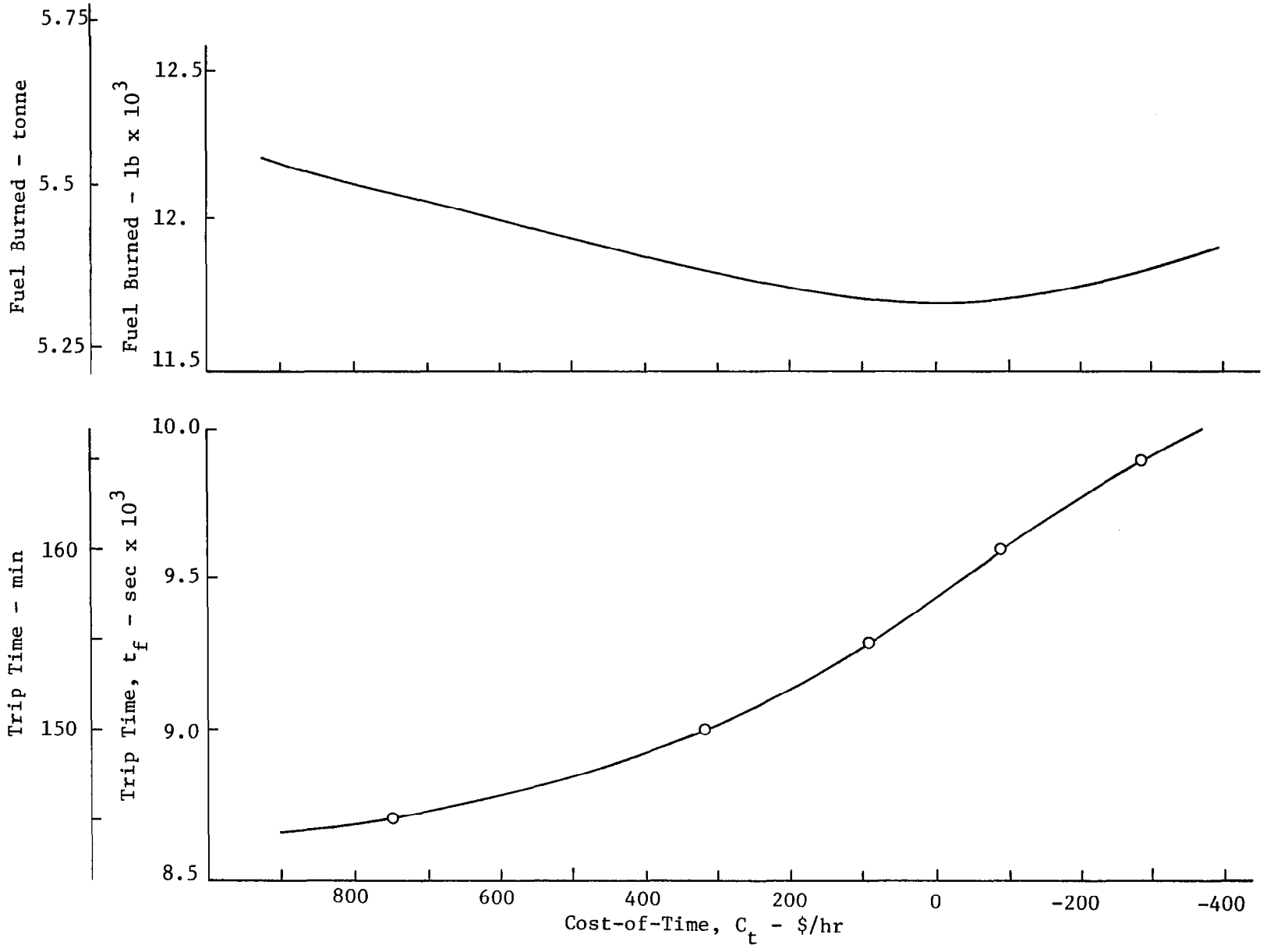

Figure 6. Trip Time and Fuel Burned as Functions of Cost-of-Time. Cruise Altitude Fixed at 10 km (33000 ft).

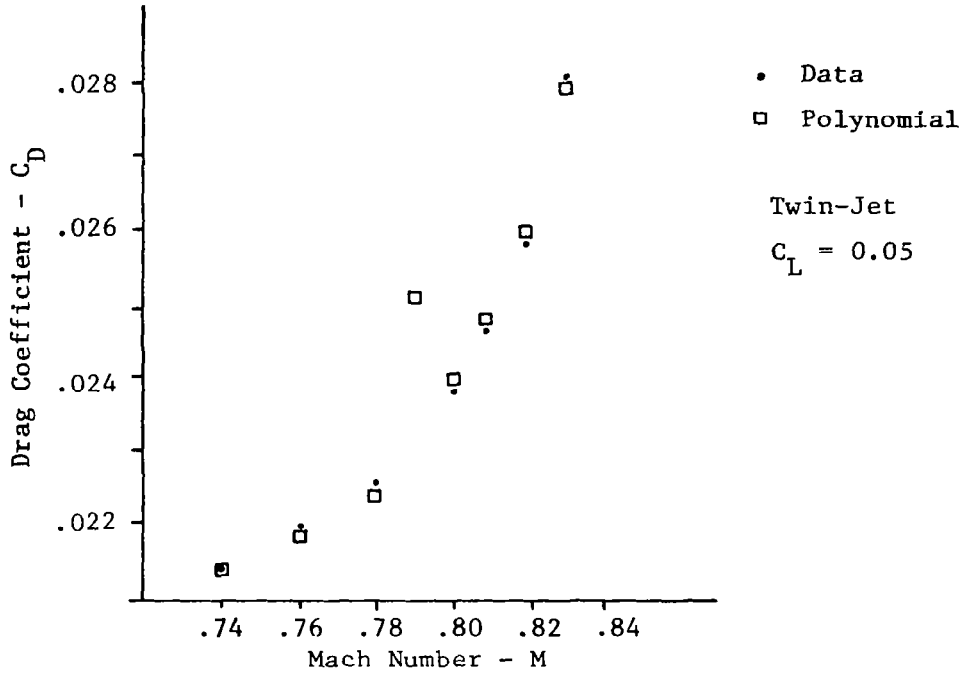

Figure 7. Portion of Minimax Fit with Lift Coefficient $C_L = .05$

Another characteristic of the minimax polynomial was that it had a polynomial denominator which had roots in the range of interest. Figure 8 shows the effect of a mismatch occuring between the roots of the numerator and denominator of the polynomial representing the drag coefficient C_D. The result is that the polynomial has local values varying between zero and infinity. This effect also shows up in the associated cost of cruise which is illustrated. Thus, this type of curve fit is unsuitable for use in minimizing costs at a given altitude (as in OPTIM).

Least Squares Solution The process of attempting to improve the polynomial representation of the C_D and T/δ surfaces took three paths:

1. Interpolation The interpolation scheme was retried with quadratic (Lagrangian) interpolation. The NASA Langley subroutine IBI was used. Results were not sufficiently more accurate than linear interpolation. No improvement in OPTIM was seen.

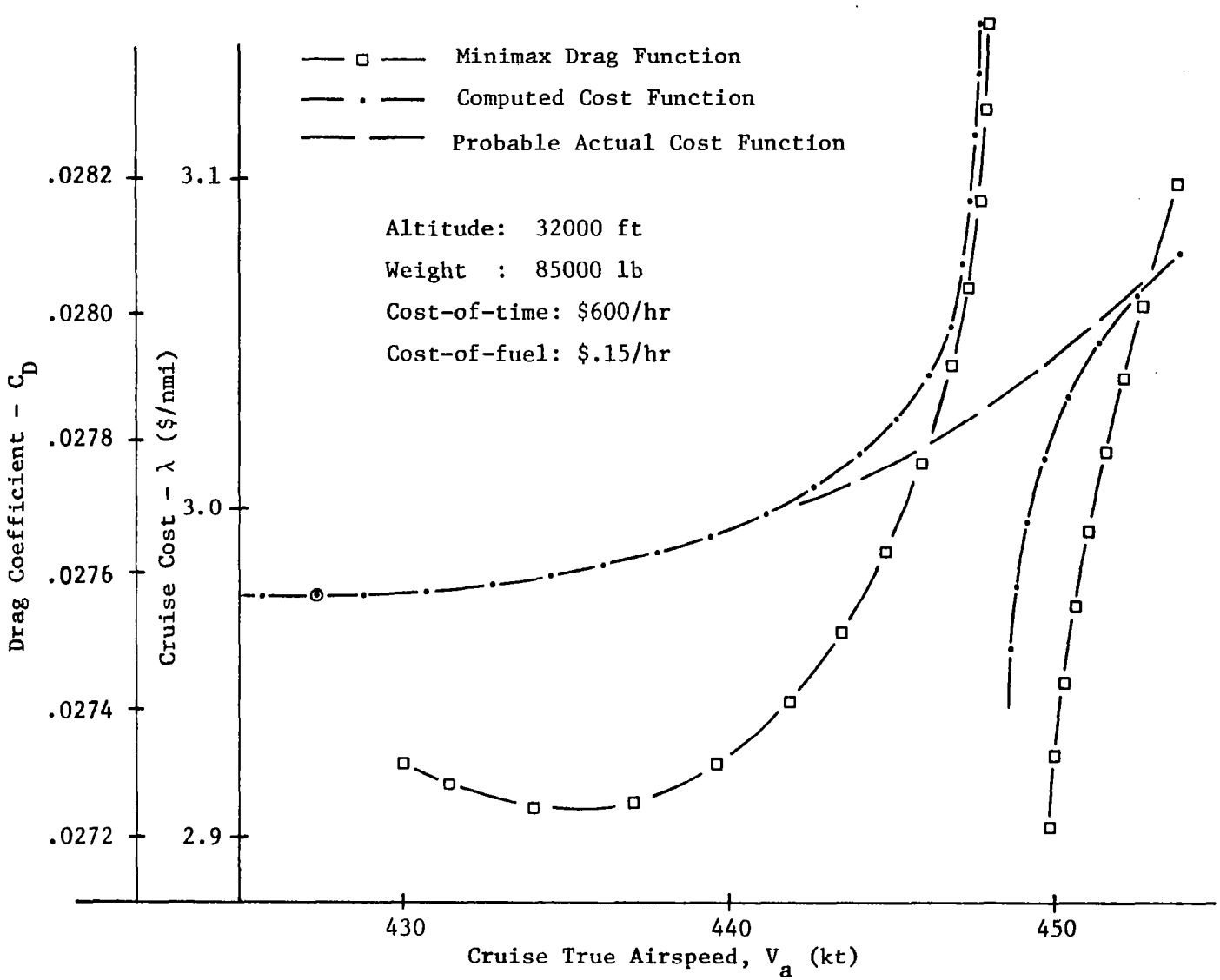

Figure 8. Cruise Cost and C_D as a Function of Airspeed at 9.75 km (32000 ft) for Cost-of-Time = $600/hour, Aircraft Weight = 38.6 tonne (85000 lb) and Cost-of-Fuel = $0.33/kg ($.15/lb).

2. Minimax Polynomials More data were used in determining the C_D surface fit by using more data points from the curves of Fig. 3. No improvement in the overall fit was achieved.

3. Least Squares Polynomials The data of Figs. 3 and 4 were used with the NASA Langley least squares regression program MRA to find polynomial fits of the form

$$C_D = \max(.199,\ a_{00} + a_{10}\overline{M} + \ldots + a_{01}C_L + \ldots \qquad (4a)$$

$$+ a_{mn}\overline{M}^m C_L^n + \ldots + a_{44}\overline{M}^4 C_L^4 .) ; \qquad \overline{M} \triangleq e^M .$$

$$T = b_{00} + b_{10}EPR + \ldots + b_{01}M + \ldots$$

$$+ b_{mn}M^m EPR^n + \ldots + b_{44}M^4 EPR^4 ,$$

where M is the Mach number limited by max {actual Mach number, .6}, and $\overline{M}$ is defined as e^M. Also, a_{ij}, b_{ij} are the least squares coefficients.

These least squares polynomials were extensively tested in OPTIM. In preliminary tests, they were shown to have the following advantages over the minimax polynomials:

1. In all tests, OPTIM computed the correct cruise table values without restricting the independent variables.

2. The fits were single precision and required only 25 coefficients for each surface. The improvement in run time over the minimax fit is shown in Table 1.

3. The fit was smooth between data points and had a maximum error at data points $\leq$ 2%. This appeared to be sufficient for OPTIM convergence. Figure 9 compares a particular cruise table summary for minimax and least squares fits. It is obvious that the least squares results are more realistic.

4. The least squares form had no denominator and therefore no roots in the denominator.

Least Squares Modifications One disadvantage of the least squares polynomials (the drag fit in particular) is that they do not correspond to the known physical relationship between C_D, M, and C_L. (It has been documented for other aircraft that C_D can be described as varying directly

Table 1. Comparison of Run Time, in CPU seconds, for Two Typical OPTIM Runs Using Three Methods of Determining C_D and T_h/δ

Run Time, CPU Seconds

Run No.	Interpolation Scheme	Least Squares Polynomial	Minimax Polynomial
1	159	189	464
2	157	193	448

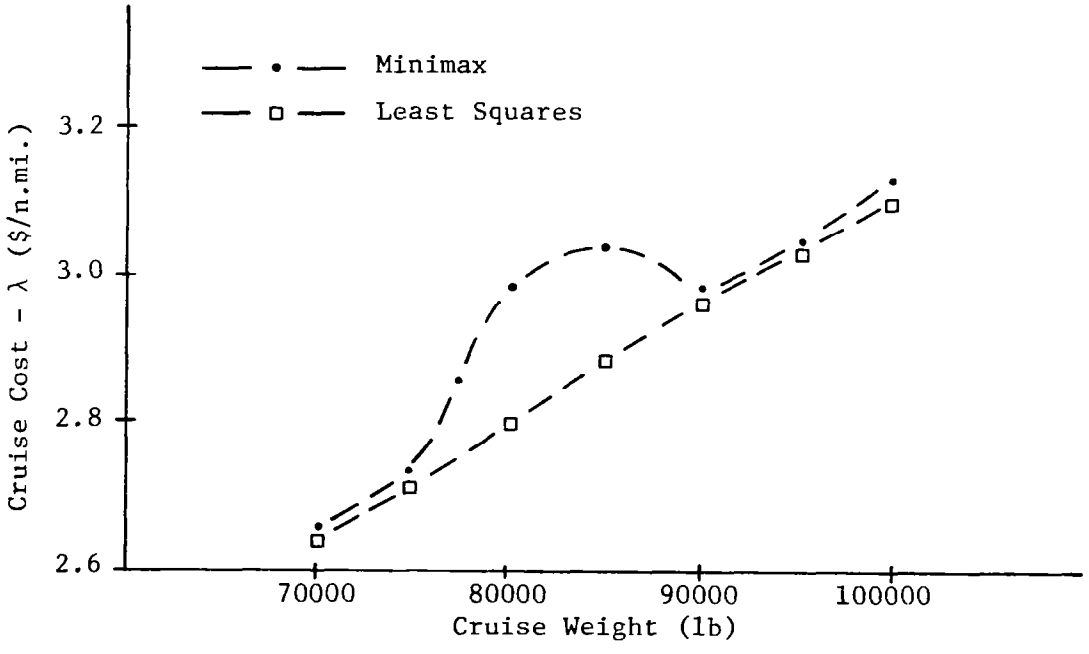

Figure 9. Comparison of Cruise Cost as a Function of Cruise Weight for Minimax and Least Squares Polynomials.

with the square of C_L and inversely with a polynomial in M [7].) In addition, use of the least squares surfaces did not always produce a cost curve having a single minimum as a function of altitude. The oscillations in the cost function were generally in the fourth significant figure (less than $.01/nmi.). However, this was enough to produce convergence problems, as was uncovered by further testing.

In testing the time-of-arrival (TOA) option for the twin-jet with the new surface fits, it was found that a convergence problem existed when the Mach number required was between 0.6 and 0.74 for certain weight ranges. The source of this problem was found by plotting drag coefficient C_D as a function of Mach number with lift coefficient as the parameter. Examples of these plots and the least squares surface fit data, for C_L of 0.025, 0.15, 0.30 and 0.40, are shown in Fig. 10. As can be seen, the surface fit results match the data points at Mach numbers of 0.6, 0.68, and 0.74, as taken from Fig. 3. However, there is oscillation in between these Mach numbers. This results in the physically unnatural situation where the computed drag could <u>decrease</u>, say at a C_L of 0.025, when Mach number increases from 0.6 to 0.64.

The solution to the oscillation problem was obtained by using the term $\overline{M}$ equal to 1/(0.9-M) instead of e^M to obtain the drag coefficient surface of Eq. (4a) for the twin-jet model. The results of this change are also shown in Fig. 10. For the tri-jet model, the term 1/(0.95-M) was used successfully for $\overline{M}$. These changes are referred to below as the modified least squares fits.

One further problem existed in the drag surface fit for Mach numbers between 0.6 and 0.68 and lift coefficient above 0.5. This problem was due to lack of higher Mach number data in this region of Fig. 3 that prevented obtaining an adequate fit. Figure 11 shows the problem which existed here using the modified least squares fits for C_L of 0.70 and 0.75. Because only two data points are available on these curves, there is almost a straight-line fit between M of 0.6 and 0.68 in this region. With constant C_D below Mach 0.6, this produced a kink in the drag coefficient curve at the Mach 0.6 point. This kink causes a convergence problem for time-of-arrival runs requiring slow cruise.

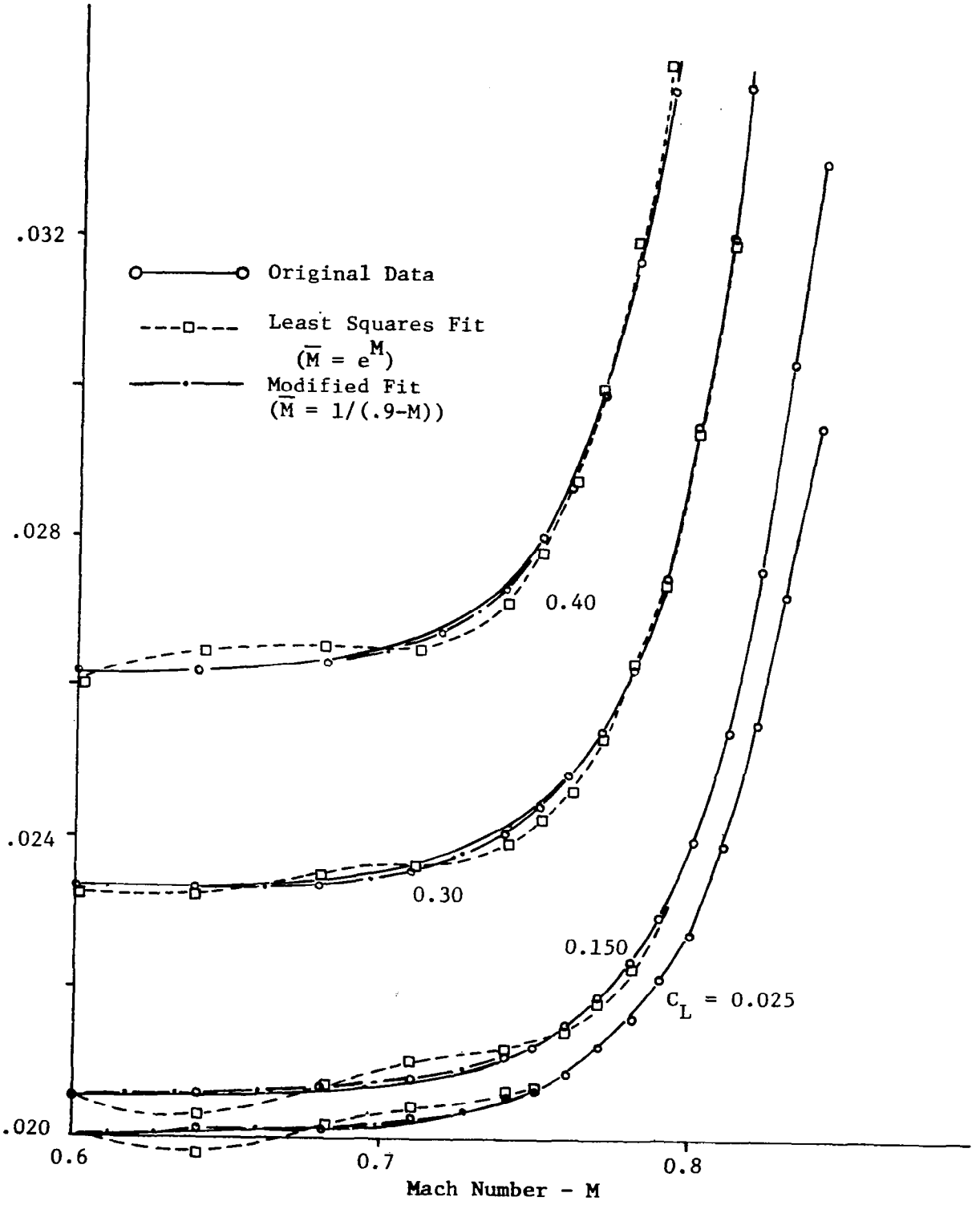

Figure 10. Drag Coefficient Surface Fit Accuracy Between Data Points at M = 0.6, 0.68, and 0.74 with C_L Given.

The solution to this problem was to assume that between Mach 0.6 and 0.68, the drag coefficient could be expressed as

$$C_D = a_1 + a_2(M-0.6)^2 + a_3(M-0.6)^3 , \tag{5}$$

for a given lift coefficient. To evaluate Eq. (5), the modified least squares surface fit is used to determine the value of C_D as a function of C_L and M on the Mach 0.6 and 0.68 lines. Also, this modified fit is used to compute the slope (dC_D/dM) on the 0.68 line. These three values are then used to solve for the three coefficients (a_1, a_2, and a_3) in Eq. (5) for a particular value of C_L. The cubic equation ensures that the result matches the surface fit (for fixed C_L) in value and slope at both boundaries, and that C_D is monotonically increasing as the Mach number increases. This is illustrated by the dashed line fits in Fig. 11.

Lessons Learned Tests of the modified least squares curve fits for drag and thrust coefficients produced good results for time-of-arrival convergence. The lessons learned from this segment of the study were as follows:

1. Numerical optimization is based on the natural existence of continuous, smooth surfaces, and any departure from this type of model to discontinuous surfaces or multiple surfaces connected with corners may produce faulty results. In the case of tables with straight-line interpolation, the optimization process will produce an answer at a tabular data point (which can be described as a corner or kink in the resulting surface made up of connected plane polygons).

2. Any error in entering the data points into tables produces points where the optimization process will either converge to or diverge from in a local search. Thus, due care must be exercised in reading and entering the data points.

3. Computer programs which produce surface fits to tabular data do not necessarily produce the desired surfaces even though each data point may be matched very well. Specifically, for thrust and drag surface representation, the following was learned:

   (a) The minimax curve fit described in Eq. (3) had surface

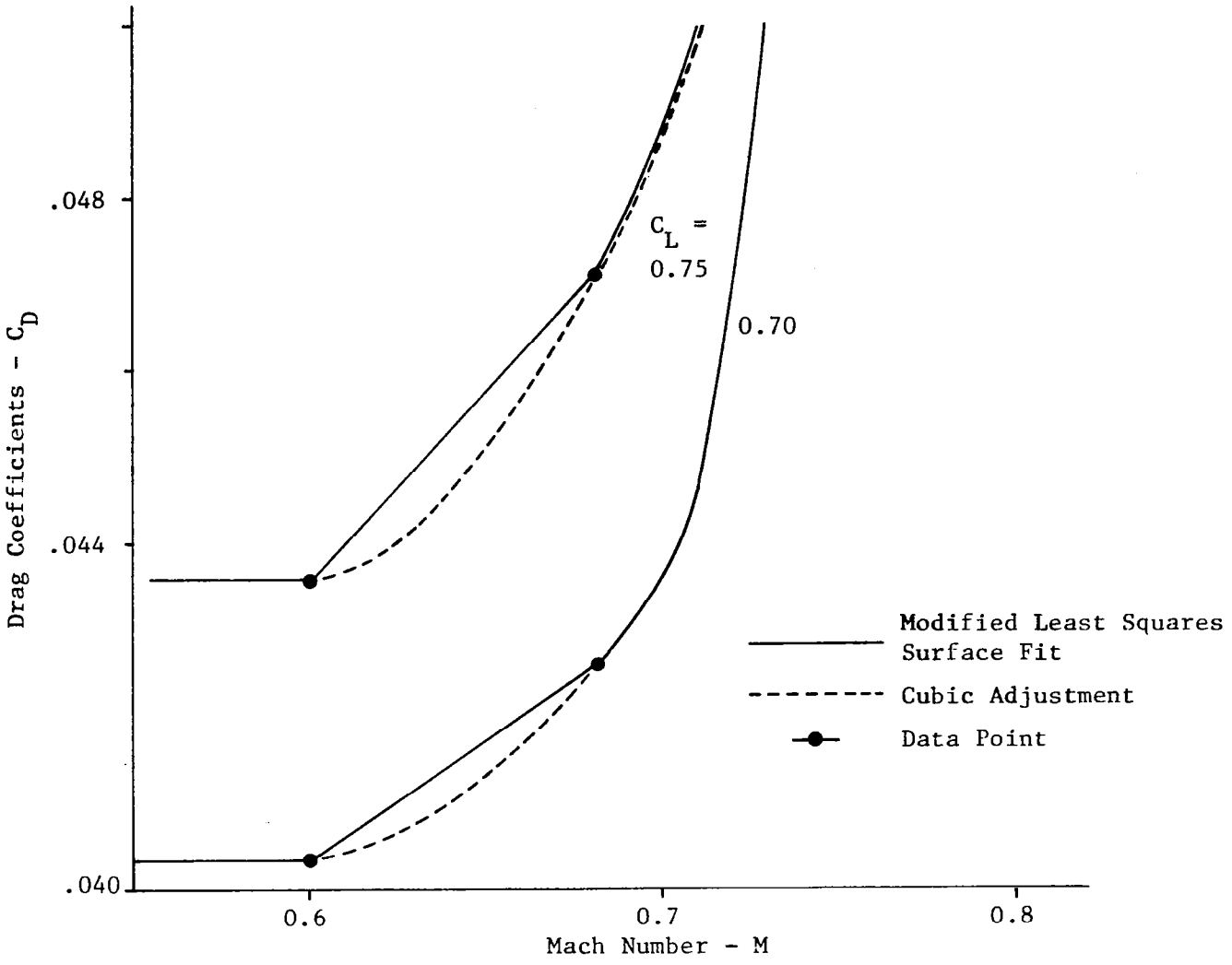

Figure 11. Kink Problem at M = 0.6 with Modified Surface Fit and its Solution with Cubic Adjustment Between M = 0.6 and 0.68.

discontinuities because of roots in the denominator.

(b) The least squares curve fit described by Eq. (4) did not always produce a monotonically increasing drag coefficient as the Mach number increased between the data points. Changing the variable M (Mach number) to (0.9-M) improved the curve fit results except in regions where original data points were limited.

(c) Special cubic fits such as Eq. (5) had to be used to produce the desired continuity in the surface derivatives.

From this sequence of trials, the following sub-points were also established:

(a) The nature of the surface fit between the data points must be examined carefully to see that "reasonable characteristics" are obtained. This is verified ultimately by use of the surface fits for the application intended (in this case, time-of-arrival convergence).

(b) Reasonable characteristics of surface fits are determined by using physical reasoning. For example, we know that drag increases monotonically with Mach number. Also, for the level of aerodynamic models used in this optimization study, there is no physical reason for kinks in the drag coefficient surfaces or discontinuities in the surface slopes.

Optimum Step Climb

Aircraft flying on IFR flight plans follow specific altitude separation rules. These rules are shown in Table 2 for continental United States travel. All air carrier turbojet aircraft file IFR plans for all flights. It can be seen from Table 2 that cruise altitude changes currently must be made in 610 m (2000 ft) or 1220 m (4000 ft) increments or steps.

Table 2. Altitude Separation Rules for IFR Flight

Altitude	Heading (magnetic) 0 - 179°	180 - 359°
Below FL180	Odd thousands of feet	Even thousands of feet
FL180 - FL290	Odd Flight Levels	Even Flight Levels
Above FL290	Odd FL 4000 ft Separation Starting at FL290	Odd FL 4000 ft Separation Starting at FL310

Previous versions of OPTIM allowed the user to compute an optimum vertical profile with either a fixed cruise altitude or a optimum free cruise altitude. The free cruise altitude is computed to be most favorable in terms of least cost per unit distance traveled (See Eq. (2)). This optimum altitude is a function of aircraft weight and the prevailing wind profile. Usually, as fuel is burned and the aircraft becomes lighter, the optimum altitude becomes higher.

At this point in time, the air traffic control (ATC) system has not evolved to a point where optimum cruise altitudes are allowable. Thus, aircraft fly by the rules listed in Table 2. However, as fuel is burned, and if ATC permission is granted, an aircraft may climb to the next acceptable flight level. Also, a climb may be warrented, based on change in the vertical wind profile. (Sometimes, the prevailing wind change may dictate that descent to the next lower flight level is desirable.)

A useful addition to OPTIM has been the ability to include step climbs from one fixed altitude to another. The step climb is a compromise between being constrained to fly at a fixed cruise altitude and flying at the optimum free cruise altitude. In keeping with the intent that the computed profile be optimum, the OPTIM program has been configured to determine where in cruise the optimum climb should begin.

According to a major airline representative, for an aircraft to make a step climb, it must be able to do so at the climb thrust rating with a rate of climb of at least 1.5 m/sec (300 ft/min). After the aircraft has reached the new altitude, it must be able to maintain cruise speed at the cruise thrust rating. This latter restriction was included in the step climb implementation.

To understand the concept of choosing the best place to begin the step climb, consider the vertical profile sketch in Fig. 12. The aircraft begins cruise at altitude (or flight level) FL_A. It later step climbs to the higher flight level FL_B with a given Mach number schedule and according to the constraints mentioned above.

In Fig. 12, the earliest the step can begin is at cruise range of R_0 which is the beginning of cruise at FL_A. It is very probable that this climb could not begin until a later range of R_1 is reached because it would to too heavy to maintain cruise at FL_B before this time. Thus, the OPTIM program establishes where R_1 is to set one boundary for the climb point. (R_1 may coincide with R_0).

The last cruise point where climb can begin is at R_f. Here, there is just enough range available to allow the aircraft to climb to FL_B before beginning final descent. This, of course, is not practical, but it establishes the other boundary for possible climb initiation points. OPTIM computes R_f as the next step in determining the optimum step climb.

With R_1 and R_f determined, OPTIM does a search between these two points to compute the optimum cruise range R_c to begin the step climb. The Fibonacci search technique is used to find R_c. The step climb beginning at this point produces less overall flight profile cost (in terms of time

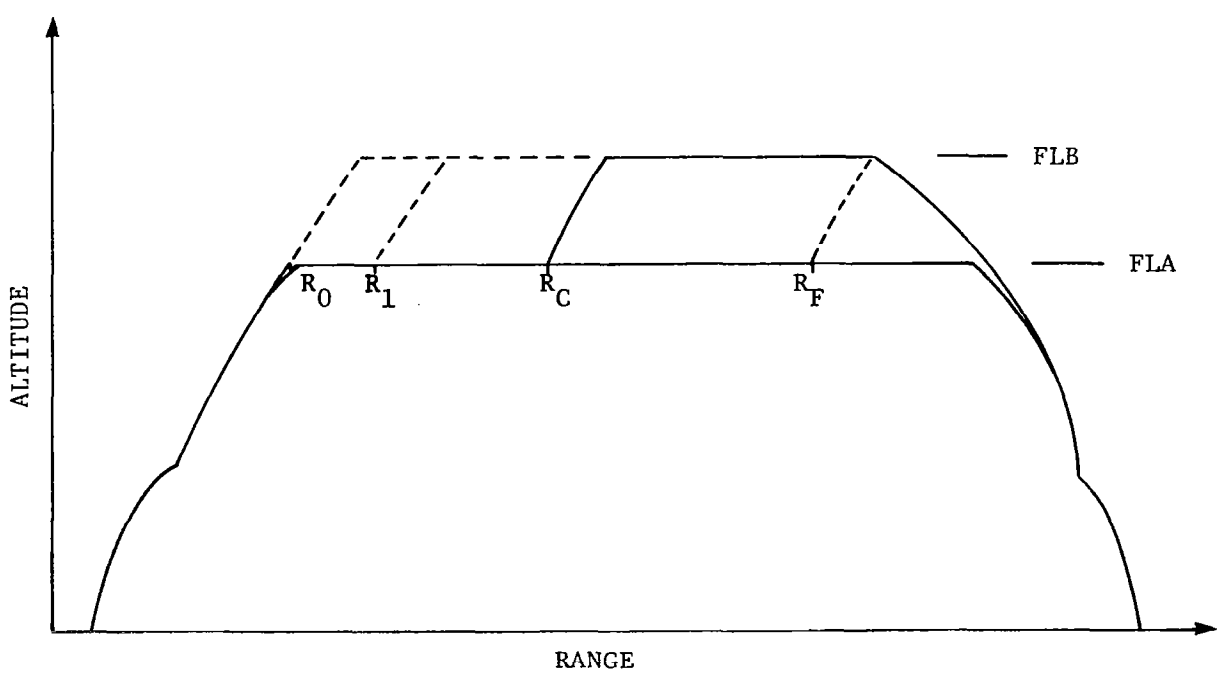

Figure 12. Sketch of Altitude vs Range Profile for Step Climb Computations.

and fuel) than step climbs beginning at other cruise points. OPTIM also checks to determine that using the step climb is better than remaining at FL_A. An example of using this program option is presented later.

Cabin Pressurization Constraint on Descent

All transport aircraft cabins are pressurized to maintain an ambient cruise pressure at some altitude higher than sea level. Typically, as the aircraft descends from cruise, the cabin is repressurized at a given rate until the landing altitude pressure is reached. Thereafter, the pressure is maintained constant. (e.g., 101348 N/m^2 (14.7 lb/in^2) for sea level.) During the pressure buildup in the cabin, it is airline practice to limit the cabin rate of descent to keep the rate of pressure increase tolerable for passenger comfort, and to not exceed the maximum differential between cabin and external pressures. This is usually done by computing an equivalent rate of descent based on pressure buildup rate within the cabin and then using this as a constraint factor.

In the past, for propeller driven aircraft, a cabin rate of descent as low as 1.5 m/sec (300 ft/min) has been used. There is disagreement on the part of the airlines as to the need for such a low cabin rate of descent when at the high altitudes of today's transport aircraft.

The rate of change in pressure with altitude is non-linear as shown in Fig. 13, and thus, one would expect the passenger comfort problem to be more critical at lower altitudes where the rate of pressure increase with decreasing altitude is greater. This is evident in Fig. 14 which shows how the time rates of change of pressure increase at given cabin altitudes for selected constant equivalent cabin rates of descent.

Two factors, or questions, are important in determining the effect of cabin pressurization constraints on optimum descent profiles:

1. What is the maximum tolerable <u>cabin</u> pressure rate of change (dp/dt) that is tolerable to the human ear? The value 19257 N/m^2/min (0.19 psi/min) is being used for design of commuter aircraft.

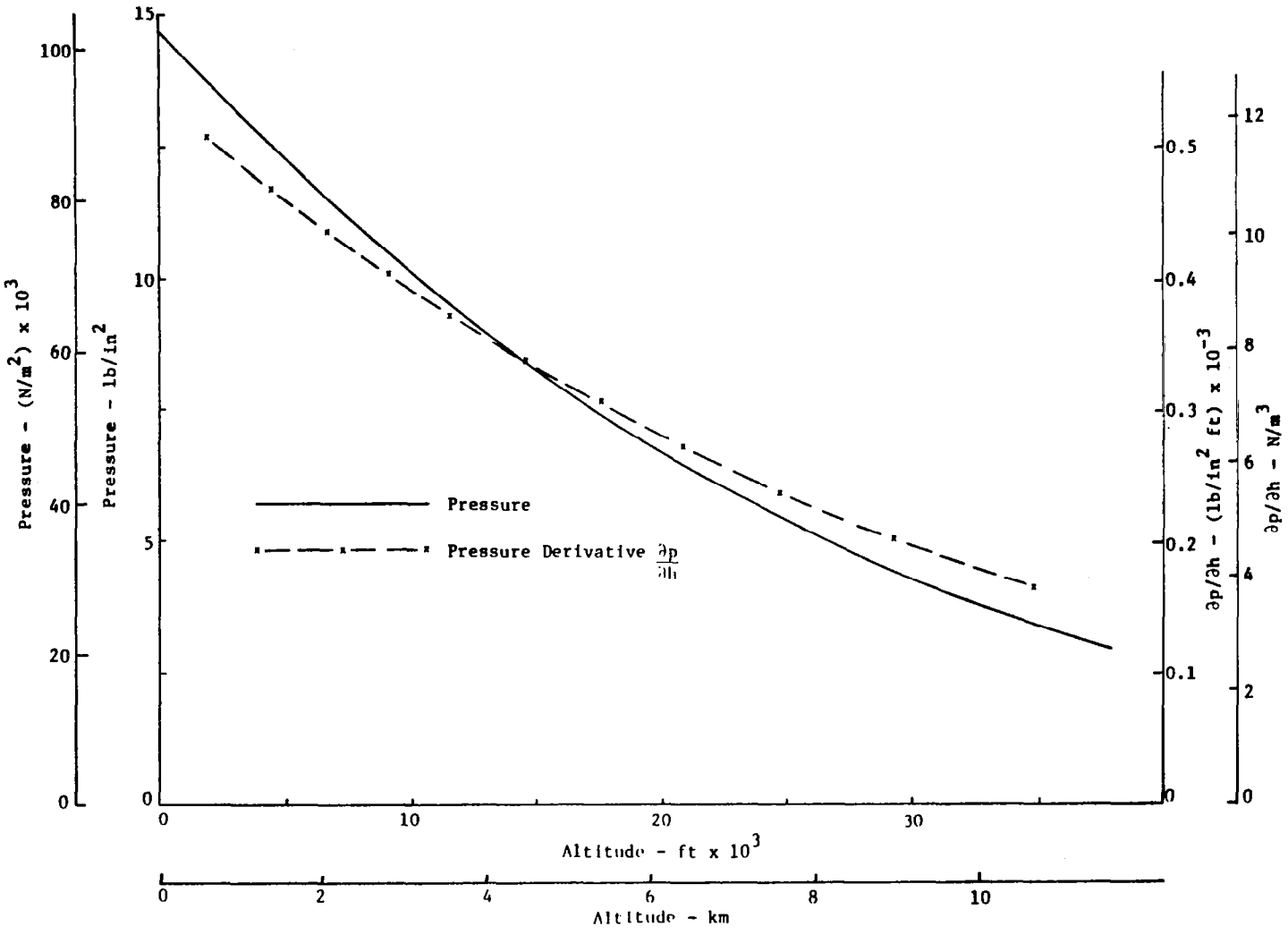

Figure 13. Air Pressure and Rate of Change of Pressure as Functions of Altitude

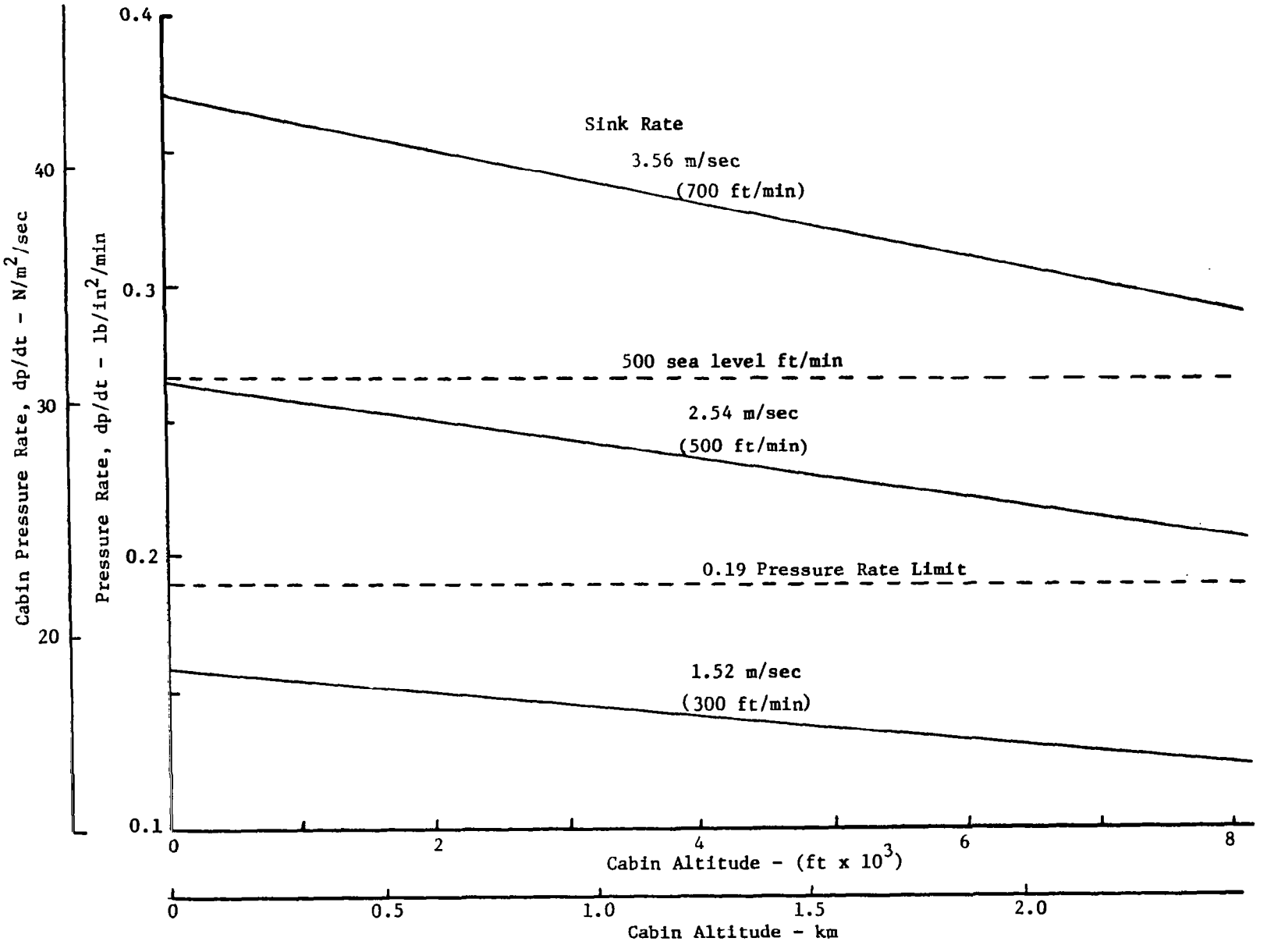

Figure 14. Rate of Change of Cabin Pressure with Time for Different Equivalent Cabin Descent Rates.

Another value which appears in aircraft manufacturers documentation is the equivalent of 2.54 m/sec (500 ft/min) sea level change in altitude. Figure 14 shows these cabin pressure rates as functions of cabin altitude rates.

2. What is the nature in which the pressurization pump functions or can function in changing the cabin pressure? Three different assumed methods can be applied to answer this question. All may be possible, but each has a different impact on the acceptable aircraft altitude rate of change limit. The three alternate assumptions are now discussed in turn.

Cabin Altitude Proportional to Aircraft Altitude In this case, the cabin pressure has the relationship that

$$h_{cab} = h_{TO} \qquad \text{for } h_{a/c} < h_p , \tag{6}$$

$$= h_{TO} + \frac{dh_{cab}}{dh_{a/c}} (h_{a/c} - h_p) \qquad \text{for } h_{a/c} < h_p .$$

Here, h_{TO} is either the takeoff or landing altitude, $h_{a/c}$ is the ambient pressure altitude outside of the aircraft, and h_p is the altitude below which the cabin pressure is maintained at the takeoff or landing altitude value. Above h_p, the cabin pressure altitude is proportional to the difference between actual aircraft altitude $h_{a/c}$ and h_p. This is illustrated in Fig. 15.

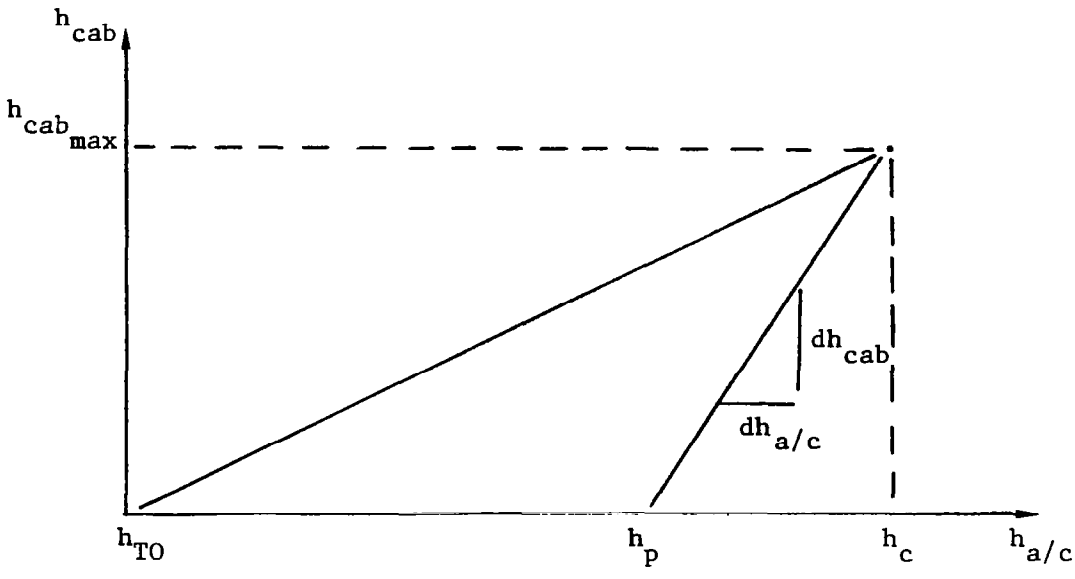

Figure 15. Variations of h_{cab} Proportional to $h_{a/c}$.

For this assumption, we can write

$$\frac{dh_{cab}}{dt} = \left(\frac{dh_{cab}}{dh_{a/c}}\right)\left(\frac{dh_{a/c}}{dt}\right) , \tag{7}$$

or

$$\frac{dh_{max}}{dt} = \left(\frac{dh_{cab}}{dt}\right)\Big/\left(\frac{dh_{cab}}{dh_{a/c}}\right) \tag{8}$$

The point h_p may be determined by the maximum overpressure the cabin is designed for. For example, for Δp of 6, 8, or 10 psig, the maximum altitudes where sea level cabin pressure (14.7 psi) could be held are 4.27, 6.10, and 8.84 km (14000, 20000, and 29000 ft), respectively.

For Δp_{max} of 10 psig, cruise altitude h_c of 11.28 km (27000 ft) and $h_{cab_{max}}$ of 2.44 km (8000 ft),

$$\frac{\Delta h_{cab}}{\Delta h_{a/c}} = \frac{8000}{37000 - 29000} = \frac{8000}{8000} = 1. \tag{9a}$$

Then, for a $\frac{dh_{cab}}{dt}$ limit of 2.54 m/sec (500 ft/min), from Eq. (8), the resulting climb or descent rate above 8.84 km (29000 ft) would also be

$$\frac{dh_{max}}{dt} = 2.54 \text{ m/sec (500 ft/min)}. \tag{9b}$$

These values are currently used in the OPTIM program, as discussed later.

For Δp_{max} of 8 psig,

$$\frac{\Delta h_{cab}}{\Delta h_{a/c}} = \frac{8000}{17000} = 0.47 , \tag{10a}$$

and

$$\frac{dh_{max}}{dt} = \frac{2.54}{0.47} = 5.41 \text{ m/sec (1064 ft/min) down to 6.10 km (20000 ft)}. \tag{10b}$$

For h_{max} of 11.28 km (37000 ft) and h_p of 0 km,

$$\frac{\Delta h_{cab}}{\Delta h_{a/c}} = \frac{8000}{37000} = 0.216, \tag{11a}$$

and

$$\frac{dh_{max}}{dt} = \frac{2.54}{0.216} = 11.76 \text{ m/sec (2315 ft/min) down to 0 km.} \tag{11b}$$

The OPTIM program is based on this assumed method of repressurization and inputs required at h_p and dh_{max}/dt. This is discussed further, shortly.

Cabin Altitude Rate Proportional to Aircraft Altitude Rate Figure 16 taken from a 737 Operations Manual indicates that cabin altitude is proportional to aircraft altitude. But the accompanying explanation states that "by climbing the cabin altitude (maximum rate 500 sea level feet per minute) "proportional" to airplane climb rate, cabin altitude change is held to the minimum rate required." This implies that the pressurization system imposes a direct constraint on the climb and descent rates.

As seen by referring to Fig. 16, if the aircraft cruises at 11.28 km (37000 ft (3.142 psi pressure altitude)) and the Δp_{max} is 52,070 N/m^2 (7.55 psi), the resulting cruise cabin pressure would be 73,740 N/m^2 (10.692 psi), or about 2.59 km (8500 ft). If cabin rate of climb or descent is proportional to the airplane rate, then

$$\frac{dh_{cab}}{dt} = c\,\frac{dh_{a/c}}{dt}\,. \tag{12}$$

For this example,

$$c \cong \frac{8500}{37000} = 0.23\,. \tag{13}$$

The aircraft rate limit would then be

$$\left(\frac{dh_{a/c}}{dt}\right)_{max} = \frac{2.54}{0.23} = 11.04 \text{ m/sec (2176 ft/min) at sea level,} \tag{14}$$

or

$$\left(\frac{dh_{a/c}}{dt}\right)_{max} = \frac{3.30}{0.23} = 14.36 \text{ m/sec (2826 ft/min) near cruise.} \tag{15}$$

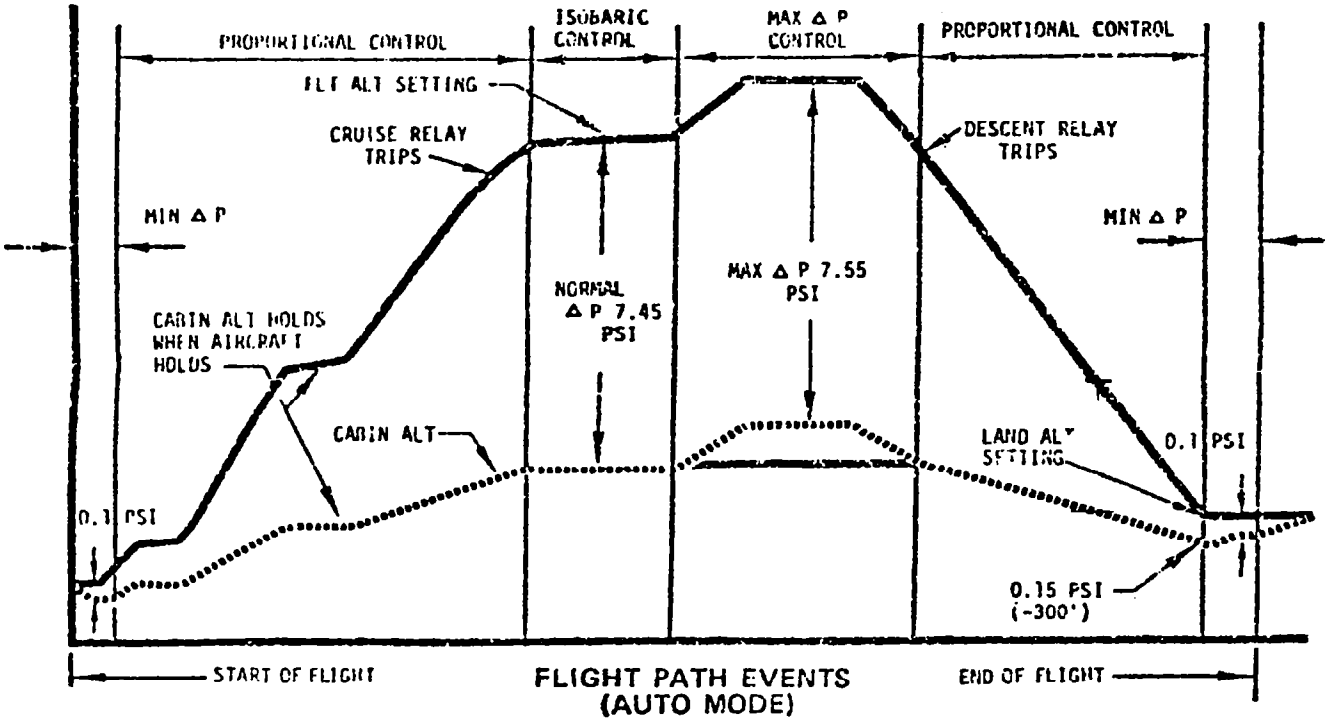

Figure 16. 737 Operations Manual Profile of Cabin Altitude as a Function of Airplane Altitude.

The 3.30 m/sec (650 ft/min) value is the equivalent to 2.54 m/sec (500 ft/min) sea level value, taken at 2.59 km (8500 ft).

These climb and descent rates would pose significant constraints on the climb and descent profiles. Typical optimum climb rates from the OPTIM program for the twin-jet model are up to 20.32 m/sec (4000 ft/min) at the initial climb point and right after leaving 3.05 km (10000 ft). These correspond to flight path angles of 9.1° and 6.7°, respectively. For descent, a maximum rate of 27.66 m/sec (-5445 ft/min) is specified right before 3.05 km (10000 ft) is reached; this corresponds to a flight path angle of -7.5°. Over the entire profiles, there are large periods of time in which climb and descend rates exceed the values of Eq. (14). Thus, hopefully this pressurization technique is not required.

Constant Cabin Altitude Rate A third alternative which offers the most flexibility is to pressurize or depressurize the cabin at a constant rate - say 2.54 m/sec (500 sea level ft/min). This is equivalent to

1860 N/m^2/min (0.27 psi/min). Going from sea level pressure of 101,380 N/m^2 (14.70 psi) to cabin pressure of 73,790 N/m^2 (10.70 psi) (~ 8500 ft) would take 14.8 min. Typical optimum climbs and descents take 16 - 18 min, so there is adequate time. Any climb and descent delays (which are likely) provide extra time to accomplish the pressure change, or allow the rate to be decreased.

This type of pressurization is possible with a constant displacement pump. However, it may not be feasible in the thinner air of the upper atmosphere. Also, caution must be taken to ensure that the pressure differential between the cabin and the ambient atmosphere does not exceed the hull limits.

Incorporation in Optimization Process Obviously, the cabin rate of descent constraint can be eliminated altogether by increasing the cabin overpressure to a sufficiently high level. An overpressure of 78,600 N/m^2 (11.4 psi) would provide sea level cabin pressure at the tropopause. However, other design and performance factors must be considered. Specifically, these factors include the effect of the overpressure on the fuselage structural requirements and weight, the amount of engine bleed air required to provide the cabin pressurization, and the pressurization pump function details.

Appendix A presents a parametric study of the effects of variations in constrained sink rate and cabin overpressure available on descent fuel and time requirements. This is based on the first pressurization method discussed above. Decreasing the rate of descent from 3.5 to 1.5 m/sec can increase descent fuel required from 100 to 250 kg (220 to 550 lb). Decreasing the cabin overpressure capability from 68,900 N/m^2 (10 psi) to 55,200 N/m^2 (8 psi) can increase descent fuel required from 150 to 450 kg (330 to 990 lb). The pressurization constraint is therefore significant concerning fuel utilization; this constraint was included in the OPTIM program as an option.

The constrained descent causes the optimum descent profile to change as depicted in Fig. 17. Descent starts earlier at range R_{f2} rather than

R_{f1}. For this pressurization method, the descent profile is constrained to follow a fixed descent rate with a Mach number linearly changing with altitude down to altitude h_p. The altitude h_p is where sea level cabin pressure is reached with the fixed cabin overpressure capability. Currently in OPTIM, the fixed sink rate is set at 2.54 m/sec (500 ft/min), and the altitude h_p is 8.839 km (29000 ft). The Mach number is commanded to vary linearly with altitude over the upper part of the profile. Values range between the one which is optimum if cruise were at h_p and the optimum Mach number at the actual higher cruise altitude h_c. The lower part of the descent profile is optimized to end at altitude h_p.

The OPTIM program generates the unconstrained optimum profile first, and then the latter part of cruise and the descent segment are modified as just discussed. This gives an immediate measure of increased time and fuel required to include the cabin pressurization constraint.

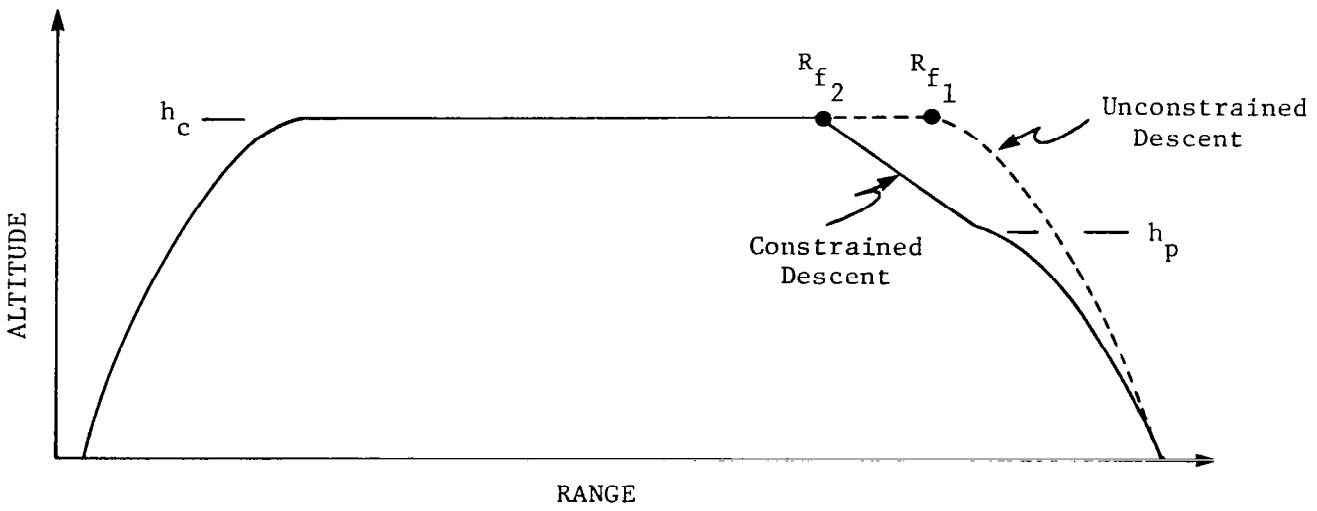

Figure 17. Sketch of Modified Optimum Profile Due to Cabin Pressurization Constraint on Descent.

Variable Wind Profiles

The biggest uncertainty in computing an optimum flight profile is in the knowledge of the wind field that the aircraft must fly through in reaching its intended destination. Airline meteorologists have achieved various levels of proficiency in wind and weather forecasting, and these forecasts are regularly used to determine favorable horizontal paths for the aircraft to follow between a given city pair. Figure 18 shows an example of twenty horizontal routes that a major airline chooses from in flying from Orlando to Chicago. Up to eight different waypoints may be used, and the distance between the westernmost and easternmost routes exceeds 500 nmi. The Atlanta to Los Angelas city pair for the same airline has more than 130 horizontal route choices.

Different computer programs have been developed to aid the flight planners in making these choices. They vary from simple programs that simulate performance along each segment of each route to relatively sophisticated programs which use graph theory [9] for computing near optimum routes. Much work remains to provide airlines and the air traffic control system with computer tools and improved weather forecasting to further reduce fuel requirements.

By examining a typical weather chart, it can be seen that wind and temperature can vary considerably over even medium range routes. Also, as seen in Fig. 18, the airline heading can change many times over the route. Thus, the vertical wind profile that an aircraft will experience can have a large variation. In computing the optimum vertical flight profile, this variation must be taken into account.

The OPTIM program computes a cruise table which minimizes the cost per unit distance traveled as defined by λ in Eq. (2). This table typically contains the optimum cruise cost λ, specific energy E, and airspeed V_a for 304.8m (1000 ft) steps in altitude and 2273 kg (5000 lb) steps in aircraft mass. Interpolation is used based on aircraft mass to determine the optimum cruise conditions (altitude, airspeed) from this table.

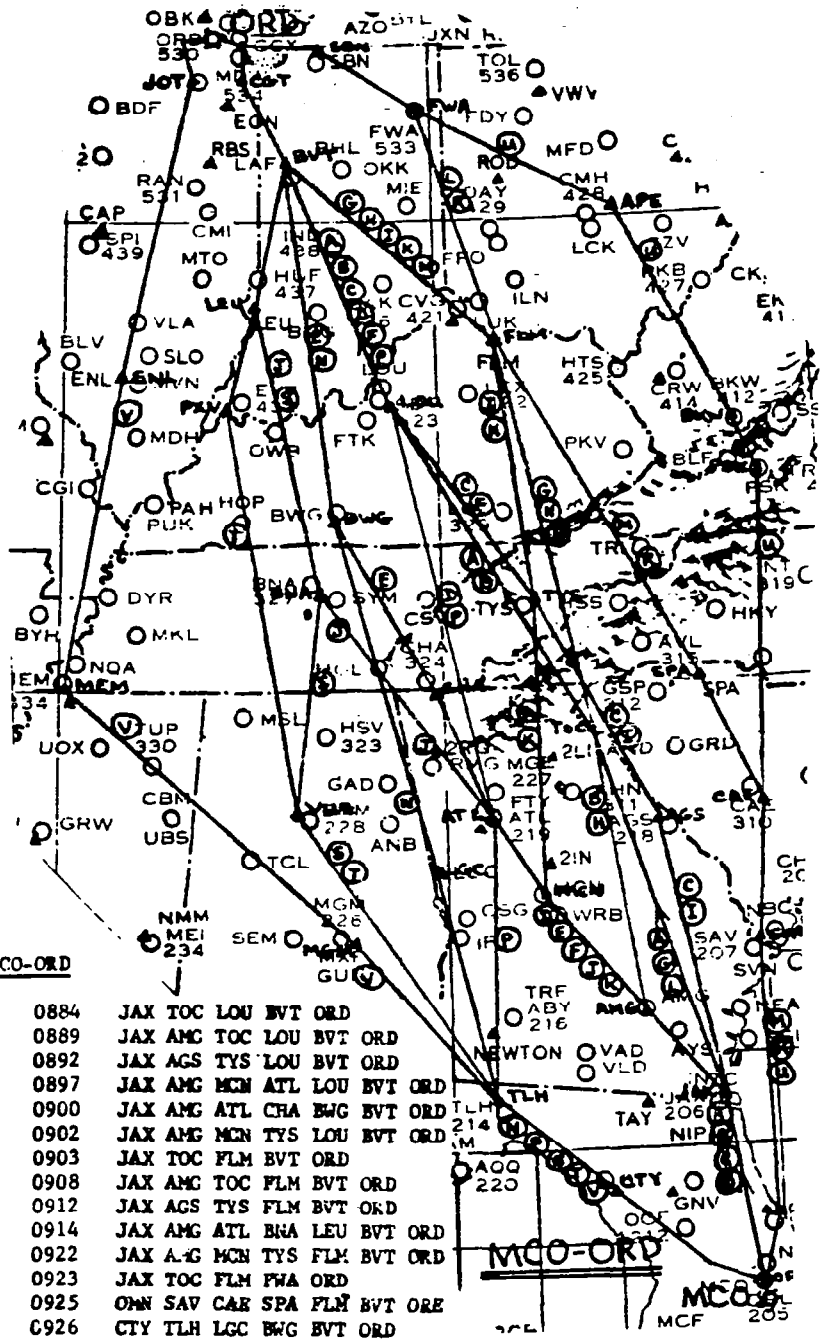

MCO-ORD

A	0884	JAX TOC LOU BVT ORD
B	0889	JAX AMC TOC LOU BVT ORD
C	0892	JAX AGS TYS LOU BVT ORD
D	0897	JAX AMC MCN ATL LOU BVT ORD
E	0900	JAX AMC ATL CHA BWG BVT ORD
F	0902	JAX AMC MCN TYS LOU BVT ORD
G	0903	JAX TOC FLM BVT ORD
H	0908	JAX AMC TOC FLM BVT ORD
I	0912	JAX AGS TYS FLM BVT ORD
J	0914	JAX AMC ATL BNA LEU BVT ORD
K	0922	JAX AMC MCN TYS FLM BVT ORD
L	0923	JAX TOC FLM FWA ORD
M	0925	OMN SAV CAE SPA FLM BVT ORD
N	0926	CTY TLH LGC BWG BVT ORD
P	0931	CTY TLH ATL LOU BVT ORD
R	0945	OMN SAV CAE SPA FLM FWA ORD
S	0952	CTY TLH VUZ BNA LEU BVT ORD
T	0957	CTY TLH VUZ PXV LEU BVT ORD
U	0999	OMN SAV CAE PSK BKW APE FWA ORD
V	1038	CTY TLH MGM MEM ENL JOT ORD

Figure 18. Horizontal Route Choices from Orlando to Chicago.

If the wind profile is continually changing, the ground speed V_g and optimum airspeed from Eq. (2) will be also changing for a given altitude and aircraft mass. Thus, the entries in the cruise table would be theoretically always changing, and the aircraft cruise conditions, as commanded by the OPTIM algorithm, would continuously change. Clearly, there is a limitation to the practicality of such an implementation.

In addressing how OPTIM could be modified to account for variable winds, the applications OPTIM can be used for had to be kept in mind. At this point, OPTIM is primarily being used for two purposes:

1. To investigate the effects of various constraints (such as constant cruise altitude and fixed arrival time) on the fuel and operating cost of the flight profile.

2. To serve as the basis for an experimental, advanced flight management system.

In the second application, it is envisioned that the horizontal path followed during cruise will be divided into short segments (e.g., 100 nmi or 10 minutes). An average wind vector can be computed for each segment at the approximate cruise altitude of the aircraft for that segment. The optimum cruise condition can then be computed for that segment, and the aircraft can be commanded to fly with the correct airspeed to minimize cost over that segment. The optimum cruise conditions for each segment of the remainder of the flight would be computed in background of the flight management system computer. As each new segment is reached, the assumed wind vector for that segment could be adjusted based on new forecast information sent from the ground or on-board wind measurements. The version of OPTIM modified for airborne implementation is constructed to follow up to twenty consecutive horizontal segments.

The first application mentioned above does not need such complex capability to study basic effects of variable wind. For analytical study purposes, three different wind profiles representing climb, cruise, and descent phases, are adequate. Thus, the basic OPTIM program has been constructed so that three different wind profiles (wind magnitude

and direction as functions of altitude) can be inserted. The second wind profile is used to generate the cruise table, and it represents the average wind at each altitude over the cruise range. Example applications of the multiple wind profile capability of OPTIM are presented later in this chapter.

Example Results

To demonstrate the utility of the OPTIM program including several of the options provided, this section presents example results. Other examples illustrating earlier options may be found in Ref. 4.

Nominal profiles Figures 19a-b and 20a-b illustrate the optimum variations in altitude, Mach number and flight path angle for the twin-jet and tri-jet aircraft, each traveling 1000 nmi in range. The three state variables are shown as functions of range and range-to-go over the first and last 120 nmi of the flights.

Also shown in these plots are the variations in profiles due to computing them in four different ways. The solid line represents the profile resulting from restricting the cruise altitude to 10 km (33000 ft), and using airspeed (V_a) only as the control variable when minimizing the Hamiltonian expressed as Eq. (1). The dot-dash line depicts the same cruise altitude restriction, but both V_a and thrust (or throttle position π) are used as controls. The dashed line represents the case with free cruise altitude, but only V_a is used for optimization. The dotted line has free cruise altitude, and both V_a and π are used for optimization.

For the twin-jet climb depicted by Fig. 19a, it is seen that for altitudes below 9 km (30000 ft), the four profiles are essentially identical. Above this point there is a difference in the flight path angle followed depending on whether thrust (π) is used as a control variable or not. If thrust is fixed at the maximum value, the aircraft achieves cruise altitude sooner by ending climb with a higher flight path angle. Mach number is fairly constant at about 0.72 above 8 km (26000 ft). This profile is achieved by setting the costs of time and fuel at \$600./hr and \$0.33/kg (\$.15/lb), respectively.

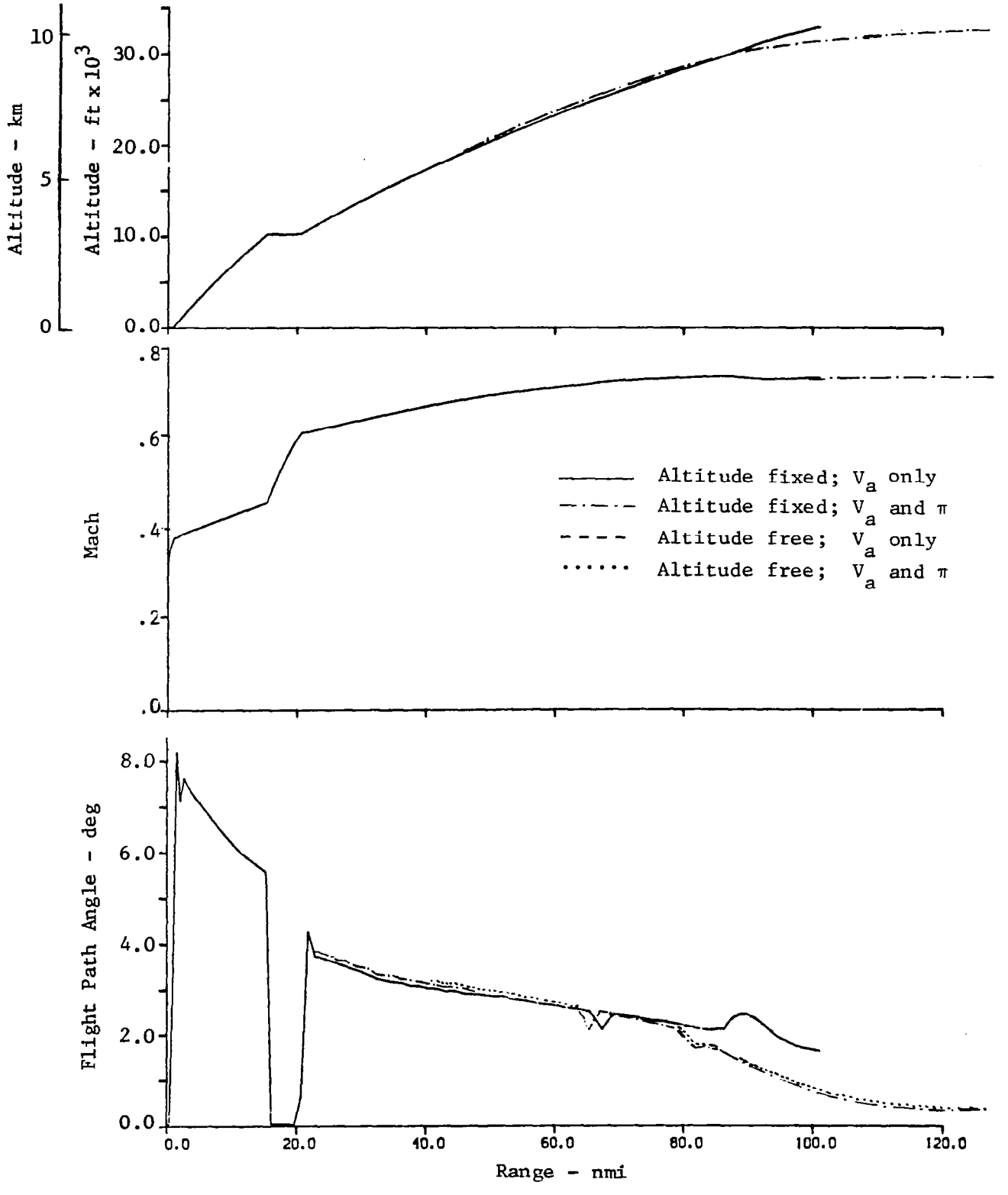

Figure 19a. State Variables for Optimum Climb Profiles of the Twin-Jet Aircraft Traveling 1000 nmi.

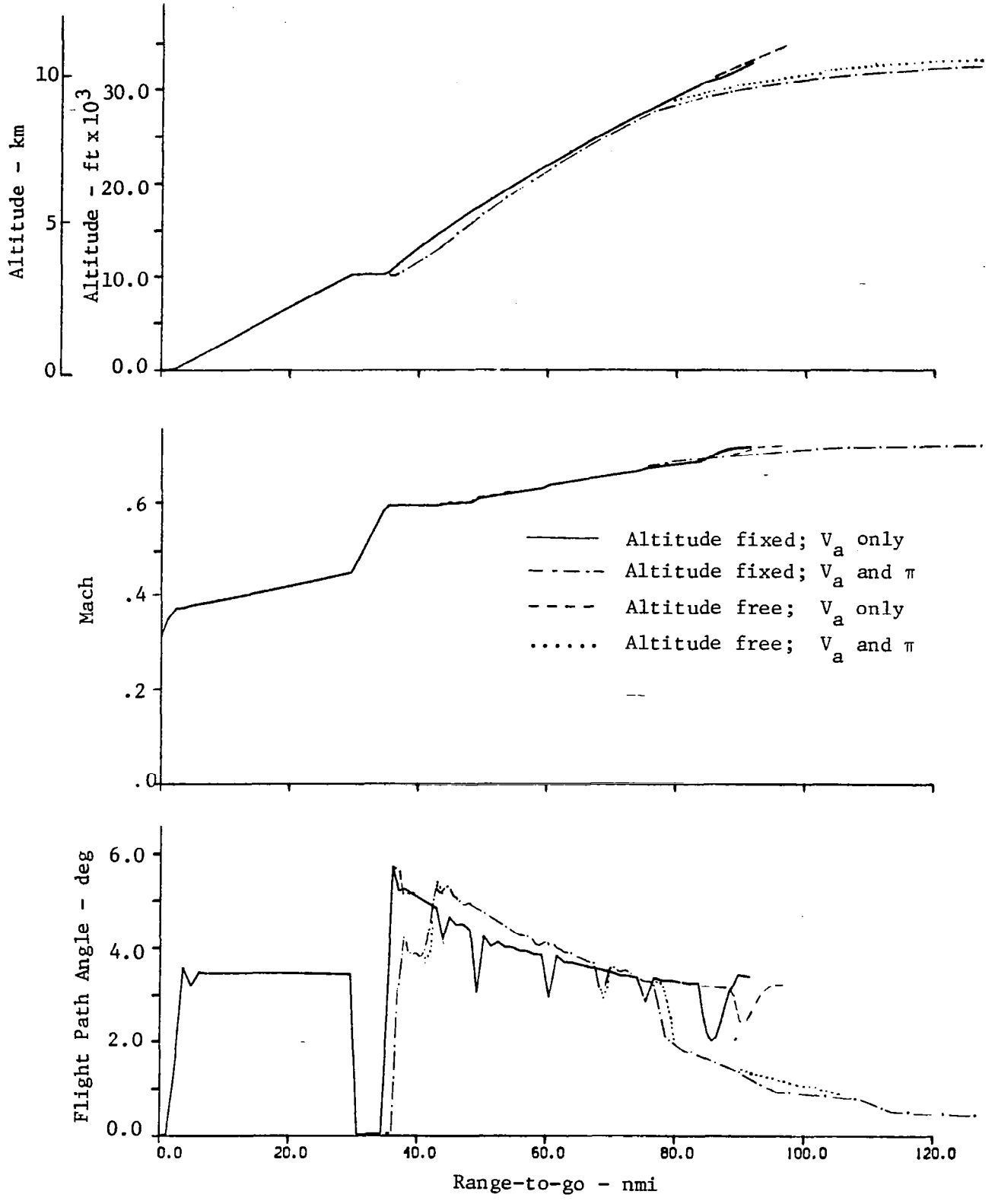

Figure 19b. State Variables for Optimum Descent Profiles of the Twin-Jet Aircraft Traveling 1000 nmi.

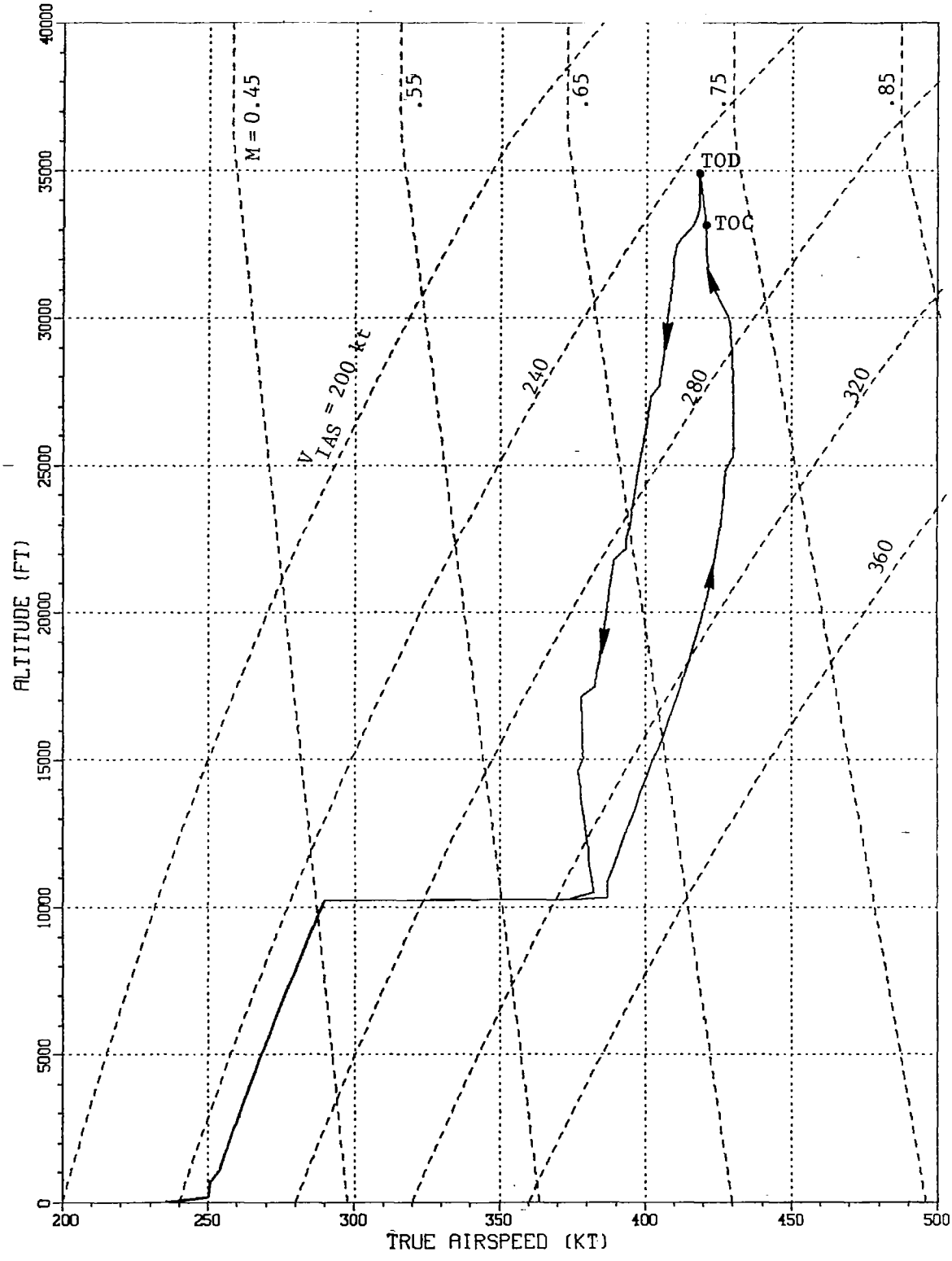

Figure 19c. Altitude vs True Airspeed for the Optimum Profile of the Twin-Jet with Cruise Altitude Free and Optimized with V_a Only.

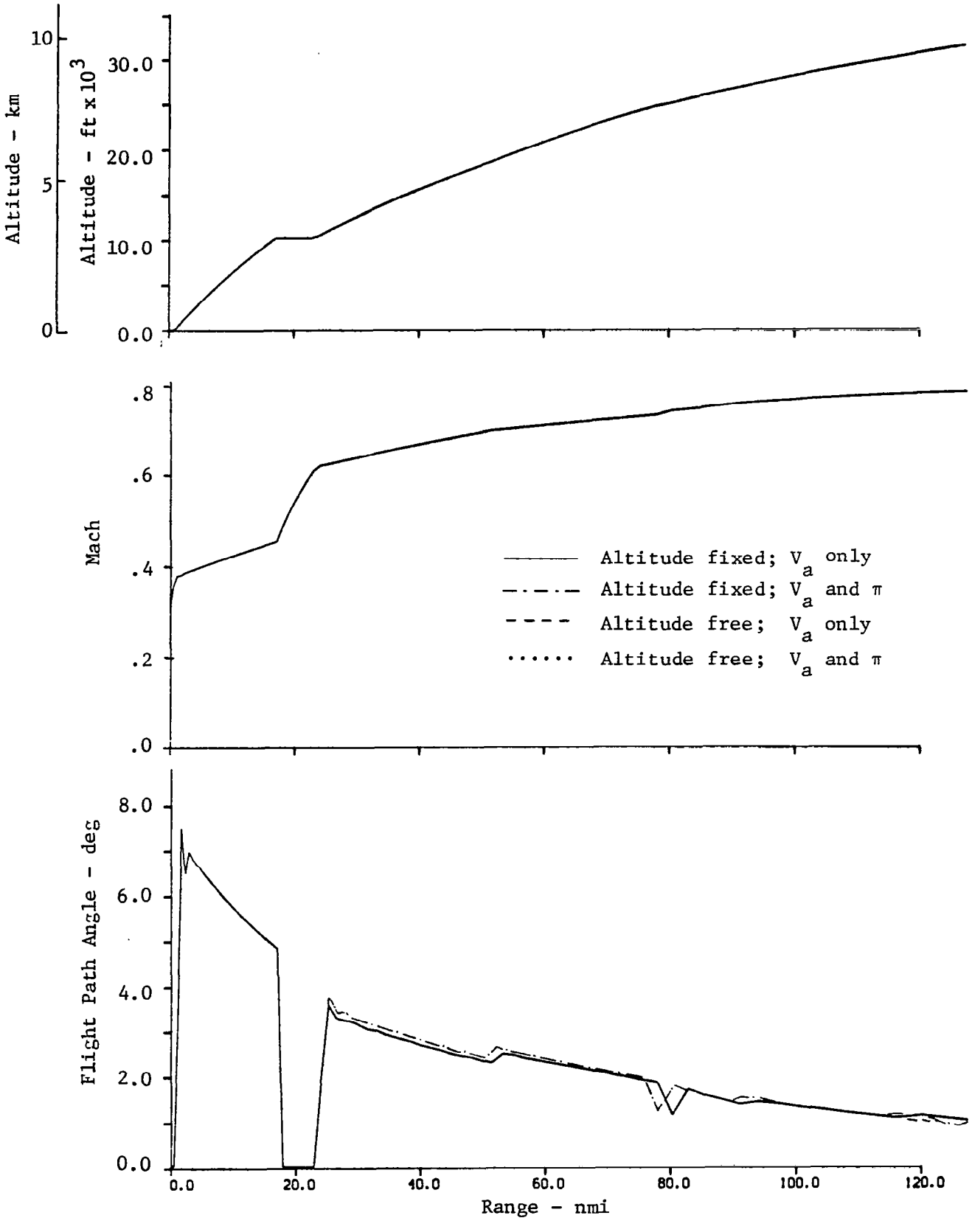

Figure 20a. State Variables for Optimum Climb Profiles of the Tri-Jet Aircraft Traveling 1000 nmi.

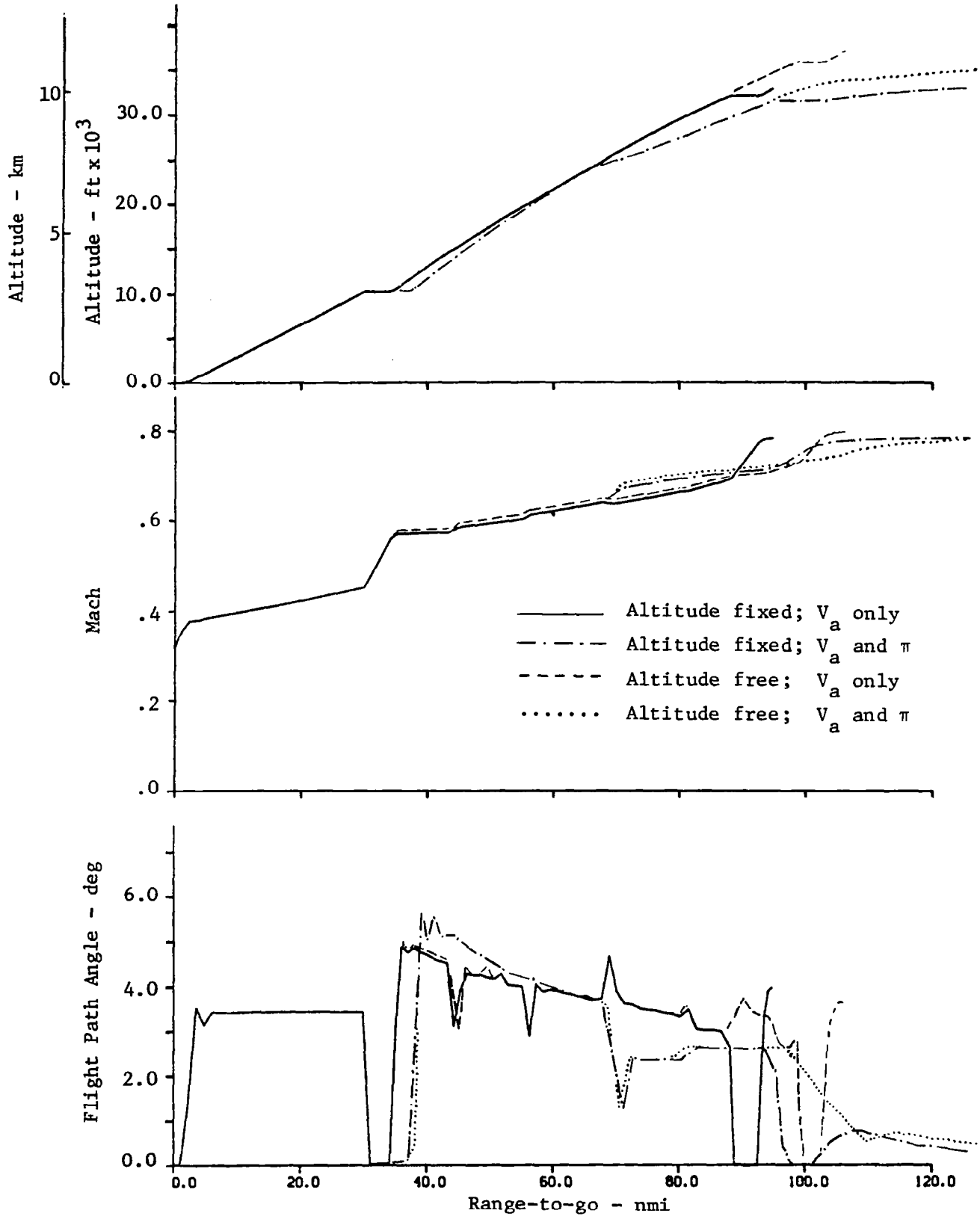

Figure 20b. State Variables for Optimum Descent Profiles of the Tri-Jet Aircraft Traveling 1000 nmi.

Figures 19b compare the descent profiles for the twin-jet aircraft. Mach number has a gradual decrease down to 3 km (10000 ft). More differences are seen in the flight path angle than found in climb.

Figure 19c is added to show altitude vs. true airspeed for the twin-jet over the entire profile (climb-cruise-descent). This is for the case with free cruise altitude, and climb and descent are optimized by varying V_a only. In Fig. 19c, the indicated airspeed and Mach numbers are shown as parameters, so it is apparent that the climb and descent profiles seldom have constant Mach number or indicated airspeed segments above 3 km (10000 ft).

The tri-jet climb profiles are shown in Fig. 20a out to 120 nmi range. It is remarkable that for this aircraft/engine model the four climb profiles are essentially identical over the range shown. Mach number never reaches a point of constant value. Flight path angle is relatively smooth.

The tri-jet descent profiles shown in Fig. 20b show more variations than the climb. As with the twin-jet, the biggest differences are seen in the flight path angle.

Figures 21a-c show the same types of plots for the twin-jet where standard day temperatures are varied $\pm$ 20°C. This is for the case with free cruise altitude, and the climb/descent profiles are optimized with airspeed only. From Fig. 21c it is seen that for the hot day, the aircraft climbs to a higher optimum cruise altitude, but at a slower rate of climb. This is reflected in the flight path angle plot in Fig. 21a. The hot-day aircraft cruises at a higher true airspeed (436 kt vs 401 kt) than the cold-day aircraft. The descent profiles are much closer than the climb profiles as seen in Fig. 21b.

The cold-day flight uses 88.5 kg (195 lb) less fuel than the hot day flight. However, because of the higher cruise speed, the hot day flight arrives about 11 min. earlier. Thus, surprisedly, the hot-day flight is $79.50 less expensive. This would not be the case if time-of-arrival was constrained. More studies are needed on the subject of effects of temperature variations.

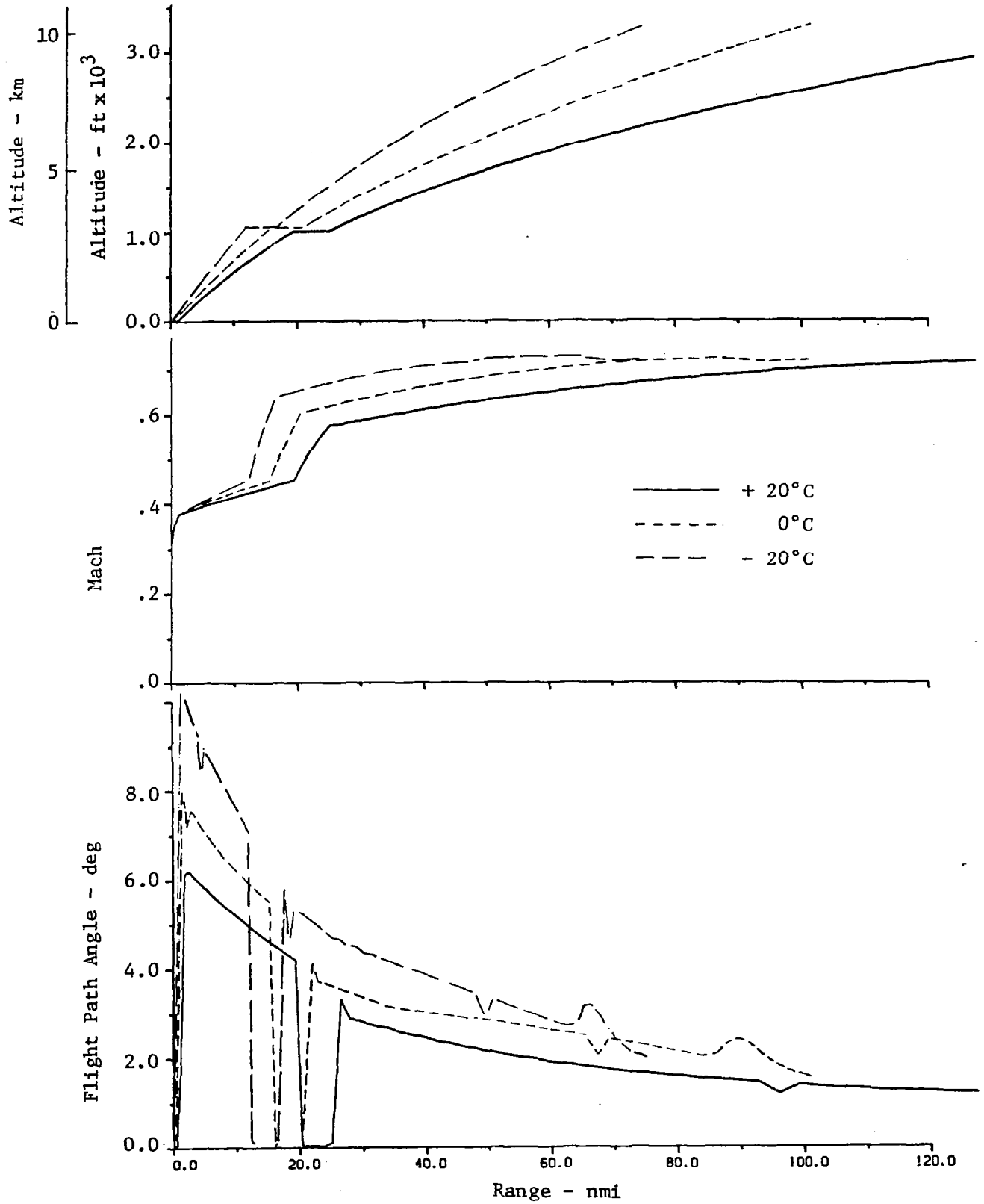

Figure 21a. Optimum Climb Profile for Twin-Jet Showing Effects of Temperature Variation.

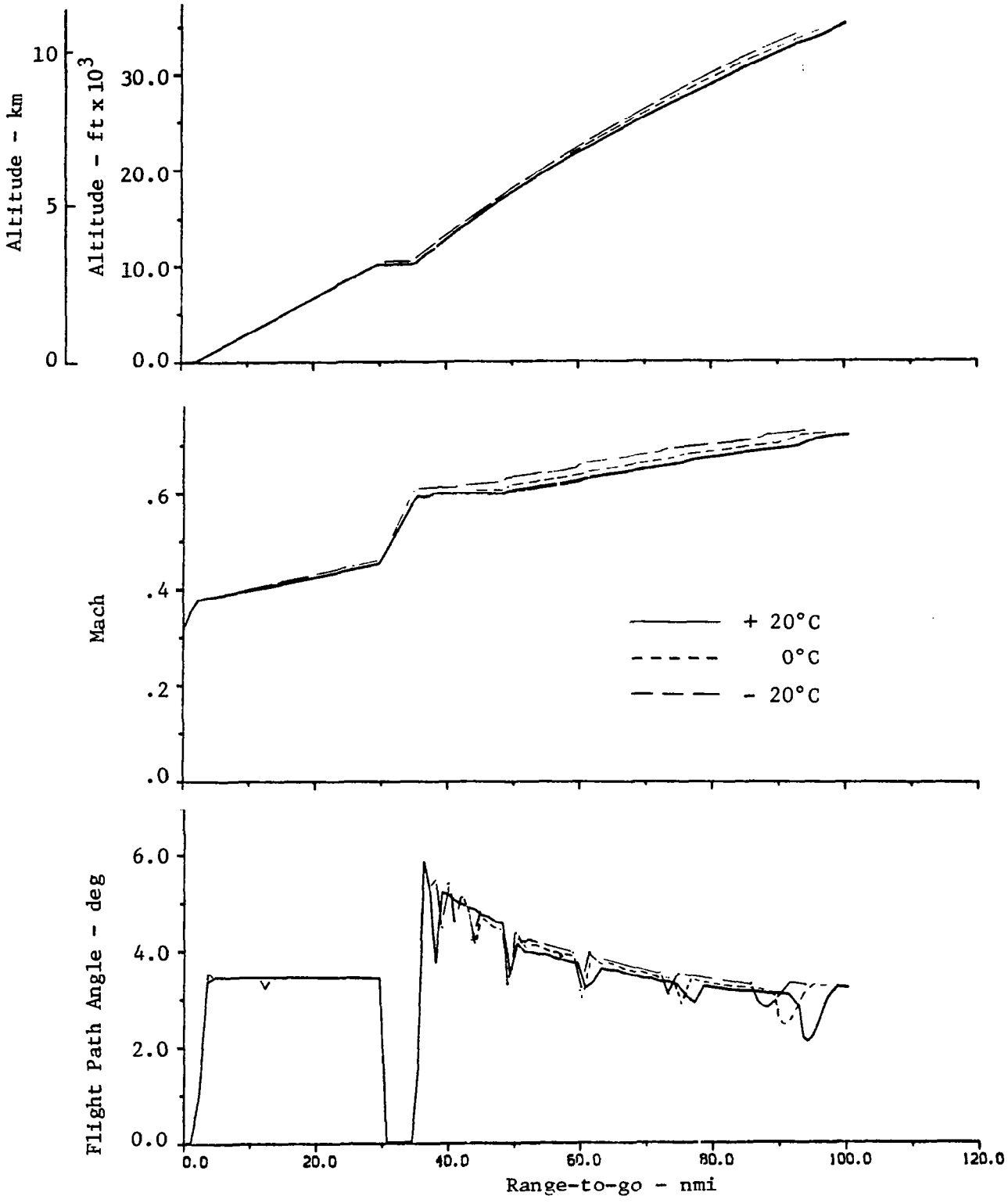

Figure 21b. Optimum Descent Profile for Twin-Jet Showing Effects of Temperature Variation.

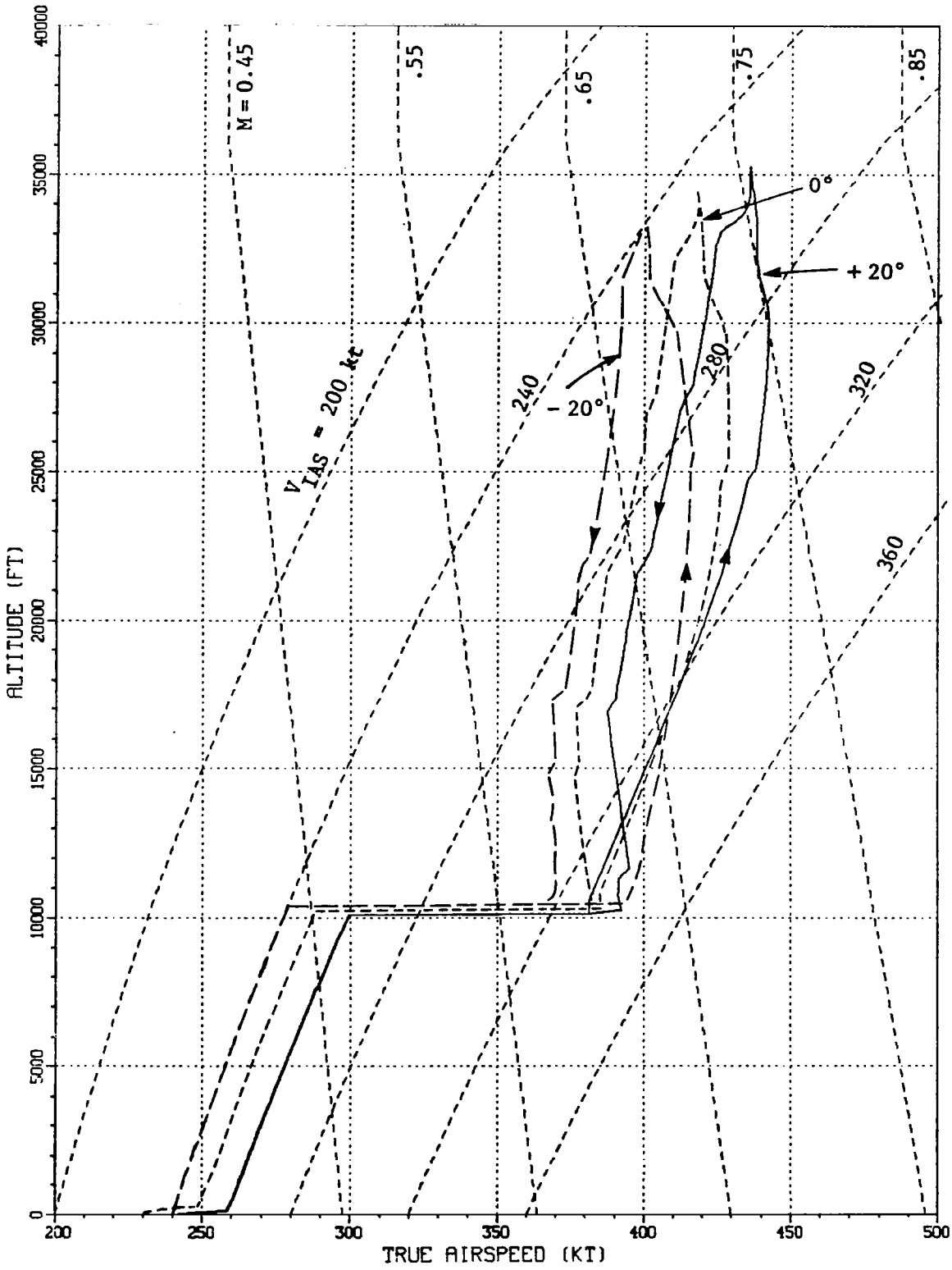

Figure 21c. Altitude vs True Airspeed for Optimum Twin-Jet Profiles as a Function of Temperature Variation.

Figures 22a-c compares minimum cost and minimum fuel profiles for the twin-jet aircraft. The differences are expecially noted in the descent speed vs. range-to-go (Fig. 22b). For these cases, the minimum cost profile, based on cost-of-time of \$600/hr, costs \$56.09 less than the minimum fuel profile. However, the minimum fuel profile uses 119 kg (262 lb) less fuel than the minimum cost profile. As fuel costs continue to climb, the minimum fuel profile becomes more important.

Speed Constraints There was some concern that the OPTIM program might compute climb or descent profiles which exceed the flight path angle or speed constraints of the aircraft. Typically, the lower speed constraint at any altitude is established by the maximum lift point (C_{Lmax}). This is also the point where lift/drag is maximum or where fuel rate is minimum.

The maximum speed is determined partially by the point where thrust equals drag. If the aircraft is climbing or descending, the flight path angle must be accounted for. For equilibrum, the equation

$$L + T \sin \alpha - W \cos \gamma = 0 , \tag{16}$$

must hold. This trim condition can be solved when thrust T is maximum, and the flight path γ is given. The lift coefficient C_L and angle-of-attack α are computed as a function of aircraft mass W and airspeed V_a. The airspeed and lift coefficient are used in turn to compute drag D. Then, for a ligitimate operating point,

$$T \cos \alpha - D - W \sin \gamma \geq 0 . \tag{17}$$

If this does not hold, then the speed V_a is too large. The maximum speed is also determined by buffet constraints.

Figure 23 shows the minimum operating speeds of the twin-jet model as a function of altitude. Aircraft weights of 454 tonne (100000 lb) and 318 tonne (70000 lb) are used as parameters. Speed constraints are shown in terms of Mach number, true airspeed, and indicated airspeed. Mach number is shown for 0° flight path angle (solid lines) and 10° flight path angle (dashed lines).

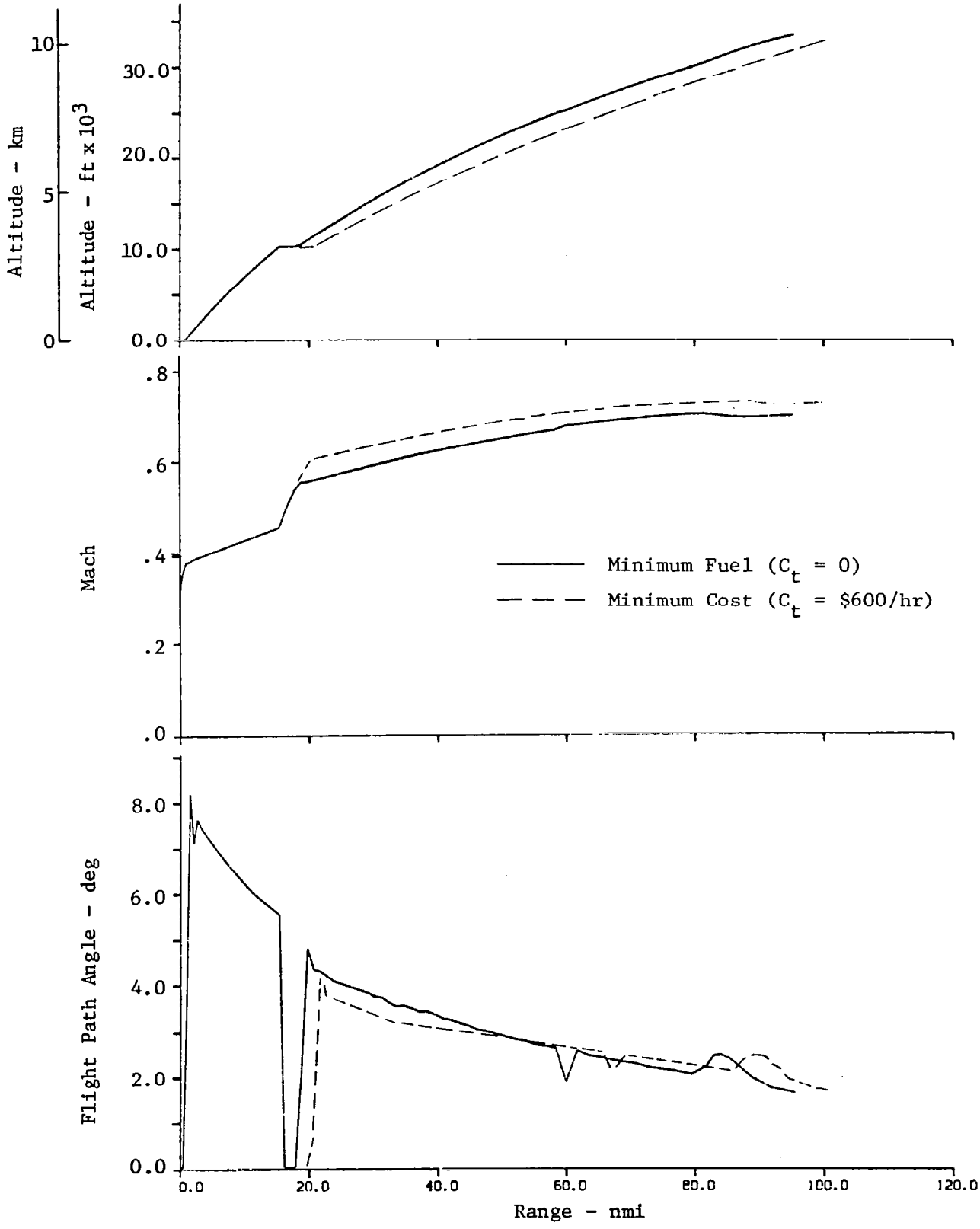

Figure 22a. Comparison of Minimum Fuel and Minimum Cost Climb Profile.

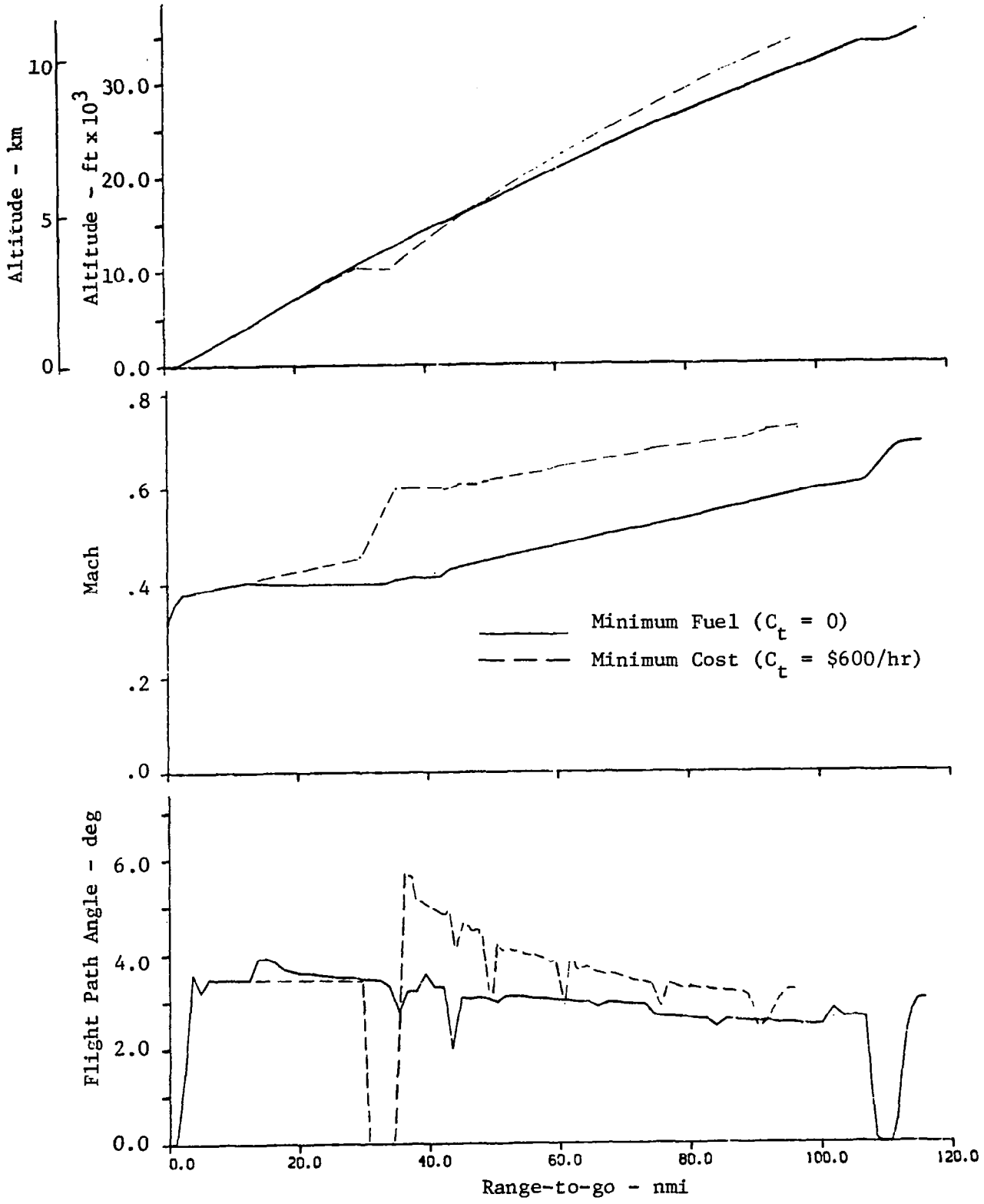

Figure 22b. Comparison of Minimum Fuel and Minimum Cost Descent Profiles.

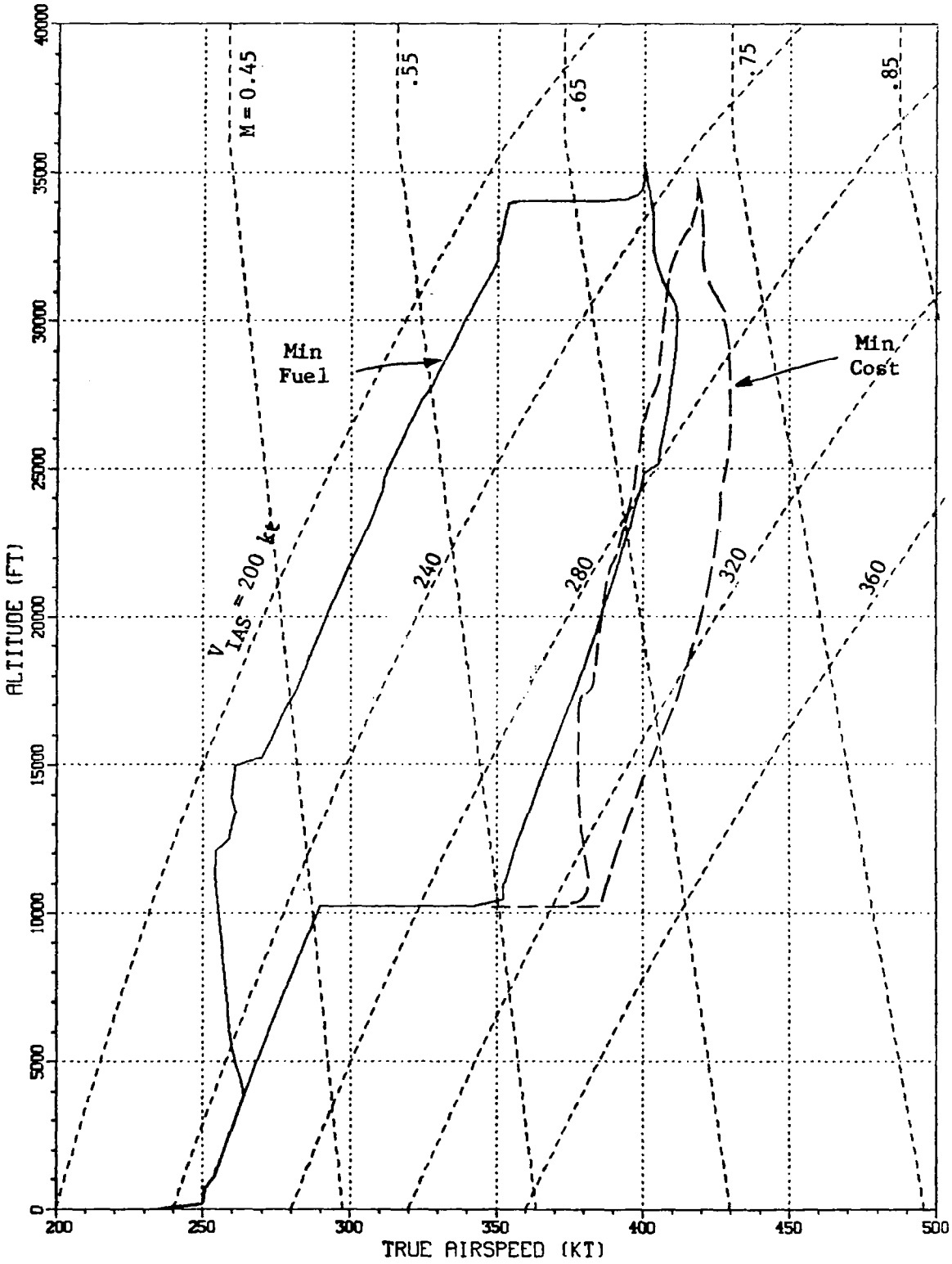

Figure 22c. Altitude vs True Airspeed for Twin-Jet Minimum Fuel and Minimum Cost Profiles.

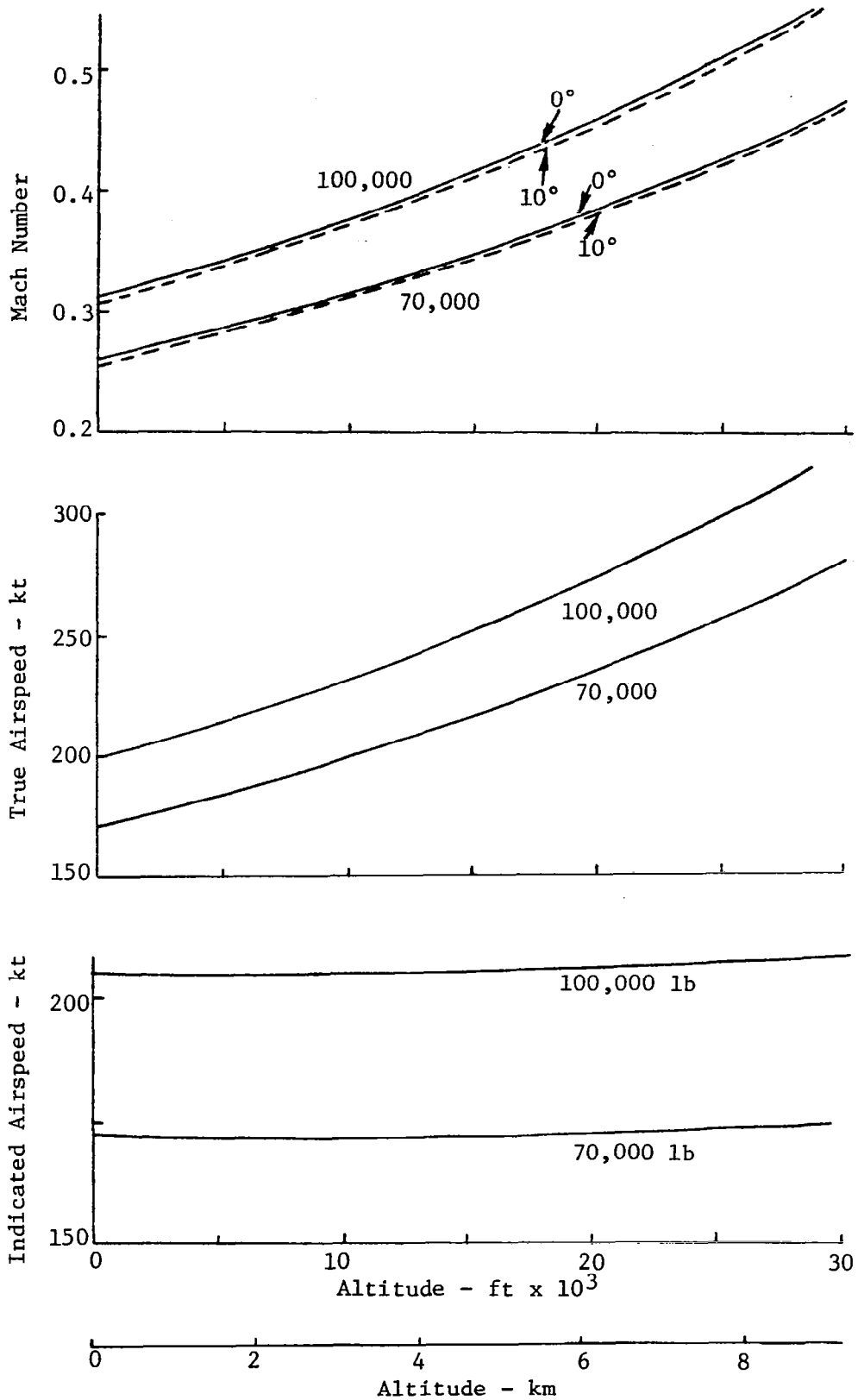

Figure 23. Minimum Speed Constraint V_{min} for Twin-Jet

Figure 24 shows several speed constraints superimposed on an altitude vs true airspeed plot. The minimum speed constraint V_{min} for a 38.6 tonne (85000 lb) aircraft is set by the C_{Lmax} constraint, and is indicated by the double line to the left of the plot. The double line boundary to the right and above sets V_{max} because of buffet constraints. The dot-dash parametric lines show maximum speed constraints for flight path angle ranging between 0° - 10°. These parametric lines were derived by solving Eqs. (16)-(17). Also shown in Fig. 24 is a typical profile as computed by OPTIM. Examination of this profile indicates that the flight path angle constraints were not violated at any point in the climb. There is also plenty of margin above the V_{min} boundary. A maximum rate of climb profile would have a flight path angle history that would match the parametric values shown in Fig. 24.

This small study of speed and flight path angle constraints was not exhaustive. However, because there seemed to be ample margin between the generated profiles and the constraint boundaries, it was not pursued further.

Wind Effects In order to examine the effects of winds with different magnitudes and directions, OPTIM was run with the twin-jet model and five different wind conditions. A 1000 nmi range profile was generated using cost-of-time C_t of \$600./hr and cost-of-fuel C_f of \$.15/lb. The cruise altitude was allowed to be free. The wind conditions were:

a) No wind;

b) A head wind varying linearly with altitude from 0 kt at 0 km to 100 kt at 12.192 km (40,000 ft);

c) A cross wind with the same linear variation;

d) A tail wind with the same linear variation; and

e) A variable head wind with linear variation with altitude from 0 to 12.192 km (40,000 ft). Magnitude varies from 0 to 25 kt for climb, 0 to 50 kt for cruise, and 0 to 100 kt for descent.

A comparison of the altitude profiles vs range of these five cases is shown in Fig. 25. A comparison of cruise altitudes, cruise speeds, fuel, time, and cost for the five cases is presented in Table 3. Note that a simple wind variation as modeled here can have a significant effect on the

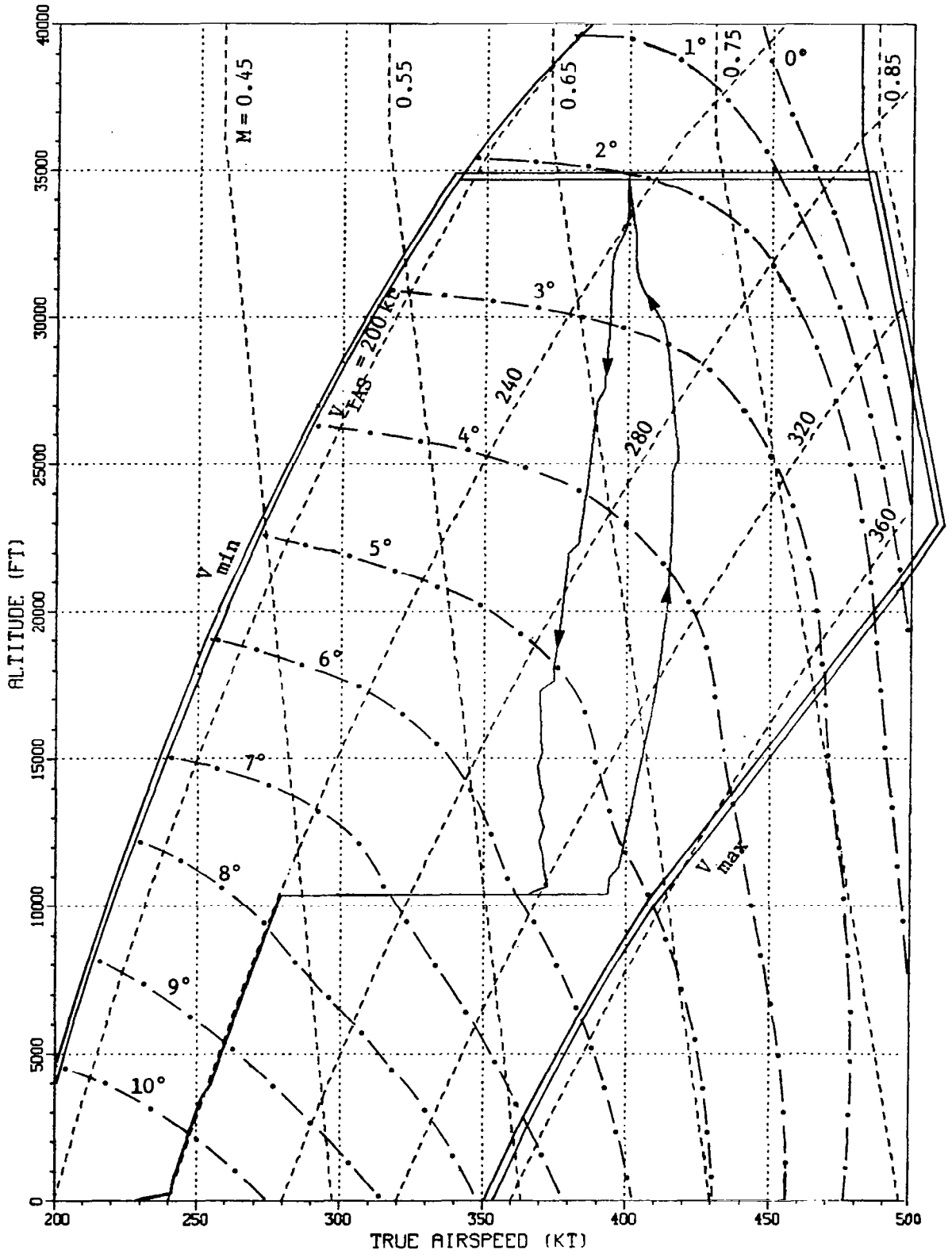

Figure 24. Chart Showing Acceptable Speed/Altitude Operating Region for a 38.6 tonne Twin-Jet Aircraft. Maximum Climb Flight Path Angle Shown as Parameter.

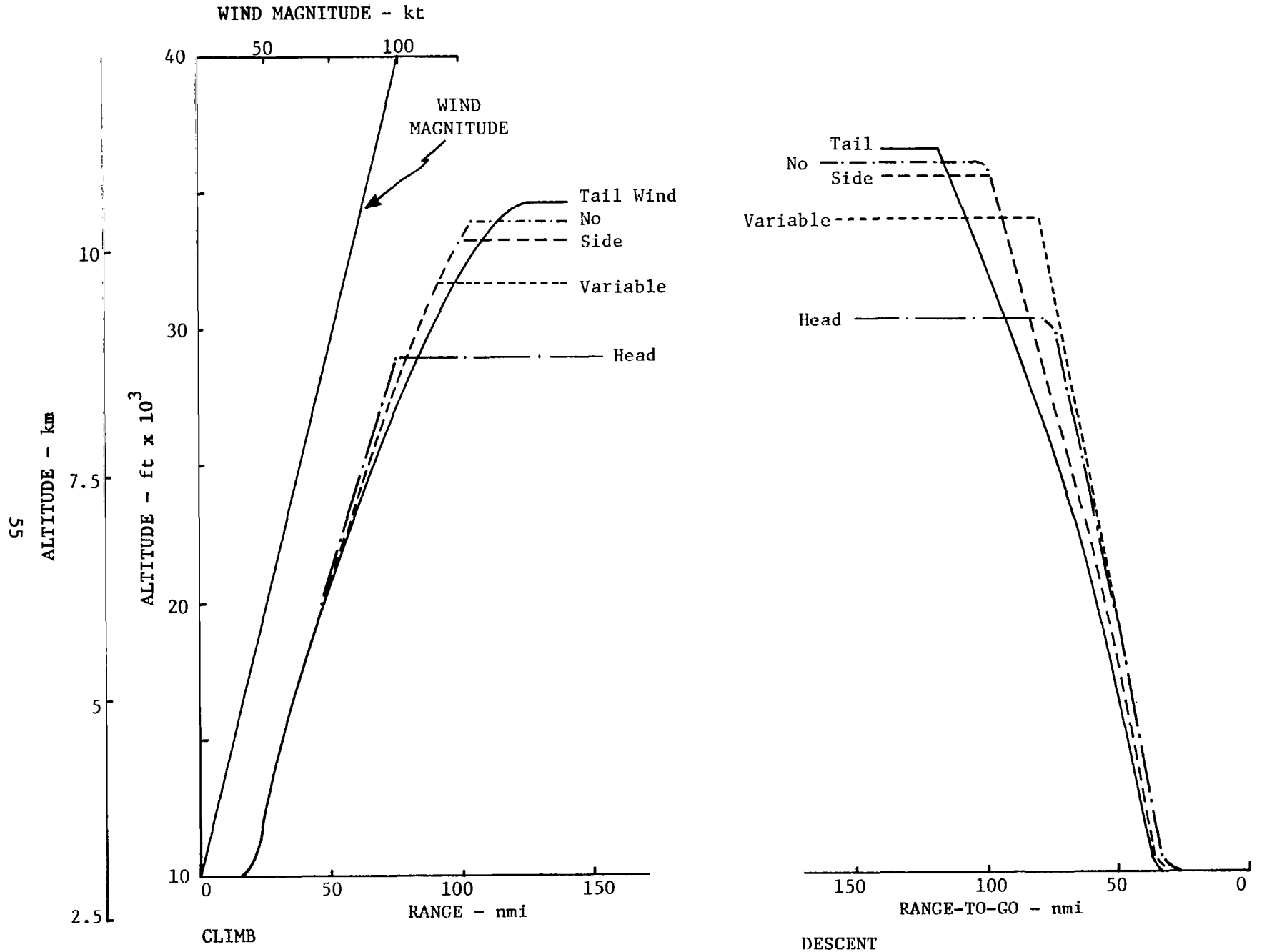

Figure 25. Variable Wind Analysis Comparitive Vertical Profiles.

Table 3. Variable Wind Analysis

Profile Performance Comparison

Type Wind	Cruise Altitudes - km(ft)		Cruise Speeds - kt		Fuel - kg(lb)	Time	Cost ($)***
	Initial	Final	Initial	Final			
No	10.42(34194)	11.01(36117)	420	418	5315.(11707)	2:27:59	3236.
Head*	8.88(29135)	9.57(31406)	433	432	6570.(14472)	2:51:20	3884.
Side*	10.20(33466)	10.84(35575)	422	420	5430.(11961)	2:20:13	3296.
Tail*	10.65(34940)	11.13(36523)	413	411	4512.(9938)	2:07:02	2761.
Variable**	9.76(32033)	10.40(34132)	426	424	5912.(13022)	2:40:24	3557.

* Head, side, and tail winds based on linear variation with altitude from 0 kt at 0 km to 100 kt at 12 km (40000 ft).

** Variable wind is head wind with linear variation to 25 kt, 50 kt, and 100 kt at 12 km (40000 ft) for climb, cruise, and descent, respectively.

*** Cost based on $.33/kg ($.15/lb) and $600/hr for twin-jet.

cruise altitude (more than 1.5 km) and cost of flight (45% variation in fuel consumed). Also as seen in Fig. 25, the range traveled to top of climb and the range-to-go to top of descent vary significantly. Predicting the optimum top-of-descent point is especially important for minimum fuel descents, and this indicates the importance of having a reasonably correct wind profile model to use in a flight management system.

Multi-segment Cruise The OPTIM-S version of the program is capable of generating an optimum profile along a path with multiple cruise segments. This version of the program can follow up to 20 consecutive segments, each with different bearings. Each segment can have a fixed or variable altitude. Also, the wind and temperature profiles can be specified at up to 20 different entry points along the route. The simulated weather at any point is then found by linear interpolation between entry points. Step climb is generated right after a waypoint by specifying a different altitude for the next waypoint.

OPTIM-S was exercised over typical multi-segment paths provided by a major airline. The route structure studied consisted of eleven different horizontal paths used to connect Chicago and Phoenix. These eleven paths were specified by 33 different waypoints (VOR stations). The wind and temperature profile forecasts were given for each waypoint for a particular flight time period.

The eleven different paths represent possibilities that the airline used to choose the desired path for that flight day. The aircraft was a B-727-200. Figure 26 shows four of the eleven routes - the ATC preferred route (shortest distance), the flight planning preferred route (shortest "wind" distance for that day), and the northern and southern routes. These routes vary from five to eight segments in length.

OPTIM-S was used to generate optimum profiles along the two preferred routes shown in Fig. 26. The tri-jet aircraft model was used with takeoff weight set at 704 tonne (155000 lb). The results of five variations in these

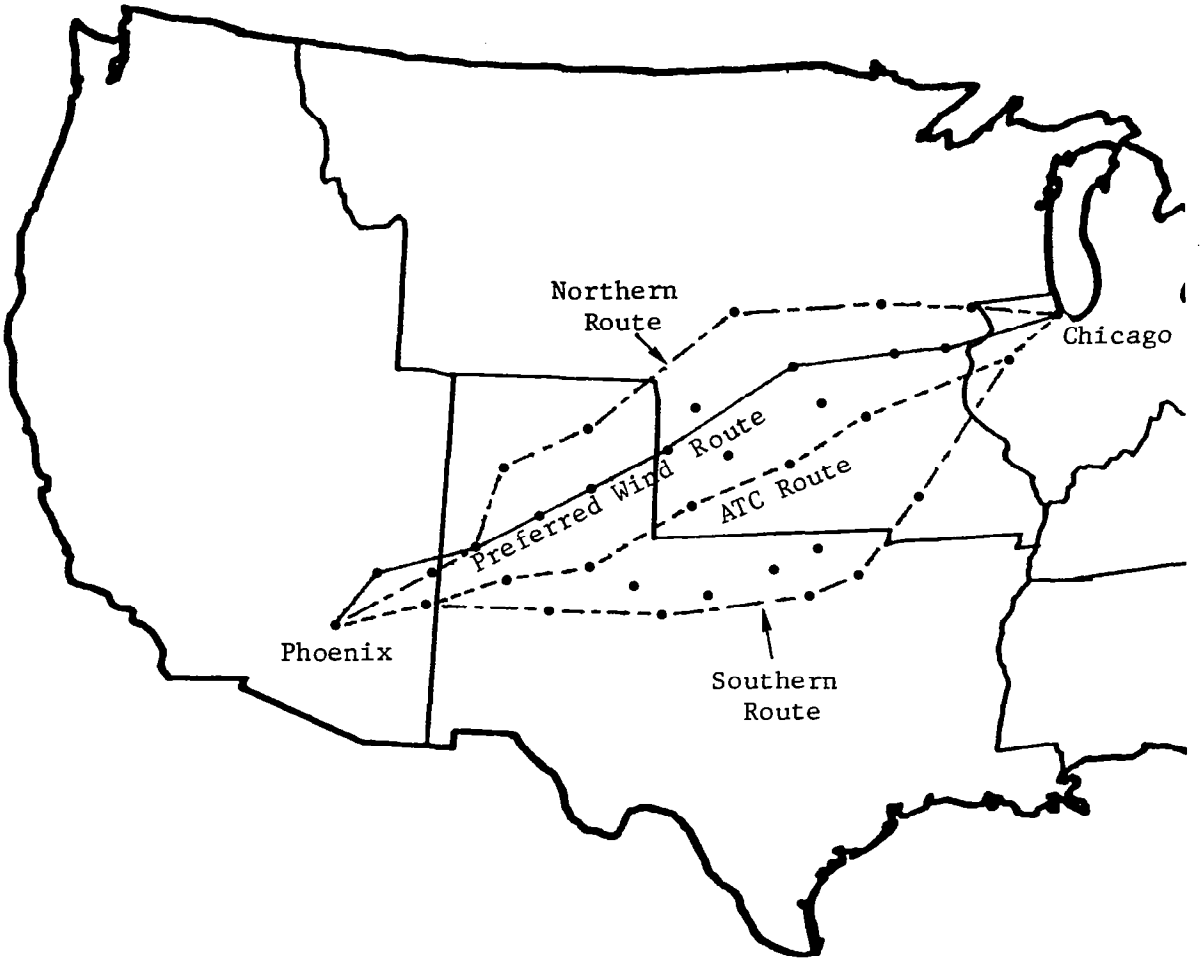

Figure 26. Typical Chicago - Phoenix Flight Plan Route Structure with Alternate Waypoints.

runs are shown in Table 4. No effort is made to compare these results with the airline flight plan because of model differences.

The shortest wind route was simulated at three different cruise altitude conditions - fixed at 35000 ft, free, and step climb from 27000 to 31000 ft midway through the flight. The actual route flown was the one fixed at 35000 ft. Free cruise altitude turned out to be a low 24000 ft because of a strong head wind. The step climb and fixed cruise cases cost about the same amount. The free cruise case saves $147.55 although more fuel is spent.

Table 4. Comparison of Time and Fuel for Variations of a Chicago - Phoenix Flight Plan with a Tri-jet Aircraft (Time: $600./hr; Fuel: $.15/lb).

Route Detail	Time	Fuel kg (lb)	Cost
Shortest wind route - cruise altitude fixed at 35000 ft; 1272 nmi range.	3:42:25	13030. (28696)	$6528.65
Shortest wind route - cruise altutude free (~ 24000 ft)	3:16:41	13365 (29438)	$6381.10
Shortest wind route - step climb from 27000 ft to 31000 ft	3:29:48	13412 (29541)	$6529.25
ATC route (shortest ground distance) - cruise altitude fixed at 35000 ft;1263 nmi range.	3:46:04	13211 (29100)	$6625.75
ATC route - cruise altitude free	3:15:01	13227 (29134)	$6320.37

The shortest ground distance route (preferred ATC route - 9 nmi shorter) was simulated at two cruise altitude conditions - fixed at 35000 ft and free (again at 24000 ft). The fixed altitude case cost $97.10 more than the corresponding shortest wind route case. However, the free altitude case cost $60.73 and $208.28 less than the corresponding shortest wind route, free and fixed altitude cases, respectively. This illustrates the potential utility of this program in determining flight paths that save direct operating costs. Note however, these numerical values are based on a hypothetical (tri-jet) aircraft model.

Step Climb As discussed previously and illustrated in Fig. 12, OPTIM has the option to compute the optimim range R_c where to begin the step climb from one flight level FL_A to another flight level FL_B. This option was exercised with both the twin-jet and tri-jet models flying 1000 nmi range profiles. Flight level FL_A was set at 10.06 km (33000 ft), and flight level FL_B was 11.28 km (37000 ft).

Figure 27 and 28 present the variations in direct operating cost and fuel carried by varying the R_c point. Here, R_c is defined as the range from the top-of-climb to begin the step climb. Figure 27 is for the twin jet model, and the cost and fuel resulting from staying at FL_A are also shown. From Fig. 27, it can be seen that the optimum point to climb to FL_B to save cost is at about 500 nmi. However, this climb cost about $2 more than remaining at FL_A. To minimize fuel, Fig. 27 indicates that the climb should begin at 450 nmi into cruise, and the potential savings is 8 kg (18 lb) when compared to remaining at Fl_A. These results are with no wind.

Figure 28a and b show similar results for the tri-jet model. Note that here the cost and fuel required to remain at FL_A are off the plot scales. Using the step climb at an R_c of 400 nmi saves about $17.25. Using the step climb at 175 nmi saves about 34 kg (75 lb) of fuel.

For this particular example flight condition, the step climb savings for the tri jet are significantly more than for the twin jet. A great deal more can be learned by study of a variety of flight levels, aircraft takeoff weights, wind variations, and profile ranges.

Pressurization Constraint Comparisons were made using the tri-jet and twin-jet aircraft models with and without the pressurization constraints described earlier. With the constraints, the aircraft was restricted to descend from cruise altitude down to 8.53 km (28000 ft) at a descent rate of 152 m/min (500 ft/min). During this period the Mach number varied linearly between the optimum value at cruise altitude and that value if cruise were restricted to 8.53 km.

Figure 29 compares the constrained and unconstrained altitude vs range-to-go profiles for the tri-jet aircraft where cruise was at 10 km (33000 ft). These are minimum fuel cases. The constrained profile starts descent approximately 60 nmi earlier, and it uses 9.5 kg (21 lb) more fuel.

Figure 30 compares the altitude/range-to-go profiles for the twin-jet aircraft where cruise was either constrained at 10 km or free. If the free cruise altitude/free descent case is used as the nominal, then the increased amounts of fuel required for the other three cases are as follows:

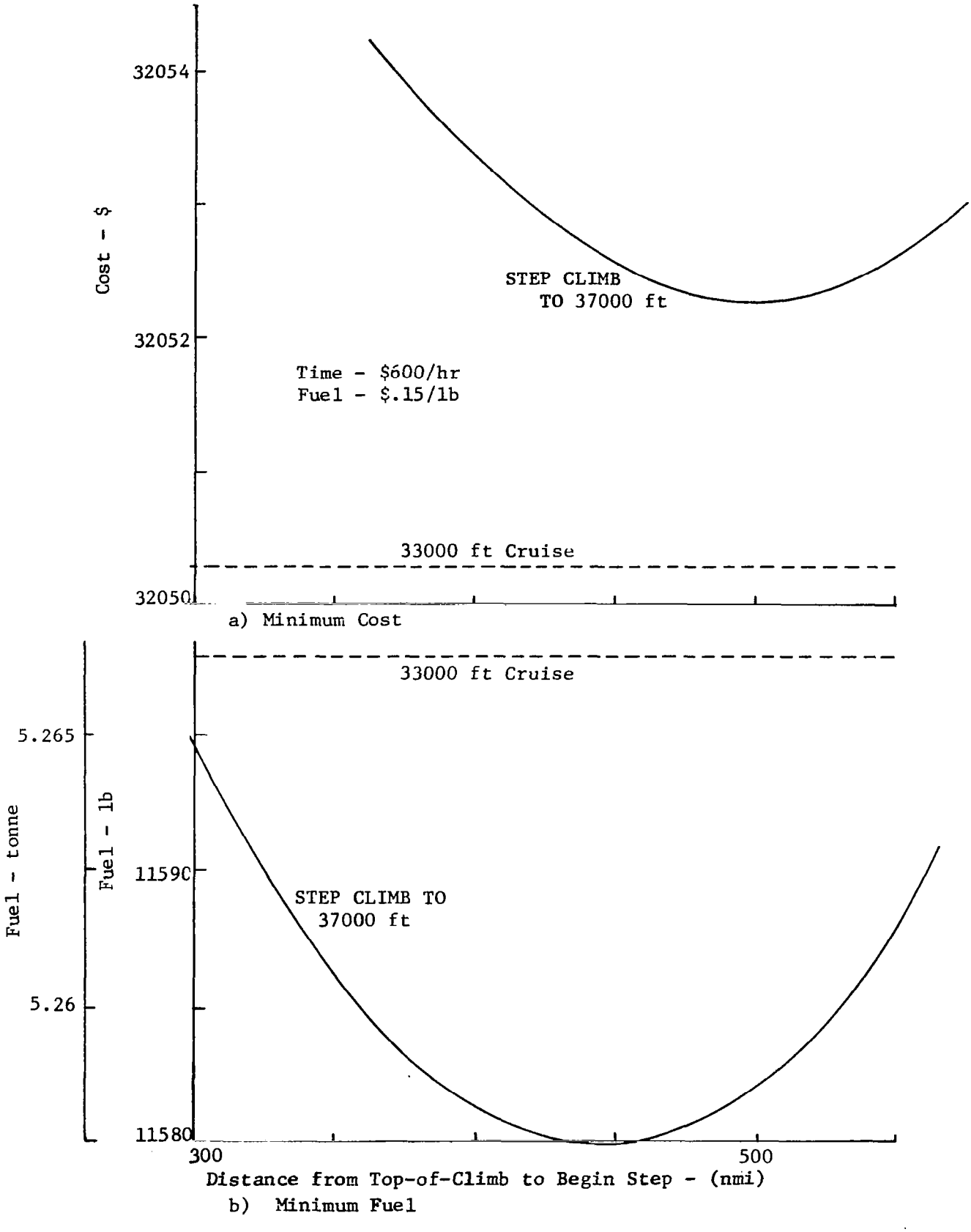

Figure 27. Comparison of Minimum Cost and Fuel for Step Climb and Constant Cruise Altitude Cases of Twin-Jet Over 1000 nmi Range.

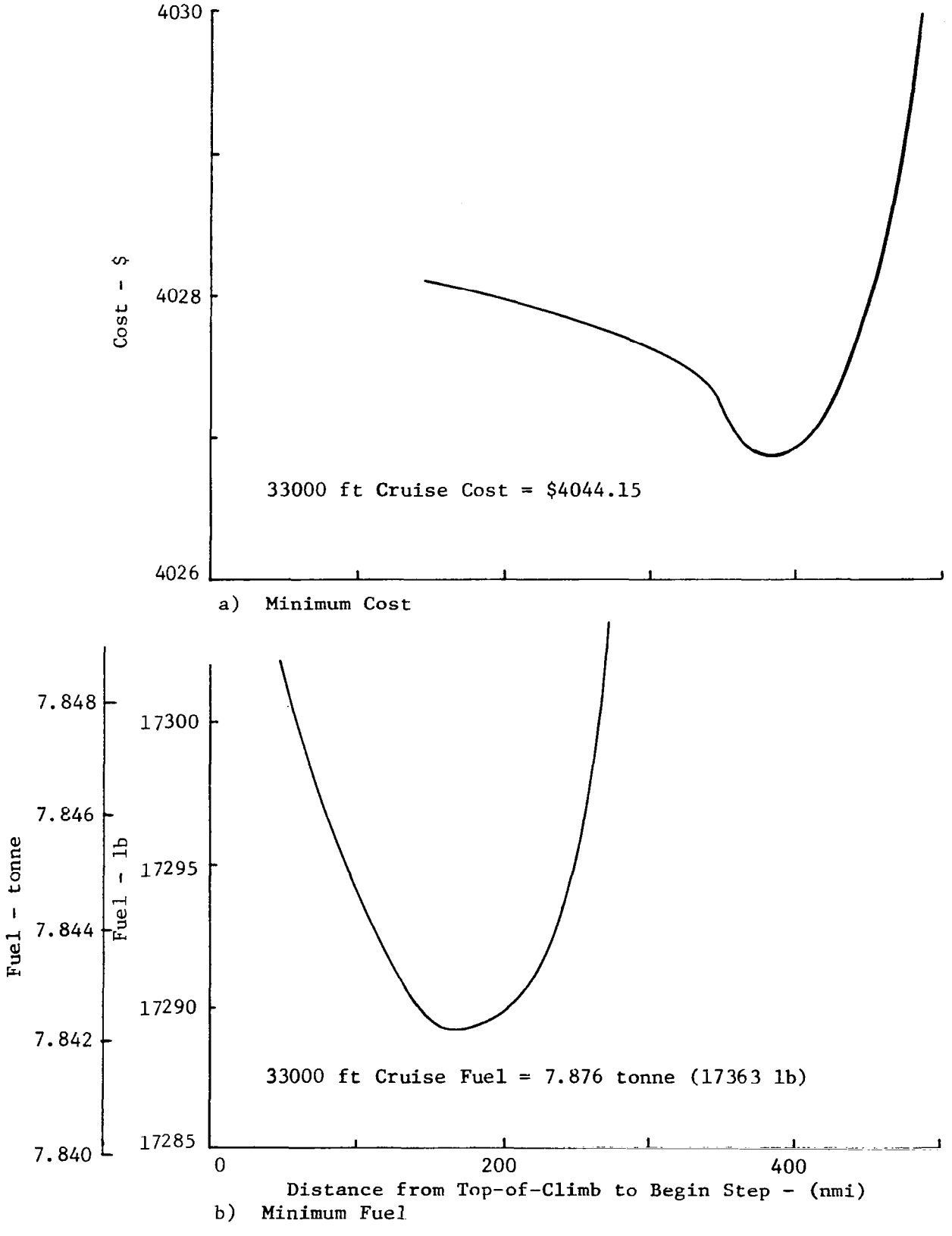

Figure 28. Minimum Cost and Fuel as Function of Range to Begin Step Climb. Tri-Jet Traveling 1000 nmi.

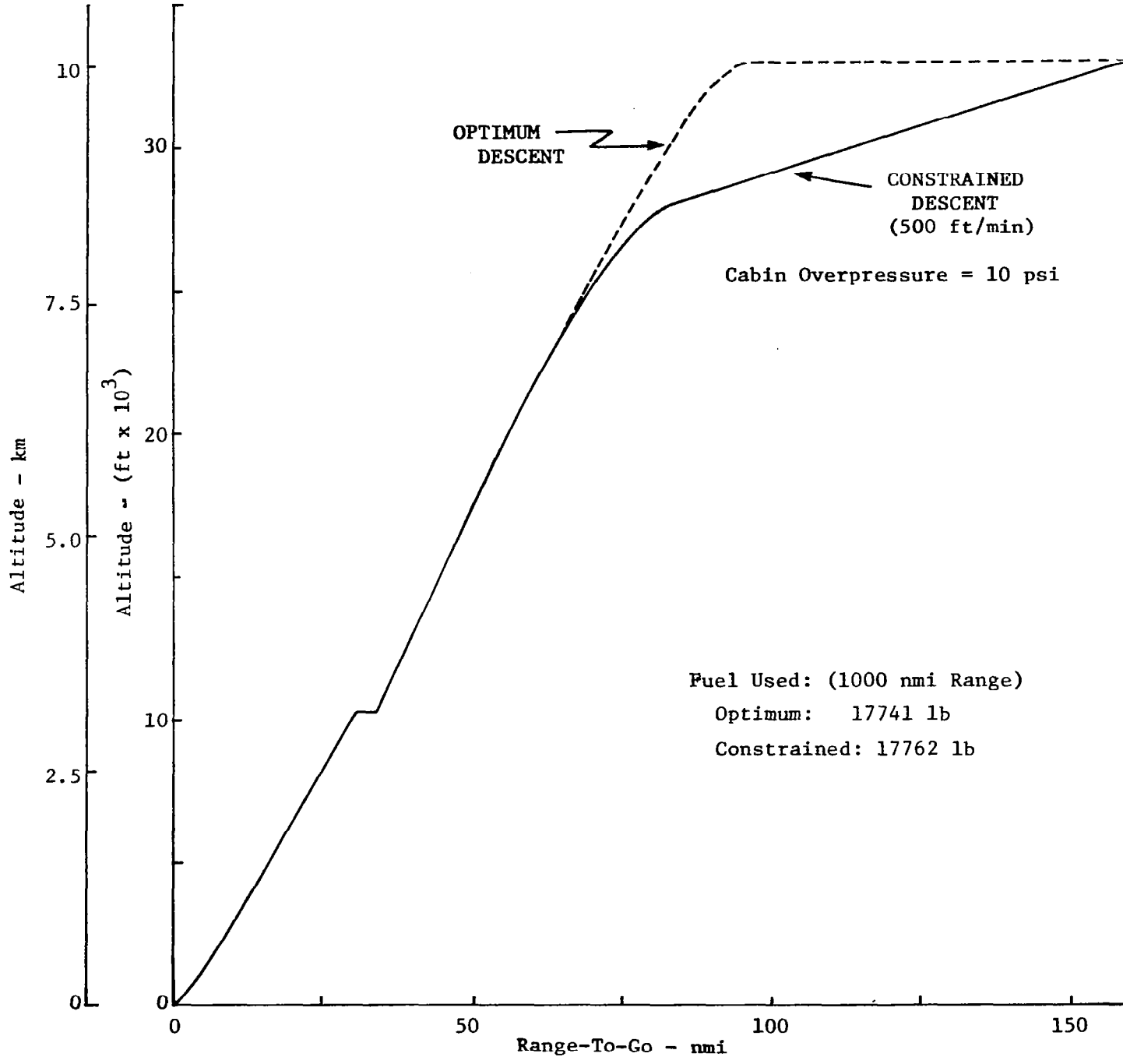

Figure 29. Comparison of Optimum and Constrained Descent Profiles. (Tri-Jet Model)

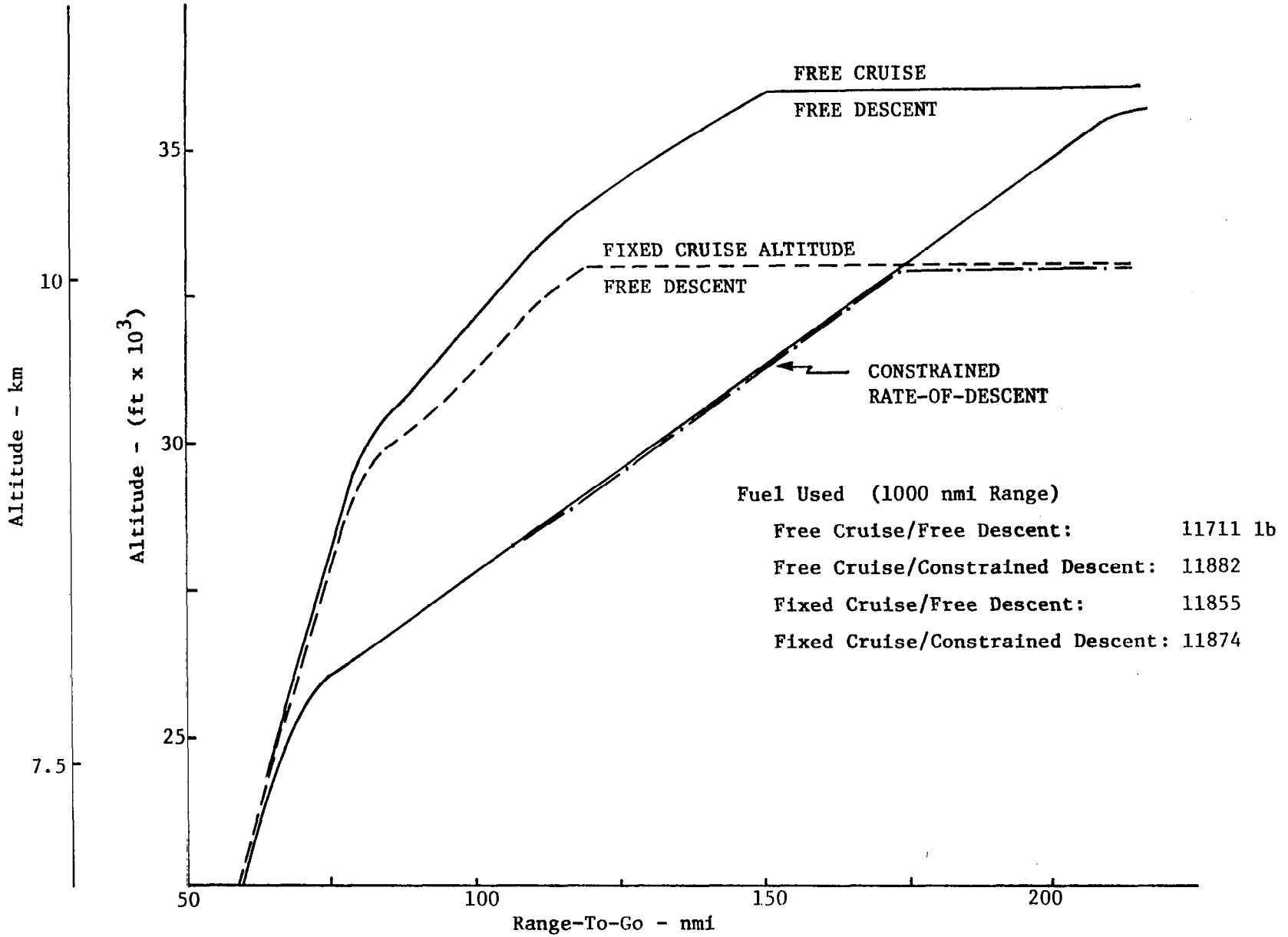

Figure 30. Comparison of Optimum and Constrained Descent Profiles (Twin-Jet)

Fixed cruise/free descent	:	64.9 kg. (143 lb)
Fixed cruise/constrained descent	:	73.9 kg. (163 lb)
Free cruise/constrained descent	:	77.6 kg. (171 lb)

This can be seen to represent a significant cost penalty. It is surprising that constraining the top of the descent profile to a sink rate of 152 m/min is more costly than constraining the cruise altitude to 10 km.

As stated before, the cabin pressurization mechanizations for different models of aircraft vary. Thus, the associated restrictions on the optimum descent profiles will also vary. The user should be careful to ensure that appropriate constraints are selected.

Benefit of Constraining Time-of-Arrival To understand the reasons why fixed time-of-arrival flight path control would be beneficial, we restate three assumptions made in Reference 2 concerning the future scenario of commercial aviation:

1. Because of the increasing cost and scarcity of jet fuel, aircraft will soon be nominally flying along near-minimum fuel vertical flight paths.

2. Because of increasing demand for air travel, increasing congestion and delays of variable length will be occuring at the major terminal areas.

3. Because of increasing capabilities being developed and implemented in communication and computer technology, the ATC system will be able to anticipate terminal area delay times. The controller will be able to inform the pilot early in the flight what the expected delay will be, and he will be able to assign the pilot an open time slot (time-of-arrival) at the terminal feeder fix or outer marker.

If these assumptions hold, the pilot will have a choice of two strategies (or options) to follow to take a fixed delay into account:

1. Continue to fly his nominal minimum fuel path and then enter a "minimum fuel flow" holding pattern to absorb the delay at the end of the cruise segment, or

2. Regulate his flight path by slowing down so that he arrives at the terminal area within an acceptable tolerance of the assigned time-of-arrival.

The algorithm developed for OPTIM generates the optimum vertical flight path between a city pair which minimizes fuel and meets the delayed time-of-arrival constraint (Option 2 strategy above). The fuel reduction of using the Option 2 strategy has been computed and presented for the tri-jet in Ref. 2 and the twin-jet in Ref. 8, when the climb segment was included. The savings are now computed for the twin-jet when the delay is introduced during cruise. That is, the climb segment is normal and cruise is underway, when the pilot is informed of a landing delay. These are two-part profiles; the pilot is informed of the delay at three example points during cruise.

The method used to generate a profile that follows the strategy of Option 1 can be described with the sketch shown in Fig. 31. It is assumed that the profile follows the segments between the sequence of points shown in Fig. 31. The segments followed are:

1-2: Maintain a minimum fuel cruise segment to the point where descent would normally begin.

3-4: Continue at cruise altitude and airspeed until the range where the minimum fuel flow airspeed is obtained during the nominal descent.

3-4: Decelerate to the minimum fuel flow airspeed while maintaining cruise altitude. This begins the holding pattern.

4-5: Remain in the holding pattern at cruise altitude and minimum fuel flow airspeed to absorb the fixed delay time period.

5-6: Continue with minimum fuel descent.

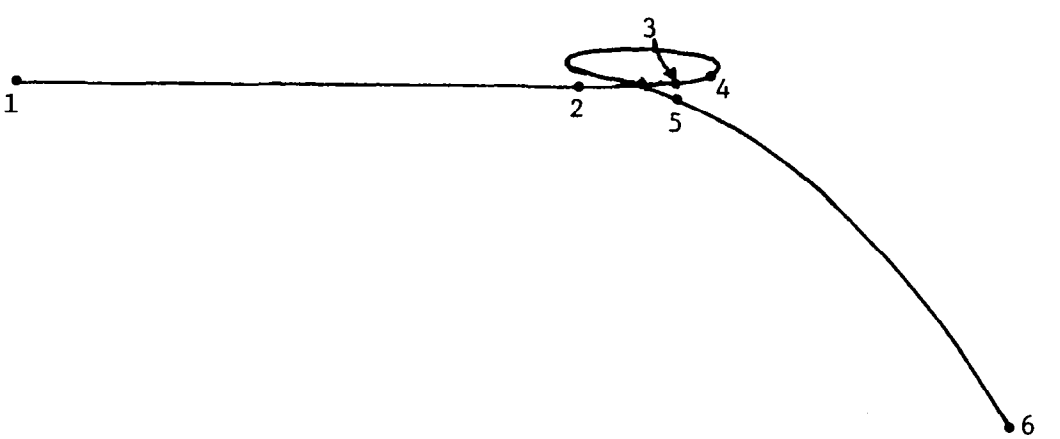

Figure 31. Sketch of Profile with Holding Pattern (Option 1).

The fuel burned during each of these segments can be obtained from the OPTIM program normal printout. This profile is optimistic in that it assumes that the aircraft enters and leaves the holding pattern (at cruise altitude and minimum fuel flow) with no discontinuity from the optimum descent profile.

Figures 32 and 33 show the amount and percent of fuel saved using Option 2 instead of Option 1. The independent variable is the arrival time delays for the medium range twin-jet aircraft with mass of 40821 kg (90,000 lb) at the beginning cruise point. The range traveled is the other variable parameter in these plots. For a 50 min delay, about 25 kg (1380 lb) of fuel can be potentially saved when range-to-go is 1500 nmi. Approximately 150 kg (330 lb) of fuel can be saved for an anticipated 5 minute delay, independent of range.

Figure 33 shows the percentage of fuel saved for the cases shown in Fig 32. Up to 11% of the fuel used by Option 1 can be saved with this controlled time-of-arrival capability. The values shown in Fig. 33 are computed by dividing the reduced fuel amount by that used for controlled time-of-arrival (Option 2).

The results just presented are conservative in the sense that the holding patterns assumed to obtain the Option 1 results are ideal. Usually, holding patterns are made at lower than cruise altitudes. Thus, further study is necessary to model a more accurate representation of the holding pattern. However, the potential savings are clearly indicated.

Related Issues

As OPTIM is now configured, it has the essential features and options which allow it to be used for generation and evaluation of several different types of near-optimum vertical profiles. There are many related issues which must be addressed when considering to use the OPTIM algorithms for either a flight planning tool or as the basis for an on-board flight management system. Two of these issues are discussed here.

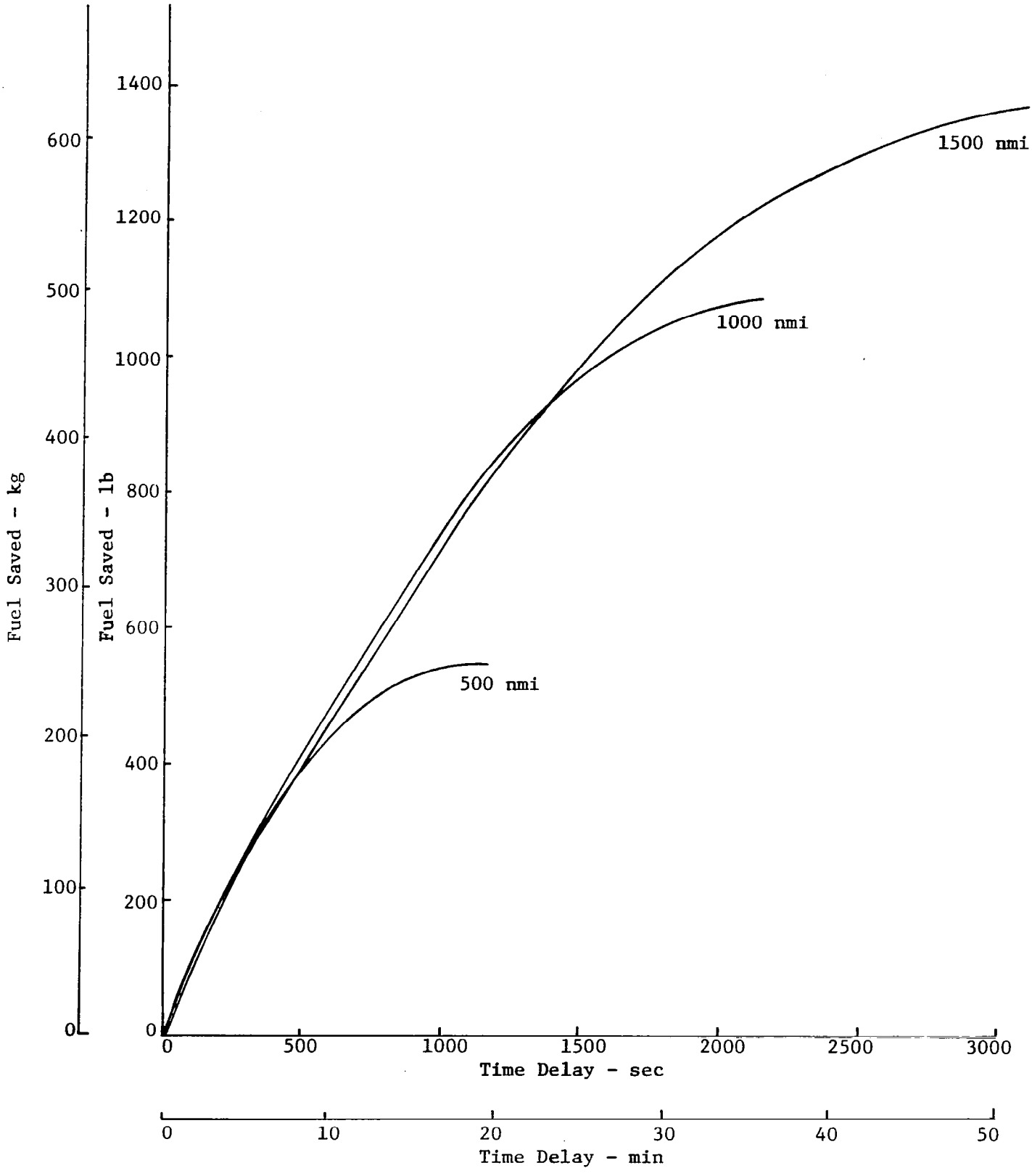

Figure 32. Fuel Saved Using Time-of-Arrival Option as Function of Time Delay and Range. (Two-Part Profile; Twin Jet Aircraft)

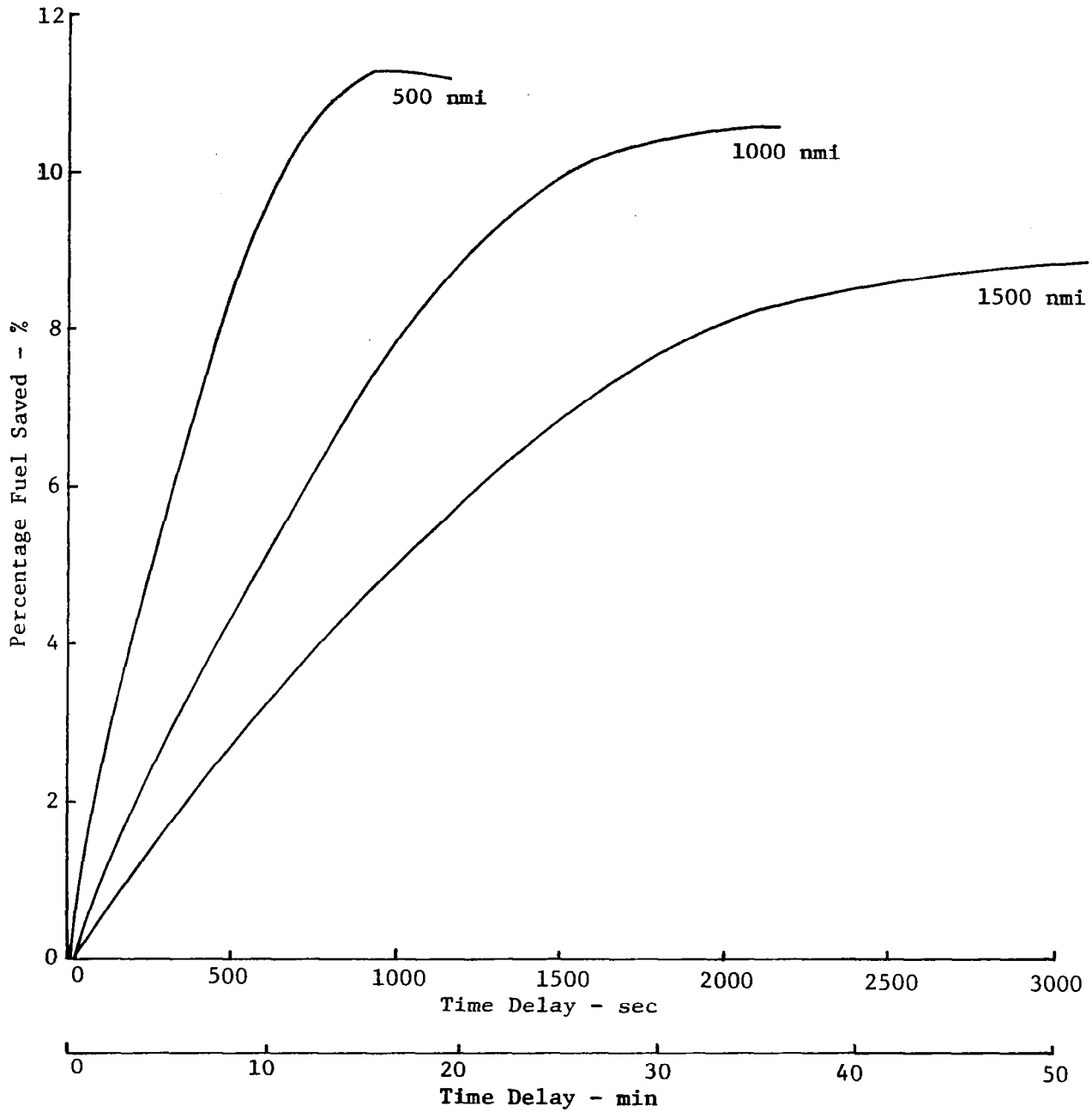

Figure 33. Percentage Fuel Saved Using Time-of-Arrival Option as Function of Time Delay and Range (Two-Part Profile; Twin-Jet Aircraft)

The models used in OPTIM for twin-jet and tri-jet aircraft aerodynamics and propulsion are based on design and test stand data. The actual aerodynamic drag and thrust per unit of fuel burned will depend on specific aircraft-dependent factors such as surface roughness and installation losses. Ideally, the OPTIM aerodynamic and propulsion models could be calibrated from flight data so that the program produces results which match particular aircraft. The process for making these calibrations and then including them in the OPTIM models remains to be developed. The first section that follows presents a brief study of the potential effects of engine losses on cruise performance.

The second issue discussed here concerns the factors which describe the take-off phase of flight. This stage consists of the period from brake release through gear and flap retraction. The end of the take-off phase establishes the boundary conditions (altitude, airspeed, initial weight) to begin the climb phase. An auxilliary program was developed to simulate take-off and to conduct a parametric study of the take-off phase. This program complements OPTIM, as does TRAGEN, and could eventually be an integral part of the TRAGEN program. The output of the take-off program can be used as input to begin the climb phase in OPTIM.

The final portion of the descent phase (terminal approach and landing) also needs to be examined to determine total fuel consumption for the entire flight. The point of ending the descent phase can be anywhere from top of descent to initial flap deployment with the current OPTIM program. However, there are many factors which affect the final descent including interaction with other aircraft and ATC, noise abatement constraints, and runway bearing. Thus, the initial phase of descent included in the OPTIM generated profile should be considered as ending at some terminal area waypoint. Fuel optimization for the terminal approach phase remains as a related research topic.

Powerplant Losses Provision is made in the twin-jet turbofan engine for bleeding air at four different locations. Three of them are shown in Fig. 34 - the eighth stage air, the thirteenth stage air (high pressure) and the fan bypass duct. A fourth location is at the low pressure compressor for low pressure air. In addition to bleed air, power is extracted

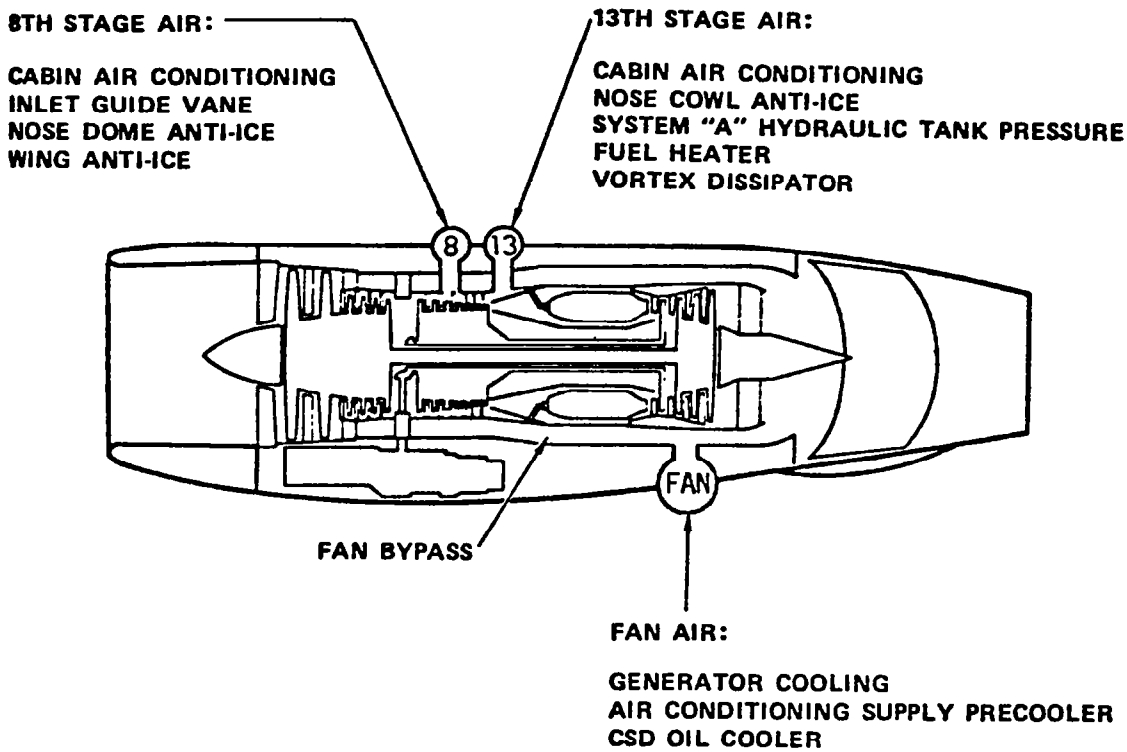

Figure 34. Location of Three Locations Where Engine Air is Bled from the Twin-Jet Model.

through a power shaft from the high pressure turbine. Also, there will be pressure losses in the engine intake system.

All of these effects will penalize the performance of the engine. The purpose of this brief study has been to determine the potential magnitude of these effects and the impact which they may have on the optimization methodology used in the OPTIM program.

The thrust penalties of the engine losses and the resulting effect on fuel flow are given in curve form in the engine Installation Handbook. The correction to thrust and fuel flow due to bleed air take the following form:

$$\Delta T_h/T_{h_i} = C_1 \ (A_{bl}/A_t) \tag{18}$$

$$\Delta \dot{w}/\dot{w}_i = C_2 \ (A_{bl}/A_t) \tag{19}$$

The corrections due to intake pressure losses take a slightly different form:

$$\Delta T_h/T_{h_i} = (1 + C_3)\ \Delta p/p \tag{20}$$

$$\Delta \dot{w}/\dot{w}_i = (1 + C_4)\ \Delta p/p \tag{21}$$

Finally, the corrections due to power extraction are of the form:

$$\Delta T_h/T_{h_i} = C_5\ \delta_{amb}\ \sqrt{\theta_{amb}}\ Hp_{ext}/Hp_{ref} \tag{22}$$

$$\Delta \dot{w}/\dot{w}_i = C_6\ \delta_{amb}\ \sqrt{\theta_{amb}}\ Hp_{ext}/Hp_{ref} \tag{23}$$

To determine the final thrust and fuel flow, one can use the equations:

$$T_h = T_{h_i}\ (1 - \sum \Delta T_h/T_{h_i})\ , \tag{24}$$

$$\dot{w} = \dot{w}_i\ (1 - \sum \Delta \dot{w}/\dot{w}_i)^{*}\ . \tag{25}$$

In Eqs. (18) - (25), the following terms are used:

$C_1 \ldots C_6$	-	coefficients specified in curve form in the Installation Handbook,
A_{bl}/A_t	-	bleed air at a particular location/total engine airflow,
$\Delta p/p$	-	intake pressure loss/total inlet pressure,
δ_{amb}	-	ambient pressure/sea level ambient pressure,
θ_{amb}	-	ambient temperature/sea level standard day ambient temperature,
Hp_{ext}/Hp_{ref}	-	extracted horsepower/reference horsepower,
T_{h_i}	-	net thrust with no penalties,
$\dot{w}_i$	-	fuel flow with no penalties,
T_h	-	net thrust with penalties, and
$\dot{w}$	-	fuel flow with penalties.

* a positive value of $\Delta \dot{w}/\dot{w}_i$ reduces fuel flow.

The curves which give the coefficients for each installation penalty have been tabulated. A subroutine entitled PLOSS has been written which contains these penalty coefficients and which can be called in OPTIM to compute Eqs. (24) and (25). The resulting effect of these engine penalties on the cost function could also be determined in OPTIM.

An example case was run where typical bleed flow ratios and horsepower extraction values were input into OPTIM. The incremental reduction in thrust and fuel flow due to these losses are shown in Table 5. The required increase in EPR and the resulting optimum cruise Mach number at the specified altitude are shown in Fig. 35. It is not known at this point what specific values represent any given aircraft. However, the ratios given for the example are the same as those used in an example given in the twin-jet engine Installation Handbook for a typical cruise point. Note in Table 5 that the incremental fuel flow is positive, indicating a reduction in fuel flow. However, the total fuel flow is increased by a much greater amount due to the higher engine power setting. For the performance with example losses, the cost function is minimized at a Mach number of 0.716.

Table 5. Effect of Engine Losses on Thrust and Fuel Flow

Quantity	Amount	Resulting Effect	
		$\Delta T_h/T_h$	$\Delta\dot{w}/\dot{w}$
Inlet Pressure Loss	$\frac{\Delta p}{p} = .01$	.0159	.01
Low Pressure Bleed	$\frac{A_{bl}}{A_t} = .01$	.0190	.0106
8th Stage Bleed	$\frac{A_{bl}}{A_t} = .02$	.0407	.0199
13th Stage Bleed	$\frac{A_{bl}}{A_t} = .02$	.0466	.0159
Fan Bleed	$\frac{A_{bl}}{A_t} = .02$	.0134	-.0014
Total		.1356	.055

Cruise Altitude = 10.06 km (33000 ft)

Aircraft Mass = 40.8 tonne (90000 lb)

Bleed Air Ratios
- Low Pressure = .01
- High Pressure = .02
- 8th Stage = .02
- Fan = .02

Horsepower - 60 hp
Extraction
Inlet Pressure Loss = .01

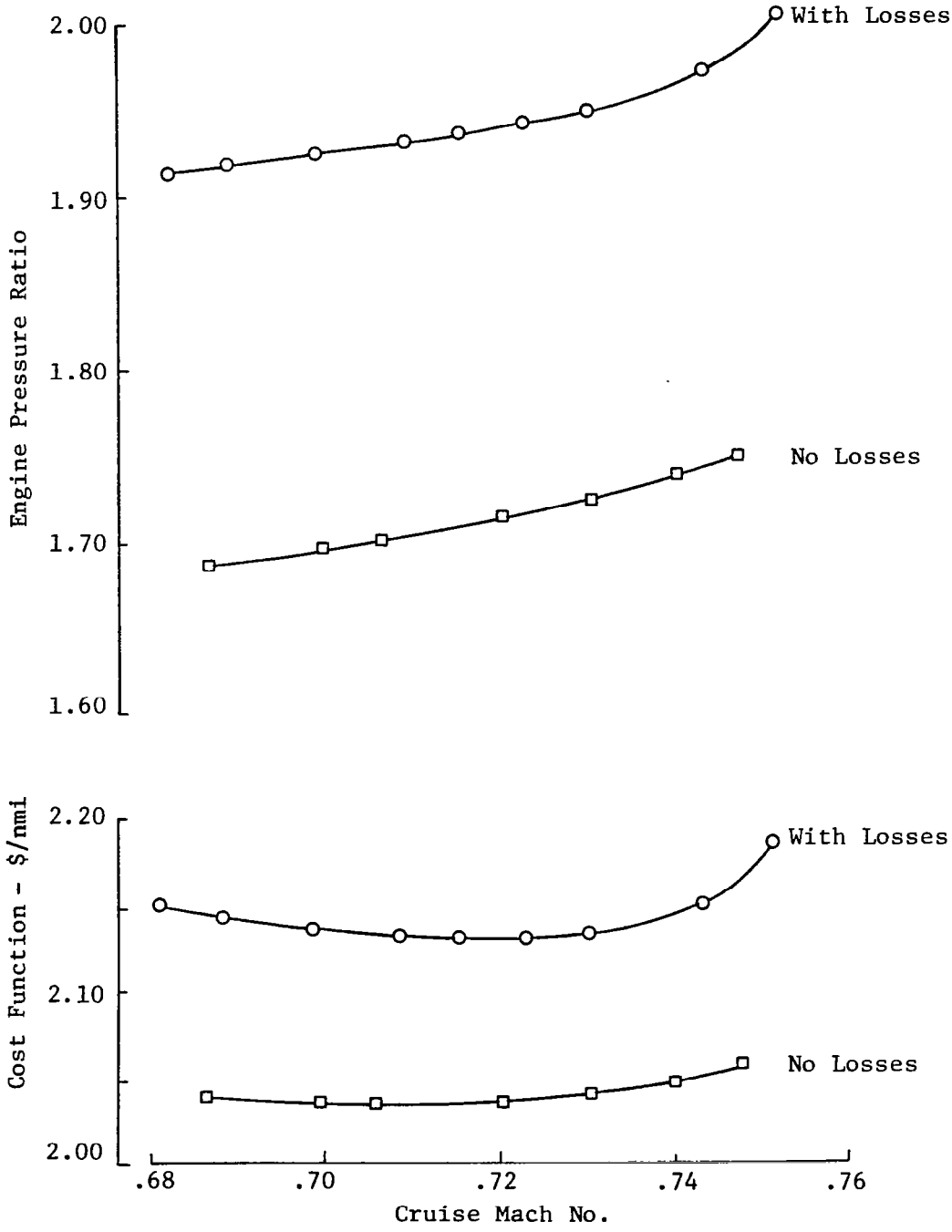

Figure 35. Effect of Powerplant Losses on Cruise Cost and Required EPR

For the bleed ratios used, the performance penalty in terms of cost per unit distance traveled is about 5%; this is substantial. The engine must be operated at a much higher engine pressure ratio to match thrust and drag. As a result, fuel flow is increased which increases the cost function.

Obviously, more work must be done to determine the magnitude of the required bleed air and power extraction and the inlet pressure loss at a specified flight condition. It appears that there is tradeoff between the overpressure level in the cabin and the performance penalty to the engine due to the eighth and thirteenth stage bleeds. Other tradeoffs undoubtedly exist, and they can be examined for both aircraft models using both the OPTIM and TRAGEN programs.

Take-Off There has been little analysis work done with regard to fuel conservation during take-off. The procedures that are followed are mostly dictated by ATC constraints and noise considerations. In addition, all aircraft are subject to last minute runway changes which has hampered fuel management planning for the take-off. Nonetheless, the fuel burned in take-off and initial climb and maneuvering is significant, particularly for short range aircraft, and it is certainly prudent to explore the potential for reducing fuel consumption during this phase of flight.

A typical take-off sequence, and the one used as the baseline case in this brief study is sketched in Fig. 36. Take-off is defined here to include each segment shown in Fig. 36, and it culminates with the initial recommended climb speed of 210 kt. This is consistent with previous work done with OPTIM and TRAGEN in which an altitude and airspeed have been specified for the beginning of climb.

Take-off profiles were modeled using the take-off simulation program documented in Ref. 10. Subroutines which model the twin-jet aerodynamics and engine characteristics were included in this program. These subroutines are essentially those used in the OPTIM program, except that aerodynamic data have been added to model the effect of the exposed landing gear on drag and lift and the transient flap deployment effects.

A complete time history of the aircraft state is generated from brake release to any specified ending speed, as indicated in Fig. 36. Take-off schedules are input to vary power setting, flap deflection and departure headings as functions of speed or altitude. The time history output from the program includes time, position (runway referenced x, y, and z coordinates), angular orientation (heading, pitch, roll, flight path angle), and performance measures (speed, acceleration, rate of climb, load factor, thrust and fuel burn).

There are numerous parameters to investigate in the evaluation of fuel burned during take-off. These include the flap setting and flap retraction schedule, the aircraft rotation process (initial rotation velocity and rotation rate (rate of change in angle-of-attack)), and the maximum allowable load factor. Also, airport altitude, ambient temperature changes from standard day, and required heading changes affect take-off performance. Each of these factors has been investigated in this study to some degree, and these are presented in Appendix B. Other factors which have not been investigated (but which may have an effect on fuel burned) include reduced takeoff power schedules, altitude to begin acceleration (point 6 in Fig. 36), the maximum allowable acceleration up to V_{END}, prevailing wind effects, and noise suppression constraints. The take-off simulation program can also be used to study these additional factors.

In Appendix B, the effects of changing the take-off parameters on two measures of take-off performance - fuel burn and distance to clear the 10.7m (35 ft) obstacle - are presented in graphic form. With regard to fuel usage, Table 6 presents the range of parameter variation studied and the corresponding fuel usage changes.

As can be seen from Table 6, the fuel variation during take-off can be as great as 11% by changing the flap schedule. Several parameters can be varied to reduce fuel usage, but the allowable change depends on runway length, altitude, and atmospheric temperature. It is recommended that the take-off program be incorporated into TRAGEN, and that it be used for further analysis to optimize the take-off portion of the flight.

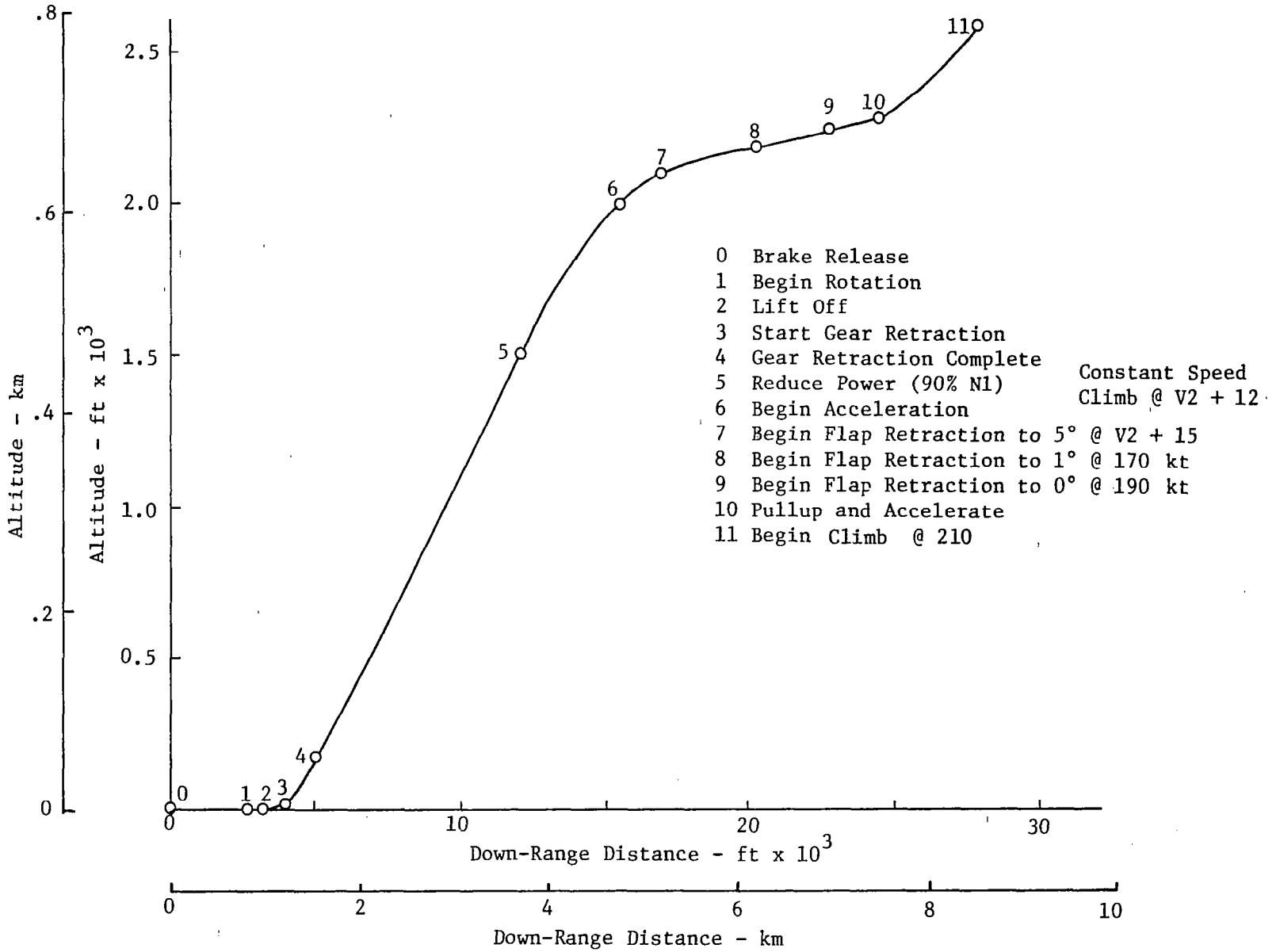

Figure 36. Typical Take-off Profile for a Twin-jet Aircraft

Table 6 Effect of Changing Take-off Parameters of Fuel Usage to 210 kt Airspeed.

Parameter: Variation	Amount of Fuel Variation (lb)	Percentage Increase
Flaps *: 1 - 15.	460 - 510	11%
Rotation Speed: 115 - 125 kt	505 - 530	5%
Rotation Rate: 2 - 5°/sec	485 - 510	5%
Rotation Load Factor: 1.10 - 1.17	480 - 510	6%
Airport Altitude: 0 - 1.5 km	510 - 550	8%
Temperature Variation: 0 - 40°F	510 - 535	5%
Departure Heading: 0 - 180°	510 - 555	9%

* See Appendix B for definition

Program Modification for Airborne Implementation

Along with the previously described studies, a considerable effort was made during the last eighteen months to reorganize the OPTIM code so that it could more appropriately serve as a basis for an advanced flight management system. This effort included the removal of redundant code, redefinition of program control variables, and reorganization of the commons. The size reduction accomplished is shown in the following Table 7.

As defined earlier, OPTIM6 is the latest version of the program designed for general studies such as those presented earlier in this chapter. OPTIM-S is the version of the program modified to include only one aircraft model - the NASA Langley Advanced Transport Operating Systems (ATOPS) aircraft (referred to as the twin-jet model). OPTIM-S is designed to reduce both size and run time, but it gives up some of the OPTIM6 version's capability. OPTIM-P is the OPTIM-S version converted to operate on a PDP 11-70 minicomputer. Here, the size increases from 11000 words to 32000 words because the PDP 11-70 is a 16-bit machine with real

Table 7. OPTIM Program Size Reduction Results

Version	Size (1000 words)	Comments
OPTIM4	52	Initial version - May 1981
OPTIM5	32	Reorganization with three new options - step climb, variable winds, and constrained descent.
	25	Printer plot capability removed to allow running interactively on NASA Langley computer.
OPTIM6	28	Program reorganized to remove known minor bugs and to improve output accuracy and computation efficiency.
OPTIM-S	11	Tri-jet model removed; step climb optimization removed; multiple cruise segments and variable wind models added. Intended for cockpit simulator usage.
OPTIM-P	31	Conversion of OPTIM-S to run on PDP 11-70 minicomputer. (16 bit words).

variables defined by two words. The CDC 6600 which OPTIM-S operates on has a 60-bit word.

Table 8 compares the run times of OPTIM6, OPTIM-S and OPTIM-P for seven different cases. Results are shown for OPTIM-S when cruise is defined with both one segment and three segments. These numbers are in-exact, and several more cases should be run to get statistical measures of run time.

The preliminary results from Table 8 show that the OPTIM-S run time can be up to 70% less than that of OPTIM6. This is primarily due to reduction in time to compute the cruise table. Also, it can be seen that optimizing climb and descent with speed (V) only as compared to using both speed and thrust (π) further cuts run time. The use of both V and π

Table 8. OPTIM Run Time Comparisons for 1000 nmi Flight

Case	CDC 7600			PDP 11-70
	OPTIM6	OPTIM-S		OPTIM-P
		1 Segment	3 Segment	
A. Fixed Altitude; V only	1.4	1.3	1.8	30.
B. Fixed Altitude; V/π	3.9	3.7	3.9	69.
C. Free Altitude; V only	11.6	3.4	3.7	68.
D. Free Altitude; V/π	12.0	5.6	5.9	103.
E. TOA; Fixed Altitude; V only (No. of iterations to converge)	9.9 (6)	8.1 (5)	9.1 (5)	192. (5)
F. TOA; Free Altitude; V only (No. of iterations to converge)	20.9 (4)	25.0 (7)	27.2 (7)	567. (7)
G. Free Altitude; V only; Wind	11.7	3.3	3.5	75.

for optimization for the twin-jet reduces fuel by a very small fraction (0.1%) compared to the V only case. Thus, the program size can be further reduced by removal of this option.

The time-of-arrival (TOA) run times are largely governed by the number of iterations required for the program to converge (currently to within 10 sec of the desired flight time). As seen for Case F in Table 8, the run time increases from 21 to 25 sec in going to OPTIM-S because the number of iterations increases from 4 to 7. The number of iteration to convergence can be limited to 3 or 4 in the future if run time is a problem. (567 sec for convergence on the PDP 11-70 seems excessive).

OPTIM-S was reduced in size to an extent limited by resources of the current contract. Further reductions are possible by removal of printout, non-necessary program options and data, and excessive storage allocations. These changes will also improve operating speed. It is suggested that these improvements be made after experience is obtained with the current OPTIM-S version operating on the ATOPS cockpit simulator

and the airborne interface requirements to the pilot, navigation system, and other avionics become better defined.

Several more issues need to be addressed to incorporate OPTIM into an experimental flight management system. These issues are now listed in the form of questions that remain to be answered (in no particular order):

1. What modifications are required to allow interface with the autopilot/autothrottle or flight director? What interface is required to the cockpit keyboard and displays?

2. What kind of interface is required to read in winds, temperature variations, horizontal profile, weight estimates, and desired arrival time? Will ground support software be required as part of the interface to assist in airborne flight management?

3. How can variations in aerodynamic and propulsion characteristics be accounted for? Is there a way to measure these parameters in flight and adjust the flight management software accordingly?

4. Should the program be modified to allow constant altitude segments during climb and holding patterns during descent? At what altitude or position relative to the destination runway should the descent profile stop? What provision should be made for interface with a terminal area flight management algorithm?

5. How often is a new reference vertical profile required? To what extent does the computation time available have to be shared with other functions such as flight control and navigation?

These questions will be answered in the course of testing OPTIM and planning for flight test experiments. The answers will govern the modifications required to convert OPTIM to an implemented airborne flight management system.

III

TRAGEN

GENERATION OF OPTIMUM AND REFERENCE FLIGHT TRAJECTORIES

References 1 - 6 describe an efficient way in which near-optimum flight profiles can be generated in an airborne computer without using the consuming numerical techniques. This method was coded into the OPTIM program, discussed in the previous chapter. Instead of iteratively solving the two-point boundary value problem, assumptions are made in deriving the OPTIM algorithm so that the dynamics are simplified to two state variables. One state variable (energy) becomes the independent variable, and the other (range) is included as the single state in the Hamiltonian. Thus, the problem of solving for minimum cost profiles reduces to minimization of the Hamiltonian at each point along the profile (as described by Eq. (1)).

Now, although this method is a convenient way of generating a trajectory, the resulting trajectory must be verified by using a more accurate model of the aircraft dynamics. Verification implies that:

1) The reference trajectory that is generated must be flyable when the full aircraft equations of motion and constraints are taken into account.

2) The trajectory cost as predicted by OPTIM must be essentially identical to that experienced by simulating more complete aircraft equations of motion.

A companion program to OPTIM was developed for verification of the optimization results. This program is referred to as TRAGEN (for trajectory generation).

With OPTIM and TRAGEN as computer tools, the user has the capability of studying the characteristics of near-optimum profiles in great detail and to examine alternate ways these profiles can be implemented on-board. Trajectory characteristics can be obtained by exercising OPTIM's options and by

making sensitivity studies with OPTIM and TRAGEN.

TRAGEN Characteristics

TRAGEN can be used to simulate the longitudinal trajectory of an aircraft commanded to follow the reference path output from OPTIM. Some details of the TRAGEN program are presented in a separate user's guide for this program [11].

In addition to verification of the optimization program's results, the TRAGEN program has the following utility:

1) It provides a means for testing guidance laws for steering the aircraft to follow the input reference trajectory.

2) It enables study of the effect of following an incorrect reference trajectory. For example, if the OPTIM results were based on one particular wind profile and initial aircraft weight, and a different weight and wind profile actually existed, the TRAGEN simulation would allow assessment of the effect of these errors on trajectory cost.

3) It can be used to determine the flight cost that would result from the aircraft being commanded to follow a reference trajectory suggested in the manufacturer's aircraft handbook. For example, for climb, handbook reference trajectories usually consist of following a constant indicated airspeed until a given Mach number is reached. Then, the reference trajectory follows this fixed Mach number until the reference cruise altitude is reached.

A five state-variable model of the aircraft is currently used in TRAGEN to simulate longitudinal motion during climb and descent. State variables are altitude, altitude rate, longitudinal range, airspeed, and aircraft mass. Currently neglected are the rapid transient dynamics of throttle response, angle-of-attack, and pitch rate (δ_T, α, q). The throttle is assumed to be set so that maximum thrust is achieved during climb and idle thrust is used during descent. The altitude control variable is taken to be the angle-of-attack which has maximum and minimum limits. This degree of sophistication is adequate for testing the OPTIM results.

To generate the control law to follow the commanded climb profile, a

linear perturbation model was made of the dynamic equations,

$$
\begin{aligned}
T \cos \alpha - D(\alpha,h,V_a) - W \sin \gamma &= m\dot{V}_a \quad , \\
T \sin \alpha + L(\alpha,h,V_a) - W \cos \gamma &= mV_a\dot{\gamma} \quad .
\end{aligned}
\tag{26}
$$

The perturbation equations and transfer functions from Eqs. (26) are given in Ref. 1. It is assumed that a perturbation $\delta\alpha$ to the nominal angle-of-attack can be used to obtain the desired perturbations in flight path angle ($\delta\gamma$) and airspeed (δV_a) to maintain the aircraft on the desired reference climb profile.

The TRAGEN program can readily be expanded to include throttle dynamics and short period dynamics during climb and descent. This would be required for further study of autothrottle and autopilot design to steer the aircraft to follow input reference trajectories. The control variables would be throttle position and elevator deflection for this expanded capability. A requirement for implementing this expanded simulation would be to obtain the necessary stability and control derivatives to complete the dynamic model.

The specification of reference profiles used in TRAGEN is based on using altitude as the independent variable for climb and range-to-go to the destination as the independent variable for descent. For climb, the reference trajectory consists of specifying airspeed and flight path angle (with respect to the air mass) as piecewise linear functions of altitude. At the 3048 m (10000 ft) point, the aircraft is commanded to level off and accelerate until the airspeed is reached where the climb should again continue. For descent, the reference trajectory consists of specifying altitude as a piecewise linear function of range-to-go.

The major additions to TRAGEN added during the past eighteen months were the following:

1) The ability to compute an accurate estimate of fuel and time required to fly over a given cruise range from a given altitude/airspeed condition to a slightly different altitude/airspeed condition. This method allows assessing the cruise performance described below.

2) The ability to combine climb, cruise, and descent segments to determine overall fuel and time requirements for a given flight profile.

3) The definition of a different wind profile for each flight segment simulated during a TRAGEN run. This allows simulating the effect of flying over a variable, range dependent wind field.

The computation of a cruise segment's performance is based on use of the Breguet equation. This equation is commonly used to determine the rate of change of range as a function of fuel burned. This equation is the key to assessing cruise performance, as is now discussed.

A single cruise segment takes place in one vertical plane. Over this segment, it is assumed that the flight path angle is small and that speed and altitude changes are negligible. Also, for now, it is assumed that there is no wind. With these assumptions specified, the following equations are valid:

$$\begin{aligned} T &= D \ , \\ L &= W \ , \\ \dot{x} &= V_a \ . \end{aligned} \tag{27}$$

In addition, the time rate of change in mass can be expressed by the equation

$$\dot{w} = -T\ (S_{FC}) \tag{28}$$

where S_{FC} is the engine specific fuel consumption.

These equations can be used to formulate the standard Breguet range equation as follows:

$$\dot{x} \ = \ (dx/dW)\dot{w} = V_a \tag{29}$$

Therefore,

$$\begin{aligned} dx/dW = V_a \ \frac{1}{\dot{w}} &= \frac{-V_a}{T(S_{FC})} \\ &= \frac{-V_a(L/W)}{(T/D)D(S_{FC})} = \frac{-V_a(L/D)}{S_{FC}} \ \frac{1}{W} \end{aligned} \tag{30}$$

The Breguet factor or range factor, R_F, is defined as:

$$R_F = \frac{V_a (L/D)}{S_{FC}} \quad . \tag{31}$$

Then,

$$dx/dW = -R_F \frac{1}{W} \quad . \tag{32}$$

From Eq. (32), one can write

$$x = -\int_{W_i}^{W_f} \frac{R_F}{W} dW \ , \tag{33}$$

or

$$x = \bar{R}_F \ \ell n \left(\frac{W_i}{W_f} \right) \ , \tag{34}$$

where $\bar{R}_F$ is the average value of R_F over the range traveled. Using the average value for the range factor, $\bar{R}_F$, is a good approximation for assessing cruise performance.

The range equation is often used to determine an optimum altitude and Mach number to maximize range. This is a relatively trivial optimization result for a commerical transport aircraft because the cost of time is not considered, and the climb and descent legs are ignored in the problem. However, for the purpose of the TRAGEN program, cruise speed, altitude and the required range of the cruise segment are specified, and it remains to find the fuel burned over the cruise segment. Thus, the range equation is rewritten as follows:

First, the fuel burned is

$$W_{fuel} = W_i - W_f \tag{35}$$

Then, the range traveled is

$$x = \bar{R}_F \ \ell n \left(\frac{1}{1 - W_{fuel}/W_i} \right) . \tag{36}$$

Thus, the fuel burned to achieve a given range x is

$$W_{fuel} = W_i \left(1 - 1/e^{(x/\bar{R}_F)} \right) . \tag{37}$$

In TRAGEN, the average Breguet factor $\bar{R}_F$ is computed by evaluating Eq. (31) at the initial and final altitude and airspeed conditions specified to be achieved over the given range. Equation (37) is used to iterate on the amount of fuel burned over this segment. This is used in turn to compute the final mass to determine the lift and drag terms of Eq. (27) and to obtain the final value of R_F from Eq. (31).

TRAGEN Results

Evaluation of Optimum Profiles Several near-optimum vertical profiles were computed by using the OPTIM program, and these profiles were used as inputs to the TRAGEN program. Table 9 presents a comparison of the results of six cases using the twin jet model traveling over a range of 1000 nmi. For these runs, fuel was valued at \$.33/kg (\$.15/lb), and time was valued at \$600./hr.

The first four cases (A,B,C,D) had no wind; Case E had a head wind varying linearly with altitude from 0 kt at 0 km (0 ft) to 100 kt at 12.2 km (40000 ft). Case F had a tail wind with the same altitude variation. Cases A, E, and F had 40860 kg (90000 lb) takeoff weight with free cruise altitude. Cases B, C and D had cruise altitudes fixed at 10.058 km (33000 ft) and takeoff weights of 43092, 40824, and 38566 kg (95000, 90000, and 85000 lb), respectively.

Table 9 compares the OPTIM and TRAGEN results in fuel, time, and range traveled for the climb, cruise, and descent segments plus the total range of flight for the six cases. Also, the total cost is compared for each case. As can be seen, all the cases compare to within 0.1% in cost. These results are considered very good; and by examining individual fuel and time elements, we see a close agreement between OPTIM and TRAGEN.

The larger discrepancies between OPTIM and TRAGEN results are for the wind cases. It is believed that these differences are because OPTIM does not account for wind dynamic effects that are included in the TRAGEN results. This point needs further study.

Table 9. Comparison of Six Twin-Jet Profiles as Generated by OPTIM and Simulated by TRAGEN. 1000 nmi. Range

Case - Comments	Phase	Fuel - lb		Time - Sec		Range - nmi.		Cost - $	
		OPTIM	TRAGEN	OPTIM	TRAGEN	OPTIM	TRAGEN	OPTIM	TRAGEN
A - Free cruise	Climb	2637	2642	948	944	100.25	100.57		
No wind	Cruise	7644	7625	6870	6872	797.05	797.00		
90000 lb takeoff	Descent	404	405	1066	1064	102.70	102.70		
	Total	10685	10672	8884	8880	1000.00	1000.27	3083.42	3080.81
B - Fixed cruise	Climb	2554	2559	864	861	89.78	90.14		
No wind	Cruise	8508	8500	6991	6998	820.52	821.		
95000 lb takeoff	Descent	374	375	963	964	89.69	89.71		
	Total	11436	11434	8818	8823	1000.00	1000.85	3185.07	3184.77
C - Fixed cruise	Climb	2359	2363	797	794	82.43	82.73		
No wind	Cruise	8324	8331	7075	7067	830.69	830.		
90000 lb takeoff	Descent	363	364	933	932	86.88	86.90		
	Total	11046	11058	8805	8793	1000.00	999.63	3124.40	3124.20
D - Fixed cruise	Climb	2176	2179	734	731	75.62	75.85		
No wind	Cruise	8161	8151	7149	7160	840.56	841.		
85000 lb takeoff	Descent	351	352	900	898	83.82	83.85		
	Total	10688	10682	8783	8789	1000.00	1000.70	3067.03	3067.13
E - Free cruise	Climb	2295	2200	744	705	69.85	68.25		
Head wind	Cruise	10789	10822	8766	8773	855.08	857.		
90000 lb takeoff	Descent	350	366	890	941	75.07	75.08		
	Total	13434	13388	10400	10419	1000.00	1000.33	3748.43	3744.70
F - Free cruise	Climb	2662	2824	984	1061	117.14	124.91		
Tail wind	Cruise	5936	5863	5428	5378	763.70	756.		
90000 lb takeoff	Descent	417	404	1102	1056	119.16	119.18		
	Total	9015	9091	7514	7495	1000.00	1000.09	2604.58	2602.02

Sensitivity Evaluation An important utility of the TRAGEN program, especially with the entire flight profile simulation capability available, is to examine the sensitivity of performance resulting from computing an aircraft profile with inaccurate inputs into OPTIM. Two errors that are quite possible are the use of the incorrect flight weight and the use of the incorrect wind profile. These possibilities were examined, and the resulting cases are shown in Tables 10 and 11.

Incorrect takeoff weight is examined in Table 10. Here, the Cases G and H were run in TRAGEN with initial weights of 43092 kg (95000 lb) and 38565 kg (85000 lb). However, the aircraft was simulated to follow the optimum profile based on a 40824 kg (90000 lb) takeoff weight. That is, the aircraft was commanded to follow the profile of Case C in Table 9. The optimum profiles for these takeoff weights would be represented by Cases B and D indicated in Table 9.

Table 10 compares Case G with Case B and Case H with Case D. This comparison represents what the penalty in fuel, time, and cost would be if the aircraft weight estimate is $\pm$ 2270 kg ($\pm$5000 lb) in error when the optimization algorithm computes the reference profile. As can be seen, the penalty for an incorrect weight estimate is very slight. The costs for Cases G and B were within 0.02% of each other (Actually, Case G was slightly better. However, this was within numerical inaccuracy of the computations). Costs for Cases H and D were within 0.13%. The incorrect initial weights caused excess fuel to be burned (23 and 18 lb), but these amounts are small. The conclusion, based on these limited runs, is that the performance predicted by OPTIM is not sensitive to typical weight estimate errors.

In Table 11, the performances of Cases I, J, K, and L are shown where the incorrect wind model was used to compute the optimum reference trajectory. Case I has a head wind, but the aircraft follows the reference profile generated for Case A of Table 9 (i.e., no wind). It is compared with Case E of Table 9 , where the correct head wind model was used. Results show an increase of 3% in overall cost.

Table 10. Effect of Weight Inaccuracy on Flight Performance

Case - Comments	Phase	FUEL - LB		TIME - SEC		COST - $	
		CASE G	CASE B	CASE G	CASE B	CASE G	CASE B
Case G at 95000 lb takeoff, but profile based on 90000 lb. Compare with Case B.	Climb	2521	2559	857	861		
	Cruise	8579	8500	7027	6998		
	Descent	357	375	910	964		
	Total	11457	11434	8794	8823	3184.22	3184.77
		CASE H	CASE D	CASE H	CASE D	CASE H	CASE D
Case H at 85000 lb takeoff, but profile based on 90000 lb. Compare with Case D.	Climb	2261	2179	756	731		
	Cruise	8068	8151	7078	7160		
	Descent	371	352	960	898		
	Total	10700	10682	8794	8789	3070.67	3067.13

Table 11. Effect of Wind Inaccuracy on Flight Performance

Case - Comments	Phase	FUEL - LB		TIME - SEC		COST - $	
		CASE I	CASE E	CASE I	CASE E	CASE I	CASE E
Case I has head wind, but profile based on no wind. Compare with Case E.	Climb	2564	2200	911	705		
	Cruise	9894	10822	9025	8773		
	Descent	552	366	1514	941		
Case I cruise altitude: 36306-38663 ft	Total	13010	13388	11450	10419	3859.83	3744.70
Case E cruise altitude: 30727-33227 ft							
		CASE J	CASE F	CASE J	CASE F	CASE J	CASE F
Case J has tail wind, but profile based on no wind. Compare with Case F.	Climb	2684	2824	955	1061		
	Cruise	6186	5863	5526	5378		
	Descent	343	404	871	1056		
Case J cruise altitude: 35772-38663 ft	Total	9213	9091	7352	7495	2607.28	2602.02
Case F cruise altitude: 37110-38857 ft							
		CASE K	CASE A	CASE K	CASE A	CASE K	CASE A
Case K has no wind, but profile based on head wind. Compare with Case A.	Climb	2305	2642	744	944		
	Cruise	8757	7625	7056	6872		
	Descent	305	405	750	1064		
Case K cruise altitude: 30733-33239 ft	Total	11367	10672	8550	8880	3130.05	3080.81
Case A cruise altitude: 36310-38666 ft							
		CASE L	CASE A	CASE L	CASE A	CASE L	CASE A
Case L has no wind, but profile based on tail wind. Compare with Case A.	Climb	2657	2642	973	944		
	Cruise	7380	7625	6826	6872		
	Descent	499	405	1364	1064		
Case L cruise altitude: 37092-38859 ft	Total	10536	10672	9163	8880	3107.57	3080.81
Case A cruise altitude: 36310-38666 ft							

Case J has a tail wind, but again the aircraft follows the reference profile of Case A. Case J is compared with Case F of Table 9, where the correct tail wind model was used. The penalty on cost of assuming no tail wind is only 0.2%.

Case K has no wind, but its reference profile is based on assuming the presence of a head wind (Case E of Table 9). Case K is compared with Case A of Table 9 where no wind was modeled. Case K has a cost penalty of 1.6%.

Case L has no wind, but its reference profile is based on use of the tail wind model (Case F of Table 9). Again, this is compared to Case A, and the overall cost penalty is 0.9%.

These examples show that inaccuracies in models of the wind can have a relatively significant effect on the achieved cost performance of a particular flight. This points out the importance of having up to date weather information.

These wind inaccuracy studies were based on rather gross modeling errors (e.g., no wind instead of a significant head wind, etc.) Typical modeling errors would be smaller, and it remains to be seen how simple the wind vertical profile can be modeled and still achieve the expected performance gains.

Profile Simplification The standard pilot handbook specifications for various aircraft recommend that aircraft should climb at a constant indicated airspeed after crossing 3.048 km (10000 ft) until a given Mach number is reached. Then, climb should continue at this constant Mach number until cruise altitude is reached. Examples for various aircraft are shown in Table 12. For example, a 737-200 aircraft climbs at 320 kt (IAS) until reaching 0.73 Mach. The climb is continued at 0.73 Mach until cruise is reached. Descent is specified to be in the opposite order.

As shown earlier, the OPTIM reference climb and descent profiles do not typically have constant indicated airspeed and Mach number segments. Rather, the airspeed and Mach number change gradually. However, these gradual changes can be approximated by a constant value IAS/Mach schedule.

Table 12. Typical Aircraft Characteristics as Specified in Manufacturer's Handbooks. [12]

Airplane Type	Final Cruise Altitude	Cruise Mach No.	Landing Weight*	Climb Schedule	Descent Schedule
737-200	8,839 m (29,000 ft)	.73	36,644 kg (80,800 lb)	320 IAS/.73 M	.73 M/320 IAS
727-100	10,668 m (35,000 ft)	.80	50,658 kg (111,700 lb)	340 IAS/.78 M	.80 M/340 IAS
727-200	10,668 m (35,000 ft)	.80	56,372 kg (124,300 lb)	340 IAS/.78 M	.80 M/340 IAS
DC-8-20	10,668 m (35,000 ft)	.80	75,011 kg (165,400 lb)	300 IAS/.78 M	.80 M/330 IAS
DC-8-50	10,668 m (35,000 ft)	.80	77,098 kg (170,000 lb)	300 IAS/.78 M	.80 M/330 IAS
DC-8-61	10,668 m (35,000 ft)	.80	88,707 kg (195,600 lb)	300 IAS/.78 M	.80 M/330 IAS
DC-8-62	10,668 m (35,000 ft)	.80	82,313 kg (181,500 lb)	300 IAS/.78 M	.80 M/330 IAS
DC-10-10	10,668 m (35,000 ft)	.83	128,844 kg (284,100 lb)	300 IAS/.82 M	.83 M/340 IAS
747-100	10,668 m (35,000 ft)	.84	194,784 kg (429,500 lb)	340 IAS/.82 M	.86 M/340 IAS

* Based on average 1973 payload obtained from CAB Form 41, Sched. T-2(b).

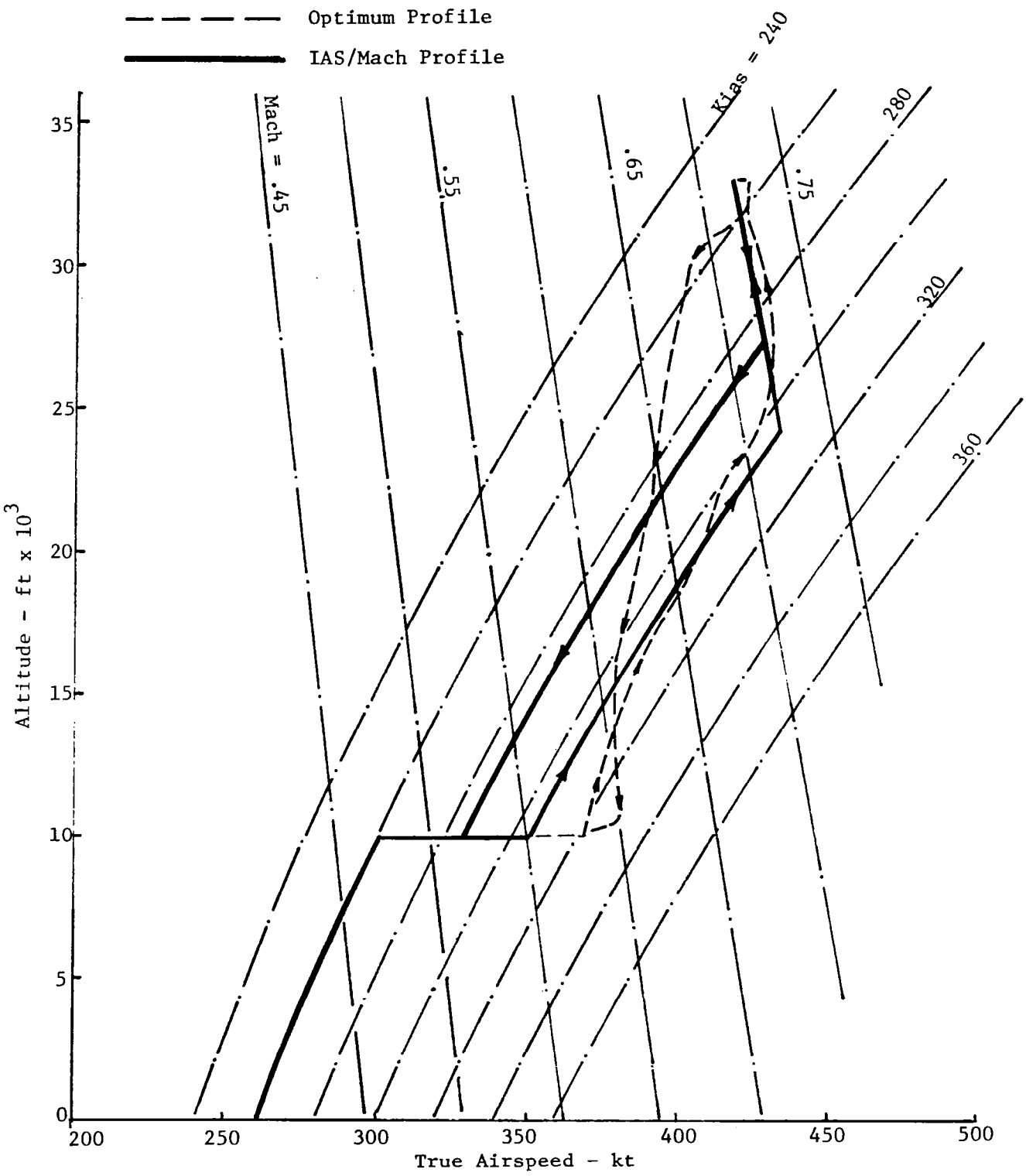

Figure 37. Comparison of Optimum and Simplified (IAS/Mach Schedule) Climb and Descent Profiles.

The advantage of constant IAS/Mach schedules are that they are easy to command, and they represent profiles which are familiar to the pilot. One question in their use is what cost penalty do they cause compared to optimum climb and descent profiles. Reference 13 indicates that these simpler profiles have essentially the same cost as the near-optimum profile. A TRAGEN run was made to examine this possibility.

A case (Case M) was run using TRAGEN where the aircraft was commanded to follow an IAS/Mach schedule of 305 kt and 0.72 Mach for climb up to 10 km (33000 ft) and 0.72 Mach and 285 kt for descent from this altitude. This is an approximation of the near-optimum profile of Case C summarized in Table 9. A comparison of the profile on an altitude vs true airspeed plot is shown in Figure 37. The resulting fuel, time, and costs of these two profiles are compared in Table 13. From this table, it can be seen that the results are nearly the same (within 0.05% in cost). The simplified profile (constant IAS/Mach schedule) is slightly better, but this is probably due to computational inaccuracies.

From this single case, we cannot make general conclusions that the simplified profile will always produce the same level of performance as that of the more complex near-optimum vertical profile. Many more examples with different costs of time and fuel, different wind conditions, and different ranges would have to be explored to reach this conclusion. However, what this example does point out is that the overall performance results may not be too sensitive to the aircraft following the exact climb and descent profiles. The characteristics of these profiles could be, perhaps, simplified. Also, there may be ways in which OPTIM could be used to compute the near-optimum profile, and then this profile's characteristics could be simplified for ease of on-board guidance command. Beyond this, it may be possible to simplify the process of computing "good" climb and descent profiles used in the OPTIM program. Rather than using the current pointwise optimization of a Hamiltonian function, it might be computationally simpler to find two optimum parameters (constant indicated airspeed followed by constant Mach number) for describing the climb or descent profiles.

These possibilities should be investigated further. OPTIM and TRAGEN provide the basis for making such investigations.

Table 13. Comparison of "Optimum" Profile and Similar Profile Approximated with Constant Mach/IAS Schedule for Climb and Descent

Phase	FUEL - lb		TIME - sec		COST - $	
	CASE M	CASE C	CASE M	CASE C	CASE M	CASE C
Climb	2337	2363	786	794		
Cruise	8316	8331	7129	7067		
Descent	353	364	917	932		
Total	11006	11058	8832	8793	3122.90	3124.20

IV

SUMMARY, CONCLUSIONS, AND RECOMMENDATIONS

Summary and Conclusions

This report summarizes the progress and results obtained during the third and fourth years of study of methods for minimizing transport aircraft direct operating costs by generation of near-optimum vertical profiles over a fixed range. The primary end product of this effort has been the development of two complementary computer programs that have a large number of applications. The first, referred to as OPTIM, computes points defining the near-optimum vertical profile of a medium range turbojet transport aircraft. The second, referred to as TRAGEN, generates an aircraft trajectory that follows either the optimum reference path or some other reference profile.

Chapter II summarizes development of the OPTIM program options, their applications, and studies conducted related to OPTIM. One of the important features of this program is the ability to generate a profile which minimizes fuel usage while achieving a fixed time-of-arrival. This profile is achieved by iterating on the cost-of-time constant in the cost function. To enable this iteration to converge required development of accurate surface fits of the drag coefficient as a function of the lift coefficient and Mach number and the normalized thrust coefficient as a function of the Mach number and engine pressure ratio. Chapter II first documents the process taken and the lessons learned in obtaining these surface fits.

Three new options added to OPTIM during this period were the ability: (a) to compute an optimum step climb during cruise, (b) to constrain the upper part of the descent profile to a maximum sink rate for cabin pressurization reasons, and (c) to use different wind profiles for climb, cruise, and descent. Details concerning their effects on optimum profile computation are described.

OPTIM was also modified by generating two new versions - OPTIM-S and OPTIM-P -- which are designed for cockpit simulation studies and eventual flight test. OPTIM-S was reduced in size and modified so run time would be greatly reduced. OPTIM-P is a version of OPTIM-S that runs on a PDP 11-70 minicomputer. Size reduction and increase in run time efficiency was accomplished by total reorganization of the program commons, removal of redundant code, and general reduction of storage requirements. OPTIM's code was reduced from 52,000 words to 11,000 words for the OPTIM-S version. Exercising OPTIM-S also indicated a decrease in run time of up to 70%.

Several example cases were run to demonstrate the utility of new options in the modified OPTIM programs. It was seen that flying into a head wind can require about 45% more fuel than flying with a tail wind on a 1000 nmi flight of a twin-jet aircraft. Also, the ideal cruise altitudes can vary more than 1.5 km (5000 ft).

The OPTIM results are also greatly effected by the temperature conditions of a given day. Results were computed for a 1000 nmi flight with the twin jet model and standard day temperature varied by $\pm$ 20°C. The hot day flight required 89 kg (195 lb) more fuel than the cold day but reached its destination 11 minutes faster based on using cost-of-time of $600./hr and cost-of-fuel of $.33/kg ($.15/lb).

Using the step climb option in going from a constrained cruise altitude of 10 km (33000 ft) to 11.3 km (37000 ft) for a 1000 nmi trip can actually cost more ($2.00) as was seen for the twin-jet model. On the other hand, it can save cost ($17.25) and fuel (34 kg (75 lb)) as seen for the tri-jet model. These results are very dependent on takeoff weight, constrained altitudes selected, and the prevailing winds, however.

The example pressurization constraint on descent limited the descent rate to 152 m/min (500 ft/min) down to 8.53 km (28000 ft). For the twin-jet traveling 1000 nmi and constrained at the 10 km cruise altitude, the pressurization constraint cost 9 kg (19 lb) of fuel. For the free cruise altitude case, the constraint cost 78 kg (171 lb) of fuel. These are

obviously considerable costs, and they have a significant bearing on design of cabin pressurization equipment and procedure.

The fixed time-of-arrival (TOA) option was exercised for the twin-jet model when the flight began in cruise. This option was shown to be able to save up to 11% of the total fuel for a 500 nmi flight or 650 kg (1400 lb) for a 1500 nmi flight. Thus, this alternative to using the holding pattern offers a significant opportunity to save fuel costs when flight time delays occur during a long range flight.

The OPTIM-S version has been configured to be able to follow multiple segment horizontal flight plans with multiple wind and temperature profiles specified along the route. This capability was demonstrated along typical airline routes between Chicago and Phoenix.

Two other topics related to the vertical profile computation were examined. They include: (a) a parametric study of the sequence of steps followed during takeoff and (b) the loss of thrust due to engine installation effects and bleed air requirements. The takeoff procedure determines the initial conditions to begin the optimum vertical profile, and they determine the initial amount of fuel consumed for a given flight. The in-flight thrust losses increase the amount of fuel required to travel a given range, and they also modify the optimum cruise speed.

In Chapter III, the applications and modifications made to the TRAGEN program are first summarized. The ability to compute time and fuel consumed during the cruise portion of flight was added to TRAGEN. Also, the program was reorganized so that a complete flight consisting of multiple climb, cruise, and descent segments can be simulated. This program can now be used to verify the accuracy of the entire vertical flight profile computed by OPTIM, or to simulate an alternate vertical flight profile established from a different source.

TRAGEN was used to simulate 1000 nmi range profiles generated by OPTIM for the twin jet aircraft model. Initial weight was varied, altitude was fixed or free, and head wind, tail wind, and no wind cases were run. In six cases examined, OPTIM and TRAGEN profile cost results (cost of time

and fuel) matched to better than 0.1%. This verifies the basic accuracy of the OPTIM profile.

TRAGEN was also used to examine the sensitivity of the profiles' cost performance to errors in initial takeoff weight and the wind model being used. For the sample cases examined, it was found that the profiles' performance was insensitive to initial takeoff weight errors of up to $\pm$ 2270 kg ($\pm$ 5000 lb). Cost differences were about 0.1 %. On the other hand, a profile generated with an incorrect wind model could have a significant increase in cost. For the four cases studied, cost increases varied from 0.2% to 3.0%.

Finally, TRAGEN was used to compare the cost performances obtained by matching an "optimum" profile generated by OPTIM with a profile containing simplified climb and descent characteristics. The latter profile was computed in TRAGEN, and it consisted of climbing with 250 kt (IAS) to 3.05 km (10000 ft), 305 kt (IAS) to intercepting Mach 0.72, and then holding Mach 0.72 until reaching cruise of 10 km (33000 ft). For descent, the reverse process was used with Mach 0.72, 285 kt, and 250 kt. These numbers were chosen so the climb and descent profiles were similar to those computed in OPTIM. The two profiles compared in cost to within 0.05%. The result indicates that there may be simpler ways to compute the climb and descent portions of the reference profiles which minimize cost, and this is a subject for future investigation.

Recommendations

The OPTIM and TRAGEN programs described in this report are developed to the point where little further modification is required for their use as analytical tools for determining ways to reduce transport aircraft operating costs. The current activity in utilization of the optimization concepts contained within OPTIM is development of a prototype advanced flight management system based on these concepts for further testing in a cockpit simulator and in flight. Effort is currently underway at NASA Langley to exercise a version of the OPTIM code in a cockpit simulator.

This effort will develop the interface to the pilot and the rest of the avionics functions. This process will also answer the questions posed at the end of Chapter II concerning development of an experimental flight management system.

The essence of the current OPTIM program is the generation of climb and descent profiles by minimization of a Hamiltonian function at successive specific energy points. An alternate method is to choose two parameters - constant indicated airspeed followed by constant Mach number - to define climb. The reverse is used to define descent. OPTIM can be configured to choose the optimum values of these parameters. It is recommended that OPTIM be expanded to include this alternate climb/descent profile computation procedure. This would enable the user to compare two computational methods in terms of profile costs and implementation requirements.

Currently, OPTIM and TRAGEN contain the aerodynamic and engine models of medium range twin-jet and tri-jet transport aircraft. Use of the programs for military and commercial applications will require inclusion of additional aircraft aerodynamic and engine models. The programs have been written to facilitate making these additions.

OPTIM has imbedded within it mathematical models of the aircraft lift, drag, thrust, and fuel flow characteristics as functions of various parameters. There is a need for a method to derive or tune these models based on the flight experience of actual transport aircraft. This requires in-flight measurement of altitude, airspeed, acceleration, throttle setting, EPR, fuel flow, ambient temperature and other variables that govern aerodynamic and engine performance. From these measurements, the required models could be identified. This process would serve all potential users of flight management systems (FMS) because they could use it to match the FMS models to the host aircraft. It is recommended that such a methodology be developed.

This report showed that various parameters could be adjusted to save fuel during takeoff. A special program has been written to simulate the

takeoff portion of flight, and this was used for the parametric study. It is recommended that this program be added to TRAGEN and that it be used for further takeoff analyses.

A recent development which promises to save fuel for short haul transport aircraft is use of the prop fan engine. This powerplant has an additional control variable - propeller pitch - in addition to airspeed and thrust, relative to the vertical profile optimization process contained within OPTIM. It is recommended that a version of OPTIM be developed with modification to optimize with three variables, and that this version be used as an analysis tool for study of prop fan applications.

The Federal Aviation Administration has a program underway to automate enroute air traffic control. This program (referred to as AERA) has the goal of generating enroute profiles that are fuel efficient, conflict free, and provide metered arrival times for all scheduled aircraft. The OPTIM algorithm, with its fixed time-of-arrival option, could be an integral part of the AERA software. Also, the Langley ATOPS aircraft, equipped with a flight management system based on OPTIM, could be a very effective research system for testing the airborne counterpart of the AERA concepts. It is recommended that investigation of this possibility be explored as part of a joint NASA/FAA research effort.

Within this context, a very important aspect of flight planning, flight management, and fuel reduction is having good weather forecasting techniques, weather measurement and reporting systems, and weather modeling capability. There is current research and development effort underway sponsored by NASA, FAA, and NOAA agencies to obtain these capabilities. As part of the AERA investigation suggested above, it is recommended that this weather modeling activity be reviewed, and that software be developed to interface the weather models with flight planning and flight management software based on OPTIM.

At this point, OPTIM is limited to determining the optimum vertical profile after the horizontal route has been determined. Computer programs exist which compute the optimum horizontal path for oceanic travel, based

on a given wind model. It is recommended that these programs and other methods be investigated to determine if they can be applied to generation of minimum-cost three-dimensional paths for continental route structures.

Associated with on-board use of OPTIM, a computer program is required to generate the desired horizontal flight path and a preliminary weather model for use by the airborne flight management system. The horizontal path would probably consist of a sequence of waypoints, and it could be input to the flight management computer via casette prior to flight. It is recommended that this technique be developed in conjunction with the 3-D optimization and weather modeling studies suggested above.

APPENDIX A

EFFECT OF CONSTRAINED DESCENT ON FLIGHT PERFORMANCE

OPTIM has been modified to include constraining the descent rate for cabin pressurization reasons. This constraint is of the form of holding the sink rate constant (e.g., -500 ft/min) until a certain pressure altitude is reached (e.g., 4.7 psi at 29000 ft). The aircraft is held at constant Mach number during this period.

In order to determine the effect of varying the different parameters (sink rate, cabin overpressure, and descent speed) on flight performance, a computer program was written to compute constrained descent profiles. Performance is measured in terms of fuel and time changes to cover the same altitude and range. The program uses as subroutines the models of the aerodynamic and the engine performance now used in the OPTIM program. The program computes a time history of descent from cruise altitude to any specified ending altitude. At every point along the descent trajectory, performance and flight dynamic parameters such as fuel flow, thrust, airspeed, rate of descent, fuselage angle, angle-of-attack, and flight path angle are determined.

Although any descent strategy (such as those described in Ref. 10) can be easily built into the program, the strategy used was to follow constant MACH - constant indicated airspeed descents. At 3048 m (10000 ft) and below, the indicated airspeed was set to 250 knots.

The baseline descent profile used in this study is given in Fig. A.1. The descent begins at a Mach number of 0.73 at 10058 m (33000 ft) and descends at a rate which limits the equivalent rate of descent in the cabin to 2.54 m/sec (500 ft/min). At 8839 m (29000 ft), the cabin pressure has built up to 101348 N/m^2 (14.7 psia), and the descent is no longer limited by cabin pressure constraints. Mach number is maintained at 0.73 until the equivalent airspeed increases to 320 knots. From that point, the

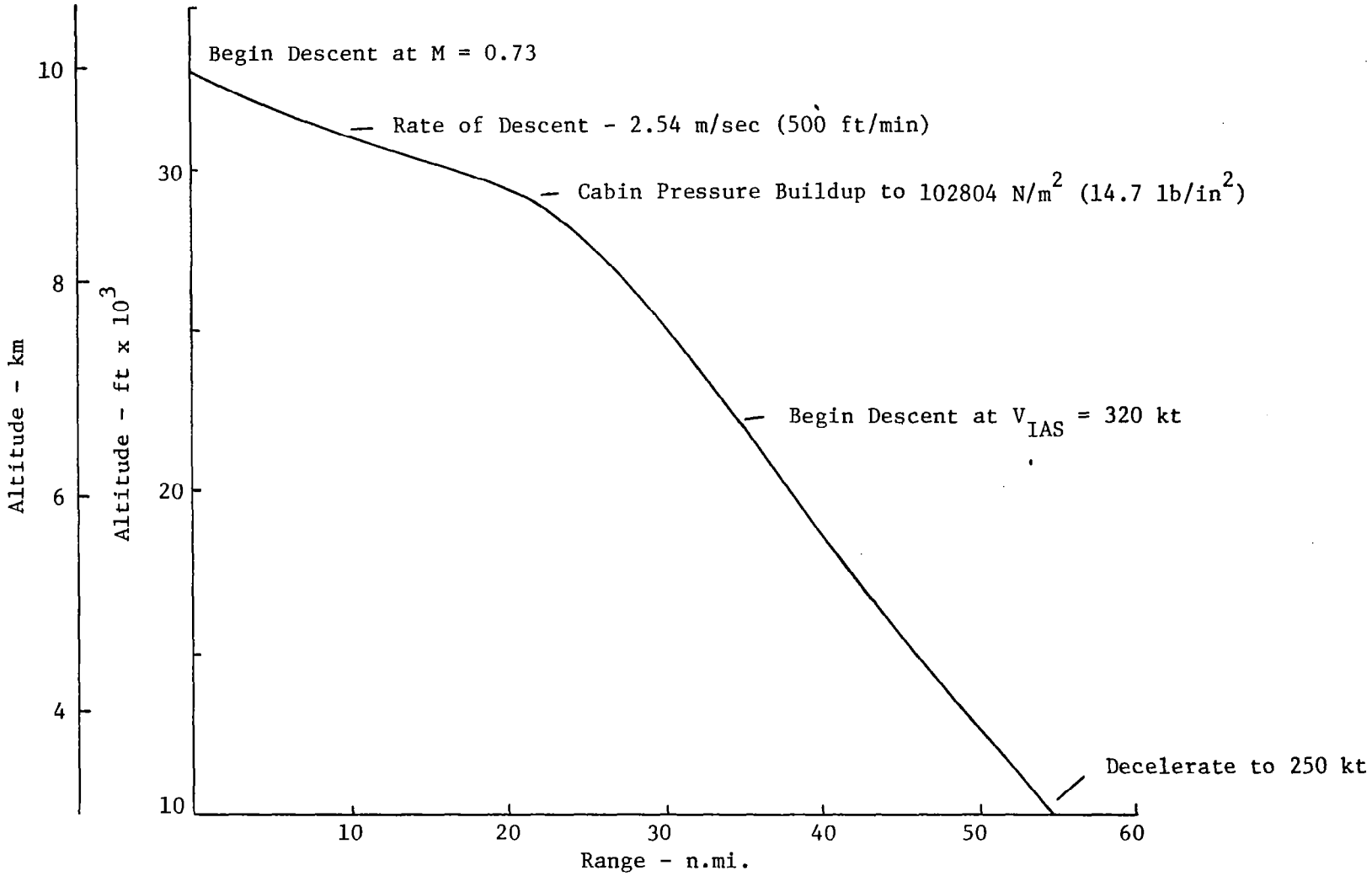

Figure A.1. Baseline Descent Profile for Study of Cabin Pressurization Constraint Effects

320 knot speed is maintained down to 3048 m (10000 ft) where the aircraft decelerates to 250 knots and maneuvers for the ATC approach. In actual practice, the deceleration to 250 knots would begin at approximately 3353 m (11000 ft) and be completed at 3048 m (10000 ft).

The descent begins with the engines at idle thrust, but two constraints are tested which can increase the thrust requirements. The first is the cabin rate of descent constraint discussed in Chapter II. The cabin overpressure is an input to the program, and the top of the descent is limited to follow a path which constrains the cabin rate of descent. The second constraint is the fuselage floor angle (pitch angle). A maximum allowable angle is input to the program, and the trajectory is modified to maintain this angle (by reducing the flight path angle and increasing the thrust). The floor angle constraint is typically 6-8 deg and is not a factor in large transport aircraft descent operations. The floor angle for all descents computed in this study was less than 6 deg.

Trajectories and performance with the rate of descent constraint have been computed for the following set of inputs which represent typical conditions for the twin-jet model:

Standard Day Atmosphere		
Aircraft Weight	-	35.56 tonne (78400 lb)
Cruise Altitude	-	10058 m (33000 ft)
Cruise Mach No.	-	.73
Begin Descent Mach No.	-	.73
Descent Speed (indicated)	-	320 kt
Cabin Overpressure	-	68944 N/m^2 (10 psi)
Maximum Cabin Rate of Descent	-	2.54 m/sec (500 fpm)

The above set of parameters represent a baseline condition. Parametric variations in maximum cabin rate of descent, cabin overpressure and descent speed have been made, and the resulting trajectories and performance measure are given in the following sections. Results are given for the descent stopping at 3048 m (10000 ft). Below this altitude, speed

is constrained to 250 KIAS, and the aircraft is usually vectored by ATC requirements.

Maximum Cabin Rate of Descent This rate of descent was varied from 1.52 to 3.56 m/sec (300 to 700 ft/min), and the resulting trajectories are sketched in Fig. A.2. With an overpressure of 68944 N/m^2 (10 psi), the sea level cabin pressure occurs at approximately 8839 (29000 ft).

Although constrained for only 1219 m (4000 ft) (10058 m to 8839 m) (33000 ft to 29000 ft)), the impact on performance is significant, as shown in Fig. A.3. Data are shown for the descent only and for a fixed range (i.e., a cruise portion is added). Comparisons at the fixed range are more meaningful. They show virtually no change in the time to descend. However, they show a decrease of approximately 54.4 kg (120 lb) of fuel in going from 1.52 to 3.56 m/sec (300 to 700 fpm) cabin rate of descent.

Cabin Overpressure The nominal value of 68944 N/m^2 (10 psi) overpressure was reduced to 62050 N/m^2 (9 psi) and 55155 N/m^2 (8 psi). The effects on the trajectories are shown in Fig. A.4; the effects on the performance measures are shown in Fig. A.5. From these results, it would appear that high cabin overpressure is very desirable. However, for overall cost performance, other factors must also be considered. First, the cabin rate of descent of 2.54 m/sec (500 ft/min) may be too low. A higher allowable rate of descent would reduce the impact on the fuel burned. Second, the higher overpressure requires more weight in the fuselage (which must be carried over the complete trip) and requires more air bleed from the engine. (See the following Appendix B on propulsion system losses).

Descent Speed Most airlines have reduced the descent speed to reduce fuel. There is an increase in descent time but with increased fuel prices, this is not considered determintal. The effect on the trajectory and the performance for reducing the constant indicated airspeed segment from 320 KIAS to 250 KIAS is shown in Figs. A.6 and A.7 respectively. For the constant range results, fuel is reduced 22.68 kg (50 lb) with an increase in time of 95 seconds when the descent speed is reduced from 320 to 250 KIAS.

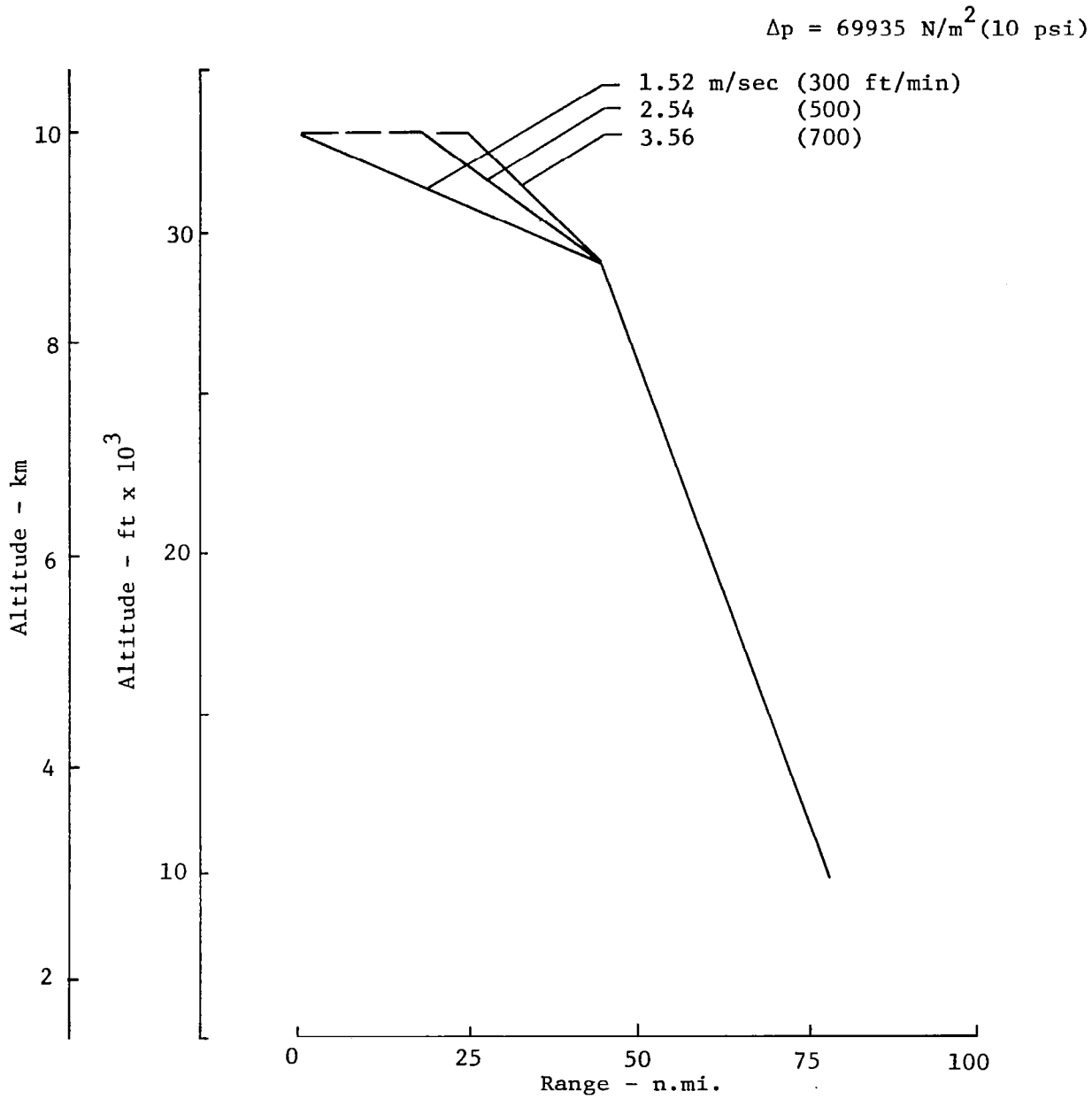

Figure A.2. Descent Profile Variations as a Function of Rate of Descent

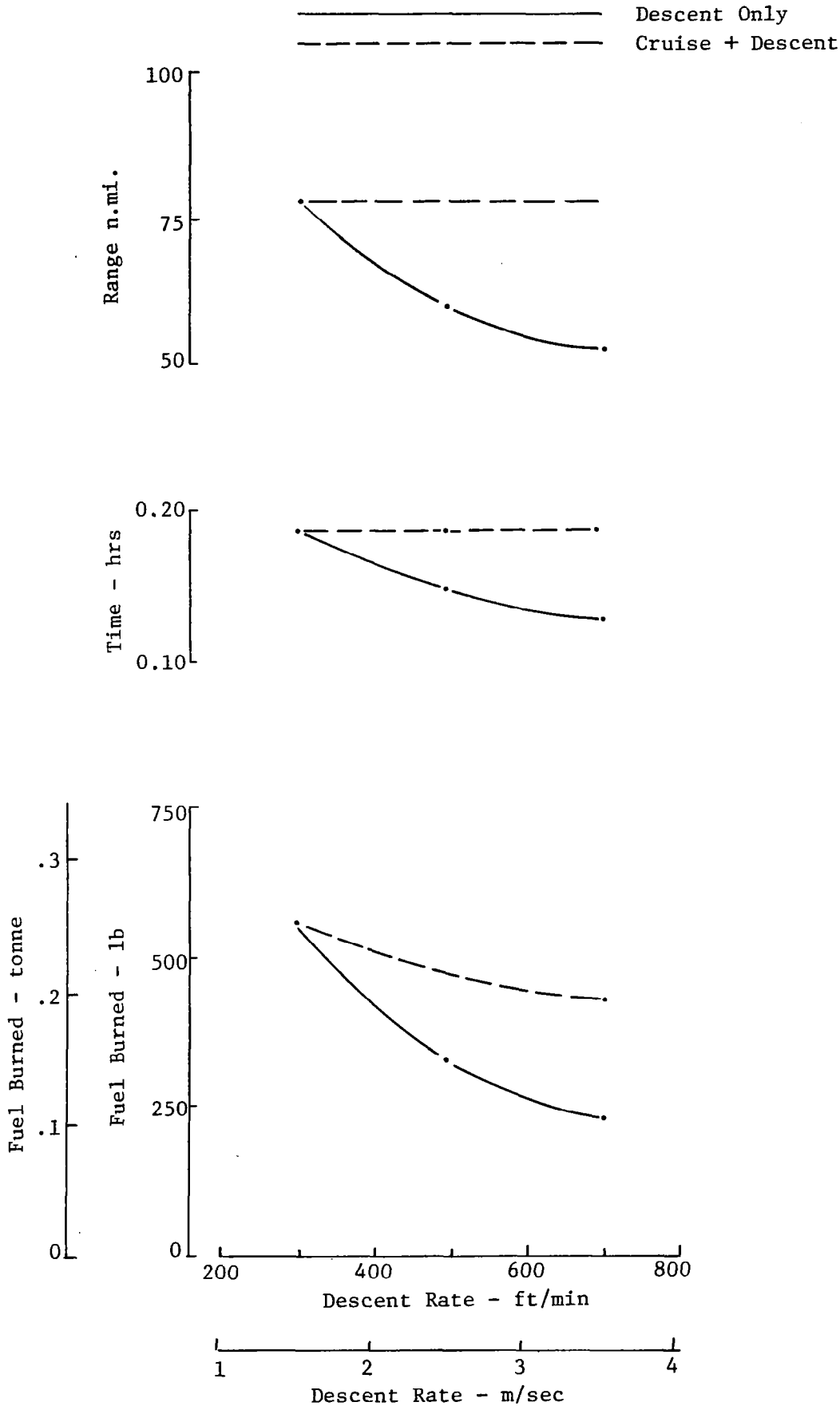

Figure A.3. Variation in Descent Range, Time, and Fuel Burned as Functions of Rate of Descent Limits

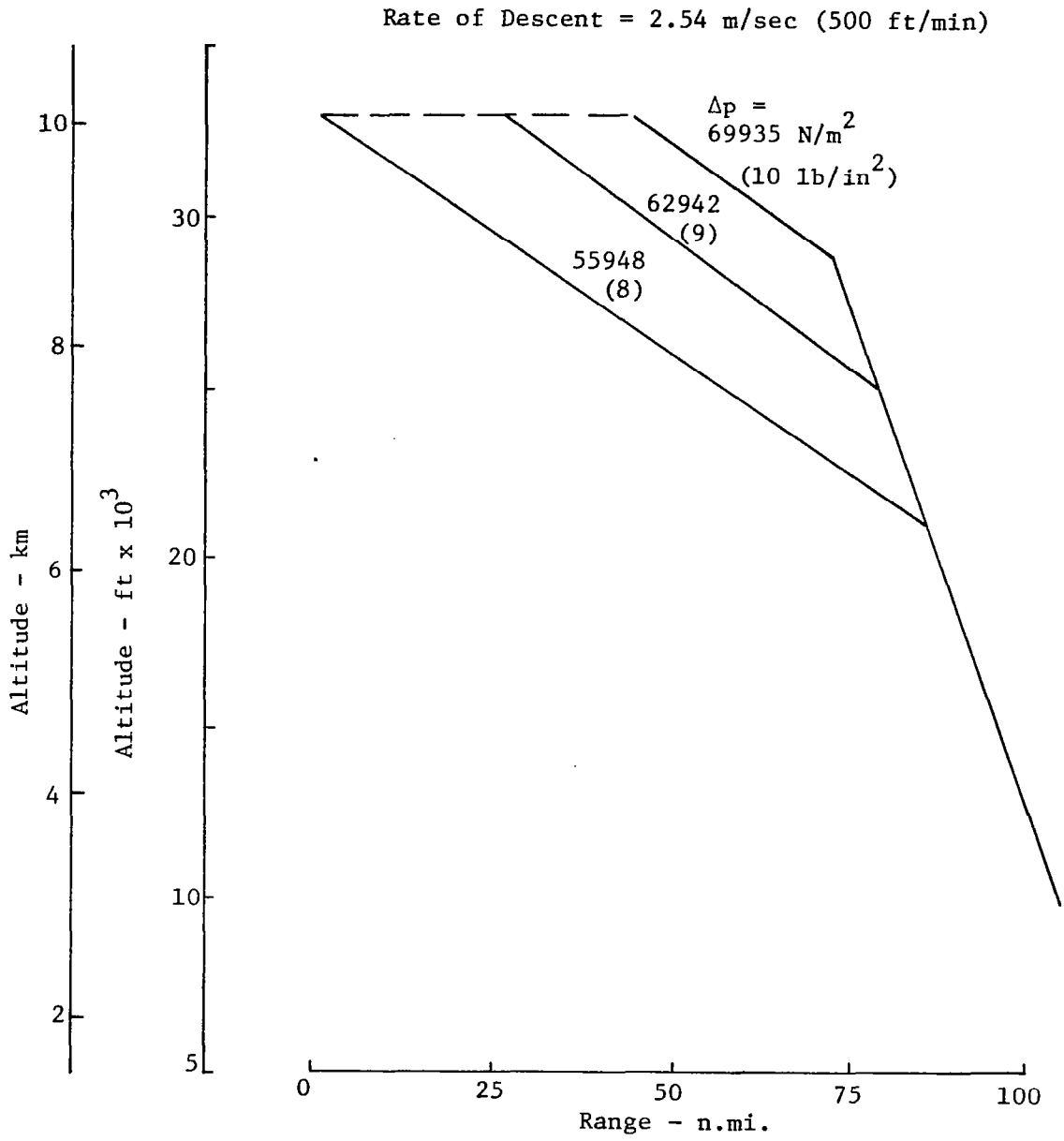

Figure A.4. Descent Profile Variations as a Function of Cabin Overpressure Constraints

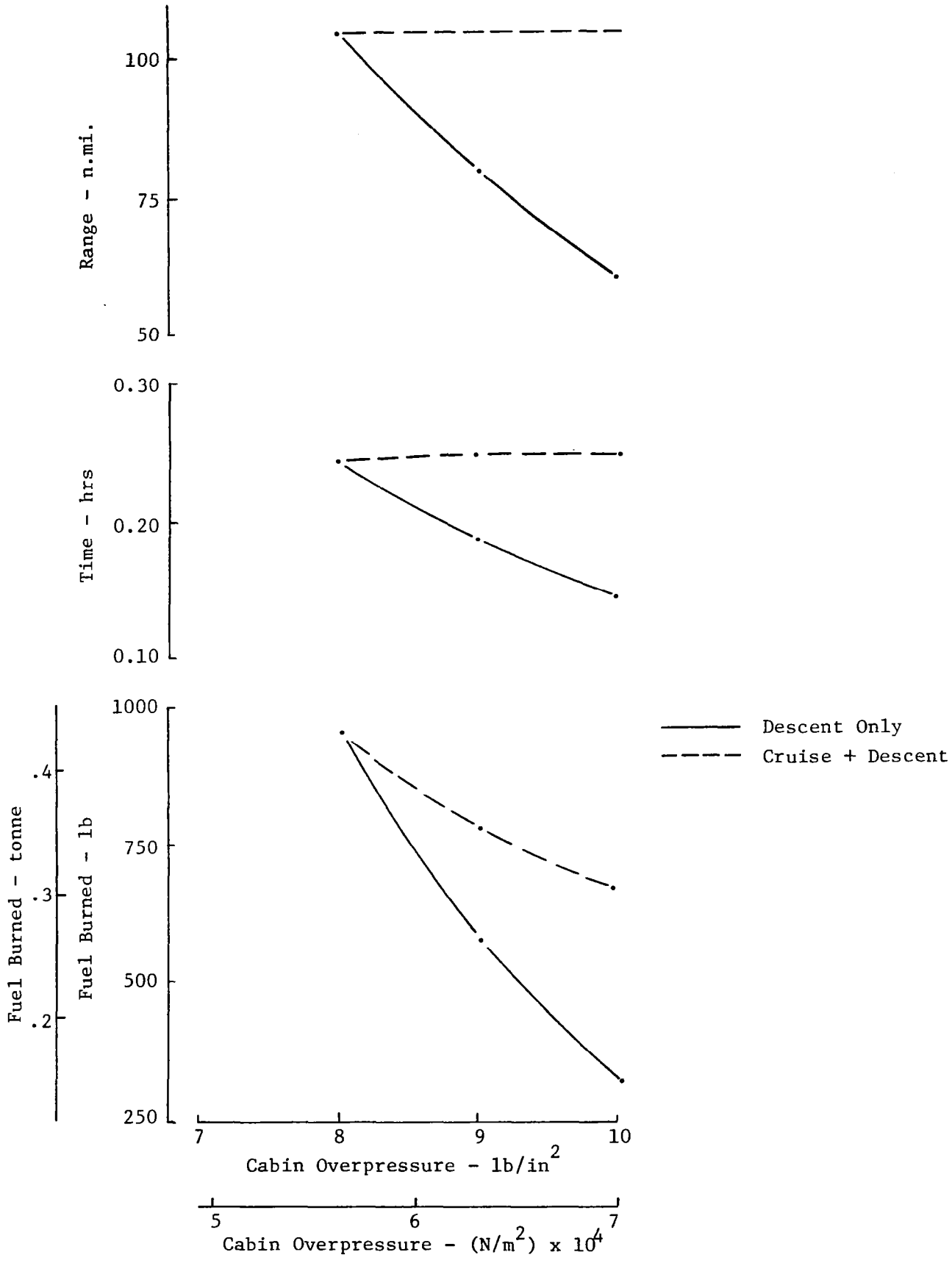

Figure A.5. Variations in Descent Range, Time, and Fuel Burned as Functions of Cabin Overpressure Constraints

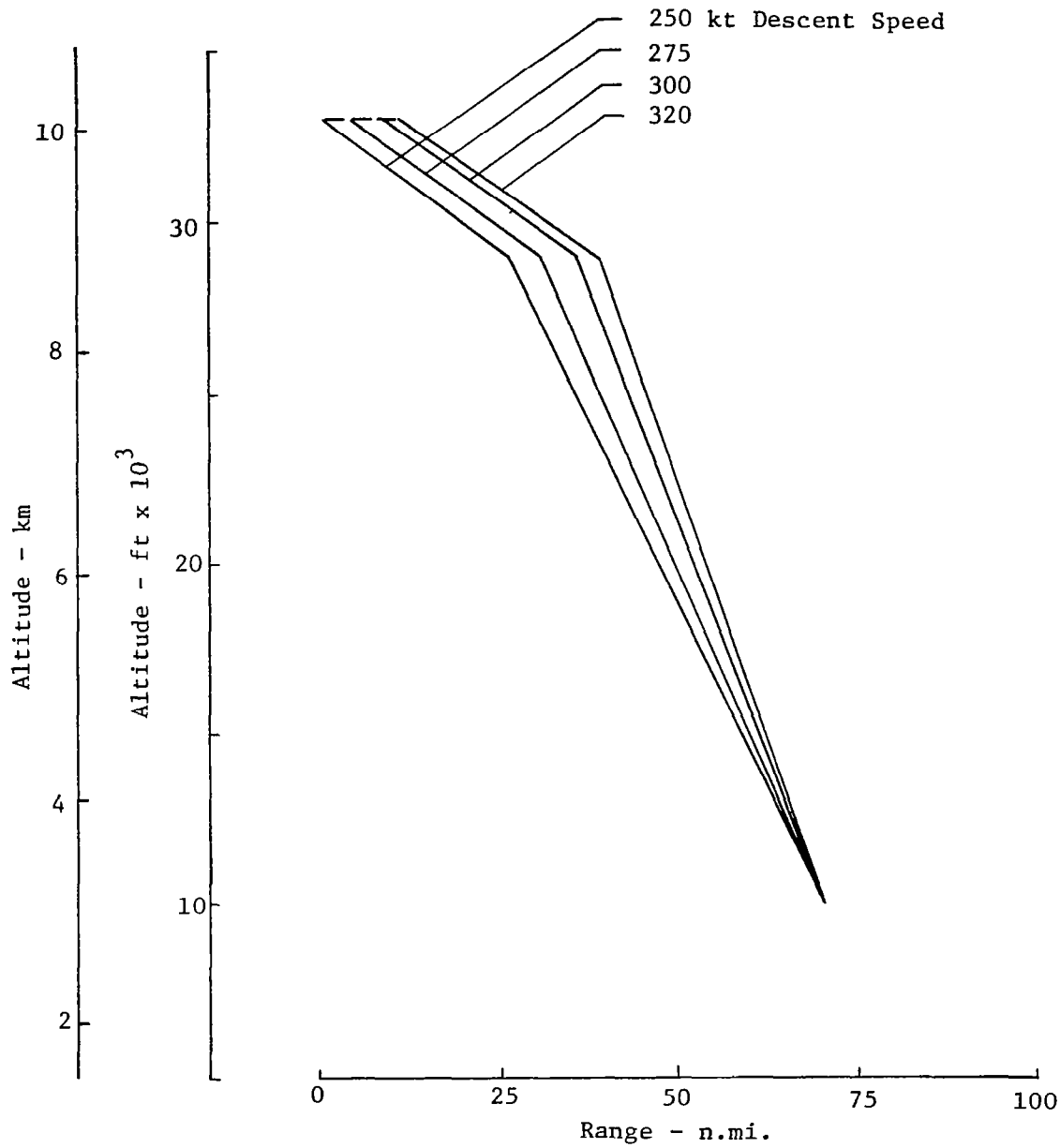

Figure A.6. Variation in Descent Profiles for Changes in the Constant Indicated Airspeed Segment

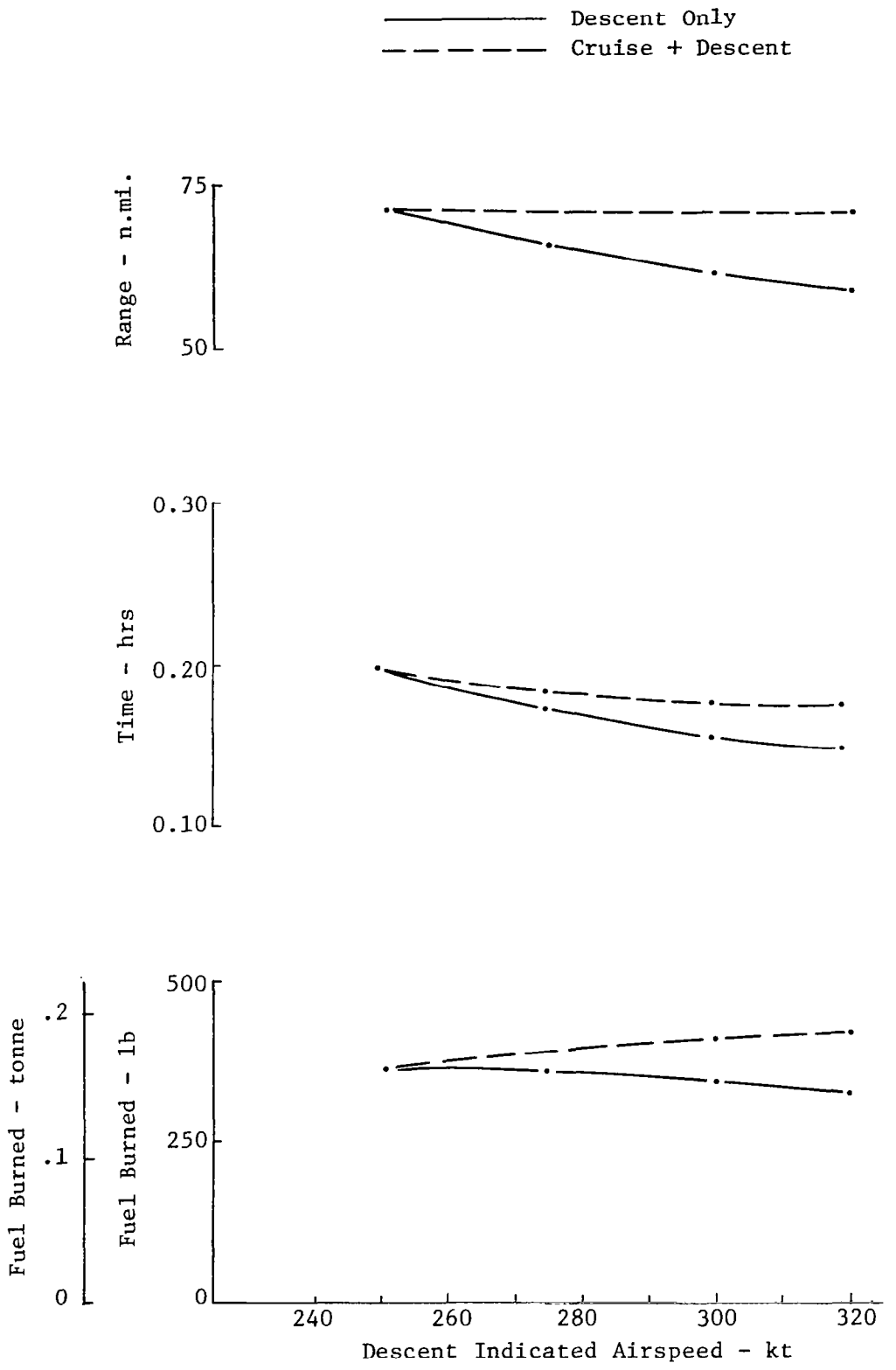

Figure A.7. Variations in Descent Range, Time, and Fuel Burned for Changes in the Constant Indicated Airspeed Segment

The above descent computations prove to be useful for conducting tradeoff studies of fuel burned and other measures of operation performance. They represent desirable applications of the TRAGEN program capability. In addition, rate of descent constraints for maintaining appropriate cabin pressure need to be included in the descent portion of the profile optimization produced by the OPTIM program.

APPENDIX B

TAKE-OFF PERFORMANCE ANALYSIS

Trajectories and performance have been computed for the following set of inputs which represent a typical condition for the twin-jet aircraft.

Standard Day Atmosphere		
Aircraft weight	-	40.824 tonne (90000 lb)
Airport altitude	-	sea level
Flaps 15 procedure for flap setting and extraction (See Figs. B.1 - B.3)		
Rotation speed	-	123 kt
Rotation rate	-	5 deg/sec
Maximum load factor during rotation	-	1.17
Acceleration altitude	-	610 m (2000 ft)
Maximum rate of climb during acceleration	-	2.794 m/s (550 fpm)
heading offset	-	0 degrees .

The sequence of take-off steps simulated are as shown in Fig. 29 . The take-off distance to the 11 m (35 ft) obstacle height and fuel burned to reach a final altitude/airspeed condition have been computed, and they are given with the data which follow.

Flap Setting Several flap setting configurations are recommended by the manufacturer for take-off. Figures B.1, B.2, and B.3, taken from the Pilots Training Manual, identify the procedures and flap retraction schedule for the twin-jet model aircraft. The tabulated data, given in Table B.1 is taken from the Operations Manual, and in it values of V_1, V_R and V_2 are specified for all combinations of take-off altitude, ambient temperature, aircraft take-off weight and flap setting.

The initial step in the study was to calibrate the program for the Flaps 15 configuration and rotation speed. The published take-off distance

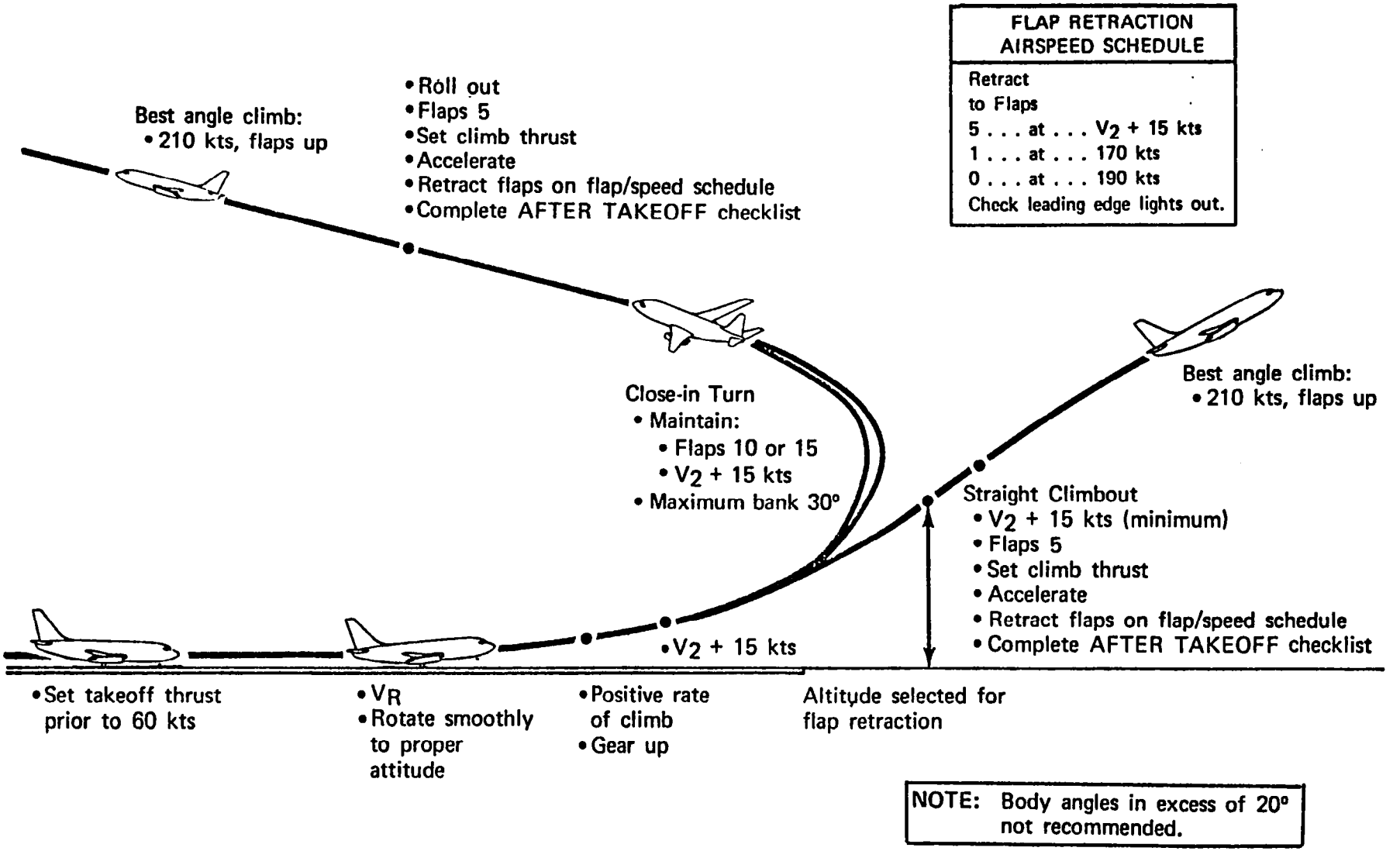

Figure B.1, Twin-Jet Take-off; Flaps 10 or 15 Schedule

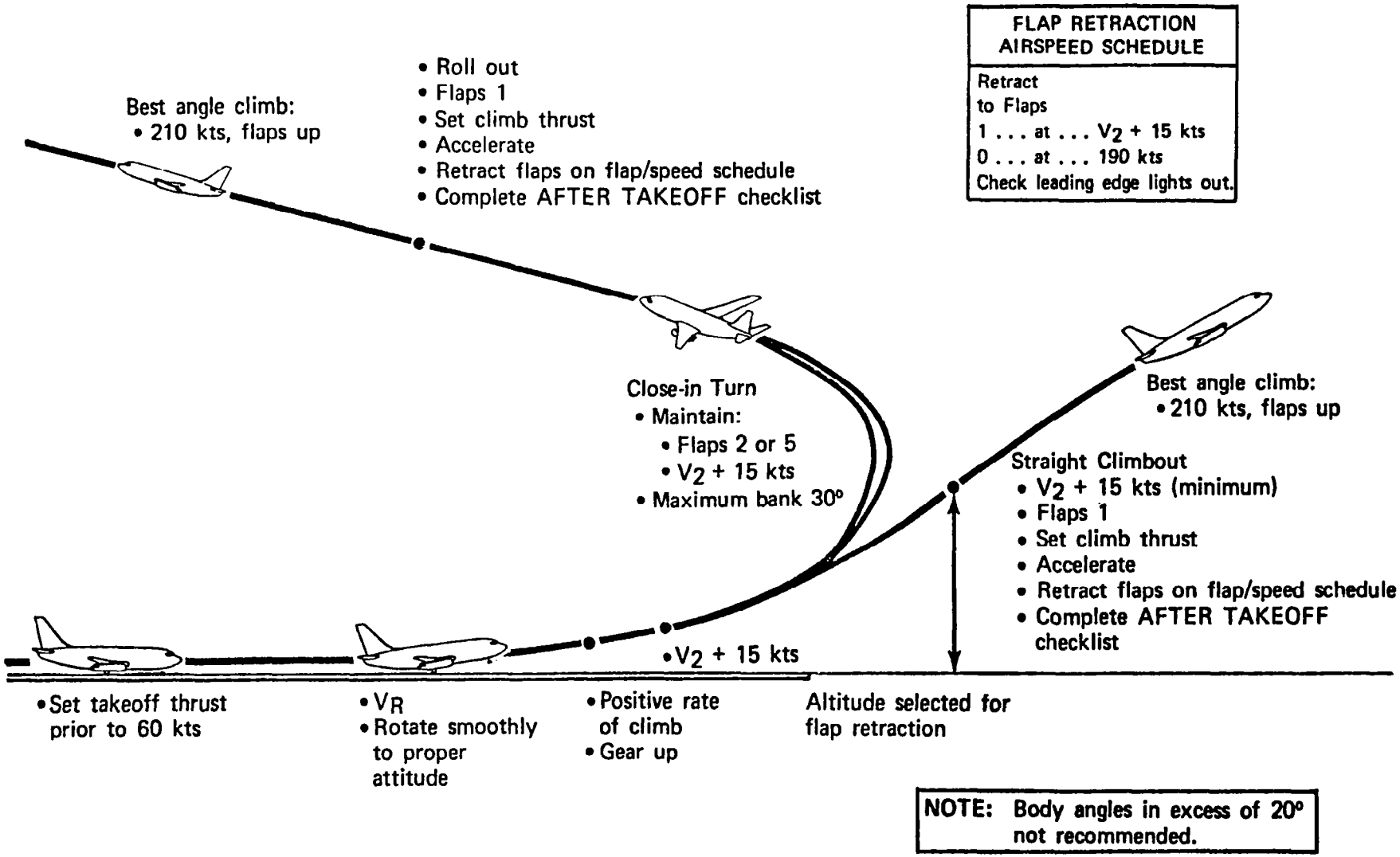

Figure B.2. Twin-Jet Take-off; Flaps 2 or 5 Sechedule

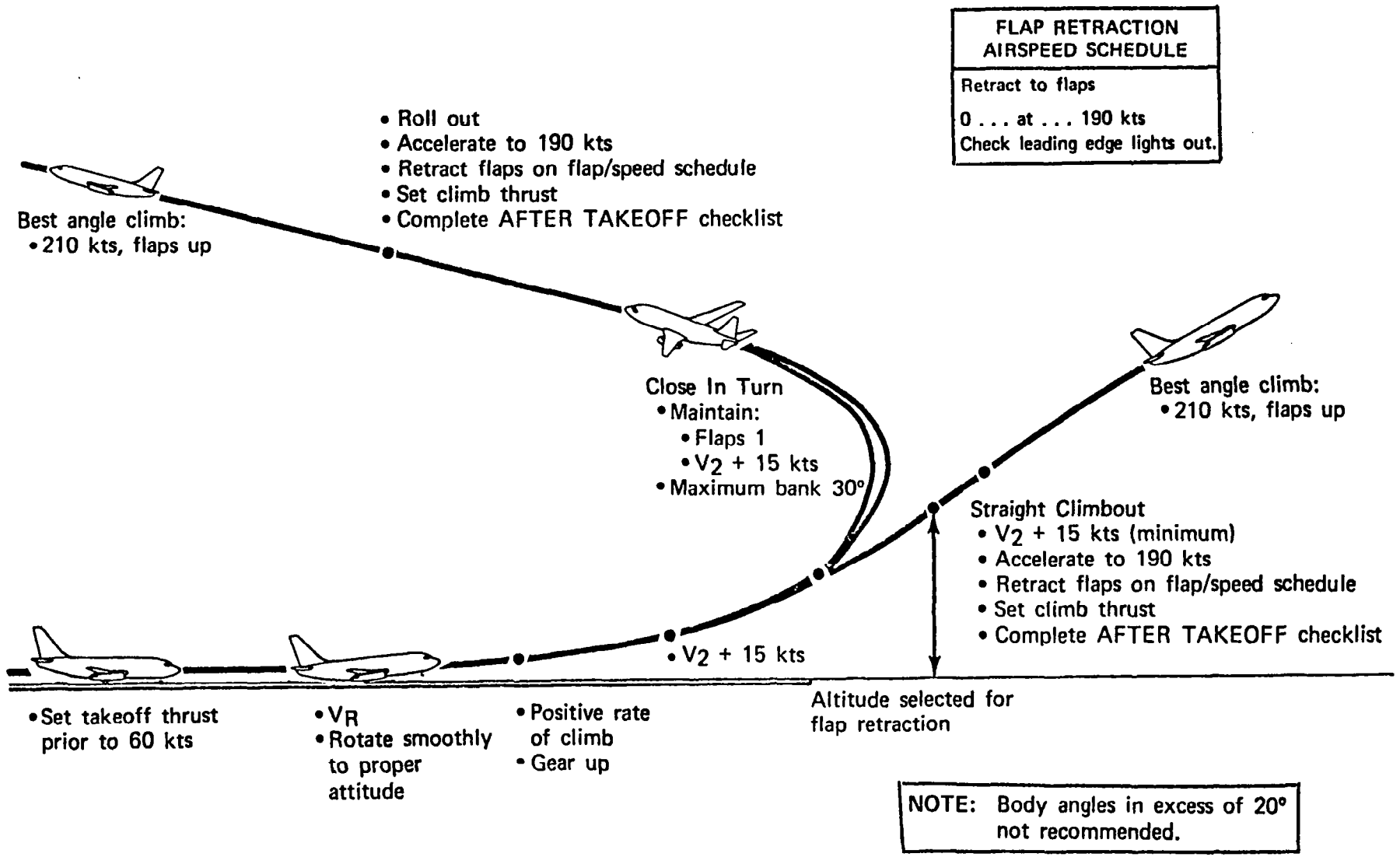

Figure B.3. Twin-Jet Take-off; Flaps 1 Schedule

Table B.1. Recommended Take-off Settings for EPR, Flaps, and Airspeed as Functions of Weight, Temperature, and Other Parameters for Twin-Jet Model

0 TO 60 KTS TAKEOFF EPR

A/C ON

EPR BLEED CORRECTIONS	Δ EPR
AIR CONDITIONING	OFF: +.03
ENGINE ANTI-ICE	ZERO

OAT																				
°F	-65	-49	-40	-31	-22	-13	-4	5	14	23	32	41	50	59	68	77	86	95	104	120
°C	-54	-45	-40	-35	-30	-25	-20	-15	-10	-5	0	5	10	15	20	25	30	35	40	49
TEMP LIMIT EPR	2.31	2.27	2.25	2.23	2.20	2.18	2.15	2.12	2.10	2.07	2.04	2.01	1.98	1.95*	1.95*	1.95*	1.94	1.90	1.85	1.78
PRESS EPR	2.23				2.16			2.10		2.05	2.00			1.95			1.91			
ALT	5000				4000			3000		2000	1000			S.L.			-1000			

① FIND TEMP LIMIT EPR
② FIND PRESS LIMIT EPR
③ USE THE SMALLER OF THE TWO LIMITS

* ADD .01 EPR @ 6-7000 FT OR .02 EPR @ 8000 FT & ABOVE

V_1, V_R, V_2

ANTI-SKID ON

PRESSURE ALTITUDE -1000 FT		OAT					
9 to 10	°F		-65 to -62	-61 to -21	-20 to 15	16 to 44	45 to 94
	°C		-54 to -53	-52 to -30	-29 to -10	-9 to 7	8 to 34
7 to 9	°F		-65 to -28	-27 to 6	7 to 36	37 to 87	88 to 106
	°C		-54 to -34	-33 to -15	-14 to 2	3 to 30	31 to 41
5 to 7	°F	-65 to -21	-20 to 7	8 to 36	37 to 85	86 to 103	104 to 121
	°C	-54 to -30	-29 to -14	-13 to 2	3 to 29	30 to 39	40 to 49
3 to 5	°F	-65 to 13	14 to 37	38 to 87	88 to 102	103 to 117	118 to 123
	°C	-54 to -11	-10 to 2	3 to 30	31 to 38	39 to 47	48 to 50
1 to 3	°F	-65 to 41	42 to 87	88 to 102	103 to 118	119 to 123	
	°C	-54 to 4	5 to 30	31 to 38	39 to 47	48 to 50	
-1 to 1	°F	-65 to 89	90 to 102	103 to 118	119 to 123		
	°C	-54 to 31	32 to 38	39 to 47	48 to 50		

FLAPS	GROSS WT -1000 LB	V_1	V_R	V_2	V_1	V_R	V_2	V_1	V_R	V_2	V_1	V_R	V_2	V_1	V_R	V_2	V_1	V_R	V_2
1	120	159	161	163	159	161	163												
	110	149	151	155	150	152	155	151	153	155	151	153	155	-	-	-	-	-	-
	100	140	142	146	141	143	146	141	143	146	142	144	146	143	145	146	-	-	-
	90	131	133	137	131	133	137	132	134	137	133	135	137	134	136	137	135	137	137
	80	122	125	130	122	125	130	122	125	130	123	126	129	124	127	129	125	128	129
	70	112	116	122	113	117	122	113	117	122	114	118	121	114	118	121	115	119	121
5	120	153	156	158	154	157	158												
	110	145	147	150	146	148	150	147	149	150	-	-	-	-	-	-	-	-	-
	100	136	138	142	137	139	142	138	140	142	139	141	142	-	-	-	-	-	-
	90	126	128	134	127	129	134	129	131	134	130	132	134	131	133	134	132	134	134
	80	117	119	126	118	120	126	119	121	126	121	123	126	122	124	126	123	125	126
	70	107	110	119	108	111	118	109	112	118	110	113	118	111	114	118	112	115	118
15	110	140	140	143	141	141	143												
	100	132	132	135	132	132	135	133	133	135	-	-	-	-	-	-	-	-	-
	90	123	123	128	124	124	128	125	125	128	126	126	128	127	127	128	-	-	-
	80	113	114	120	114	115	120	115	116	120	116	117	120	117	118	120	118	119	120
	70	104	104	112	104	105	112	105	107	112	106	108	112	107	109	112	108	110	112

SHADED AREA INDICATES PERFORMANCE AFFECTED BY MINIMUM CONTROL SPEED
MINIMUM FIELD LENGTH FOR LIGHTEST WEIGHT ABOVE SHADED AREA IS REQUIRED.

AFTER TAKEOFF NORMAL MANEUVERING SPEEDS

FLAP POS	KTS IAS
0	210
1	190
2	180
5	170
10	160
15	150

FOR MANEUVERS IMMEDIATELY AFTER TAKE-OFF EXCEEDING 15° BANK, MAINTAIN AT LEAST V_2 + 15 AT TAKE-OFF FLAPS

STAB. TRIM SETTING

– UNITS AIRPLANE NOSE UP

CG	FLAPS ALL
6	8
8	7-3/4
10	7-1/2
12	7
14	6-3/4
16	6-1/4
18	5-3/4
20	5-1/2
22	5
24	4-1/2
26	4
28	3-1/2
30	3
32	2-1/2

ENGINE LIMITS

N_1 RPM - 100.1%
N_2 RPM - 100.0%

STARTING EGT
420°C ABOVE 15°C OAT
350°C BELOW 15°C OAT

MAX CONT EGT - 535°C
TAKE-OFF EGT - 570°C

V_1 ADJUSTMENTS*	
WIND	SLOPE
ADD 1 KT PER 20 KTS HEADWIND	ADD 1 KT PER 1% UP SLOPE
SUBTRACT 1 KT PER 5 KTS TAILWIND	SUBTRACT 1KT PER 1% DOWN SLOPE

*V_1 MUST NOT EXCEED V_R

for the baseline conditions specified earlier is 1204 m (3950 ft). This distance was matched in the program by setting the rotation rate at 5 deg/sec and the maximum load factor as 1.17.*

With the program calibrated, performance was computed following the manufacturer specifications carefully. A comparison of fuel burned and distance (field length) required to clear a 11 m (35 ft) obstacle is shown in Fig. B.4 for three different flap schedules. The increased field length at the lower flap settings is very predictable, but the significant reduction in fuel burned up to V_{END} was not anticipated. At 305 m (1000 ft) altitude, well after rotation but before the aircraft accelerates, the fuel burned is approximately the same for all flap configurations. However, with the lower flap settings, the aircraft speed is higher. Thus, there is less acceleration required later to reach V_{END}.

Rotation In calibrating the take-off computer program, it became evident that departures from the specified rotation conditions lead to increasing fuel flow reductions. Figures B.5 and B.6 show the field length/fuel burn tradeoff for the beginning rotation speed and the rotation rate, respectively. Late and slow rotations will reduce fuel burn, and although the field length requirements are increased, they do not appear to be excessive. Certainly this is true for operations out of major airports.

Figure B.7 shows the effect of limiting the maximum load factor during the rotation. This limit is reached for several seconds during the rotation. The effect is to come out of the rotation at a higher speed which reduces the later acceleration required to reach to V_{END}.

These type of tradeoffs persist throughout all the data. Higher rotation speeds result in a longer field length but reduced fuel burn. Besides varying the rotation speed, it would seem that the speed schedule for flap retraction could also be optimized to minimize fuel. This, however, was not done in this study.

---

* A discussion with a major airline operations office revealed that 5 deg/sec is a pretty "snappy" rotation, but not out of the question. In fact, it is more than likely that high rotation rates were used to develop the handbook take-off data. A more typical rotation is 2-3 deg/sec.

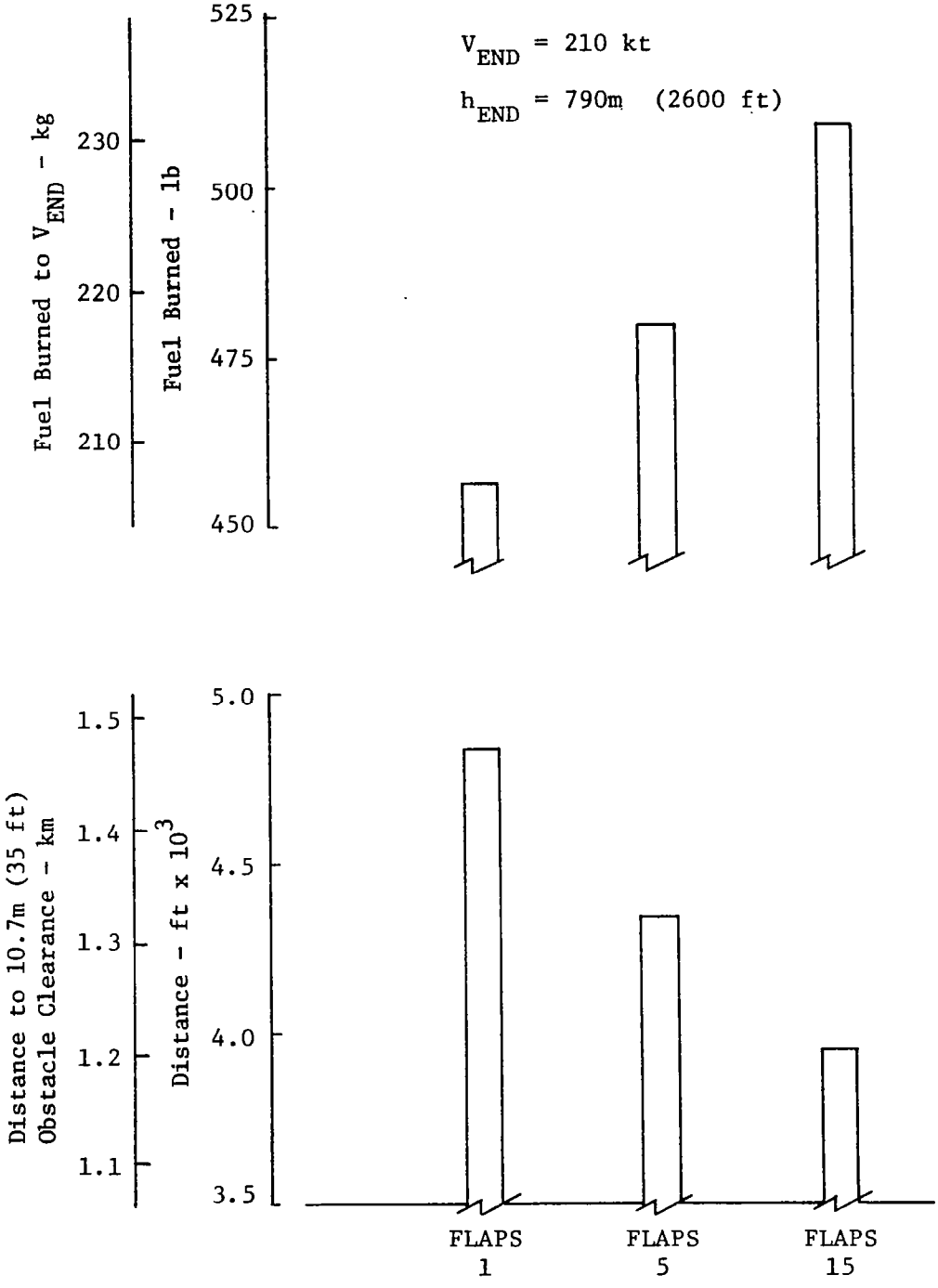

Figure B.4. Bar Chart Showing Performance Measures for Different Flap Schedules

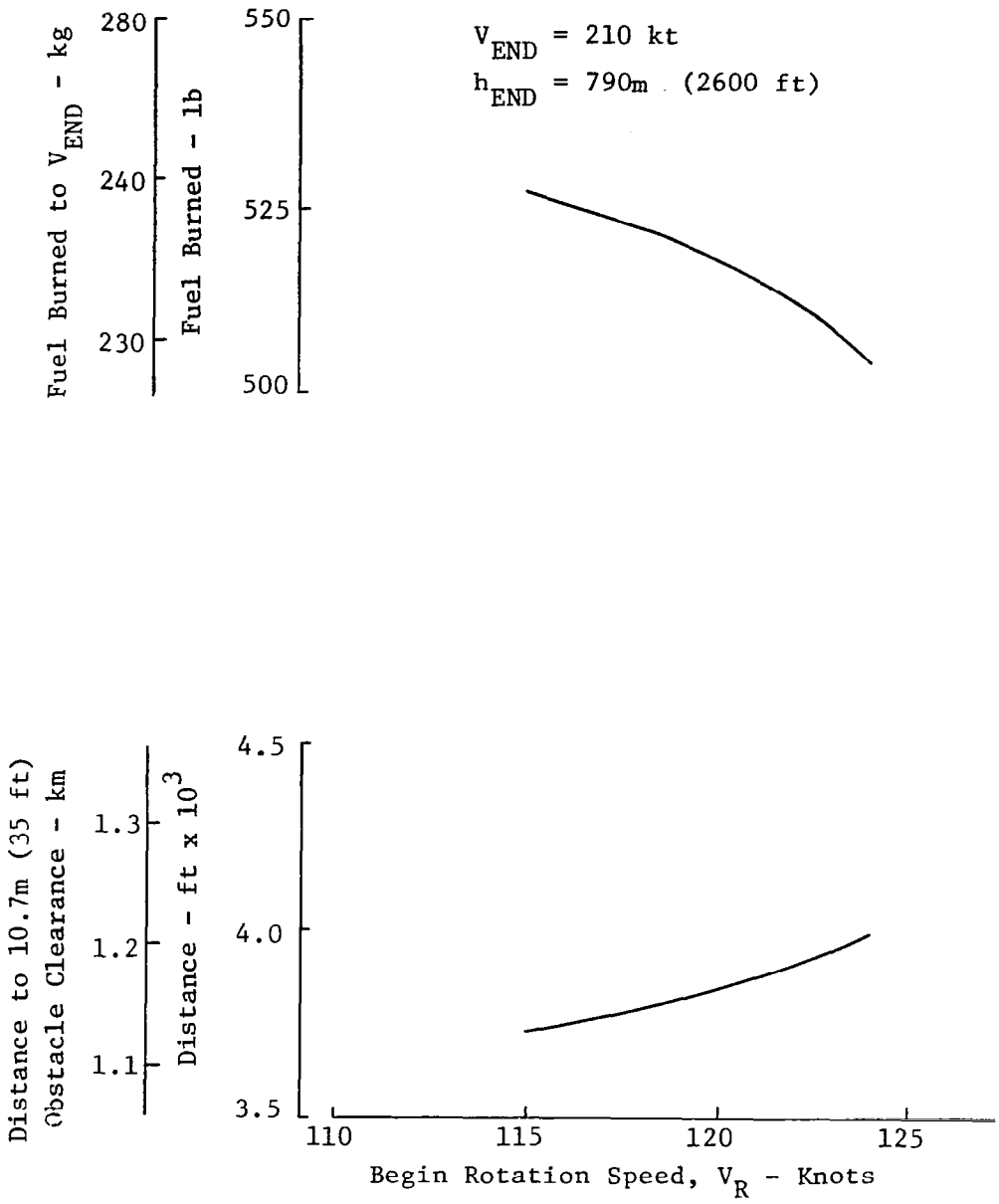

Figure B.5. Performance as a Function of Beginning Rotation Speed V_R

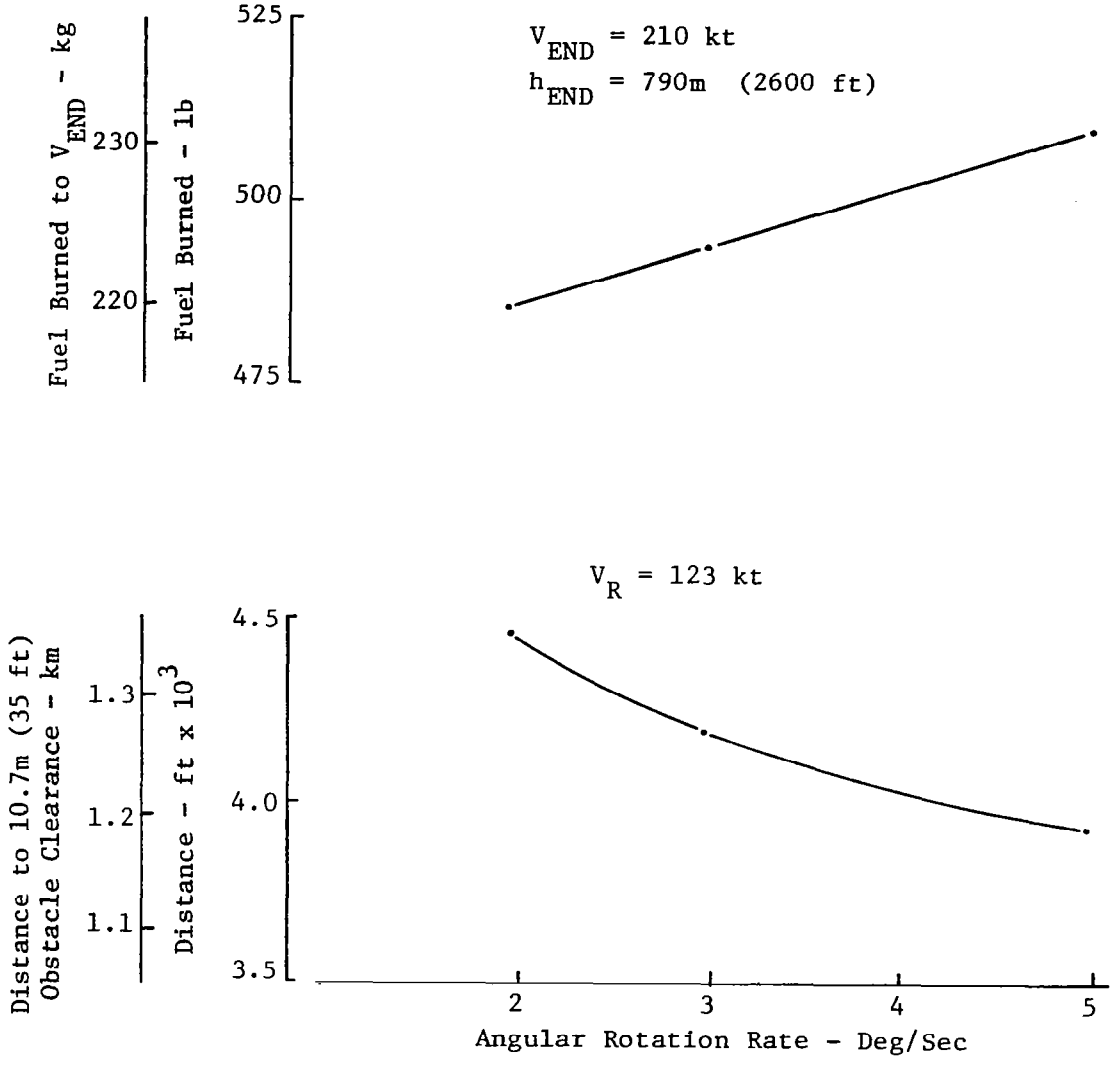

Figure B.6. Performance as a Function of Rotation Rate

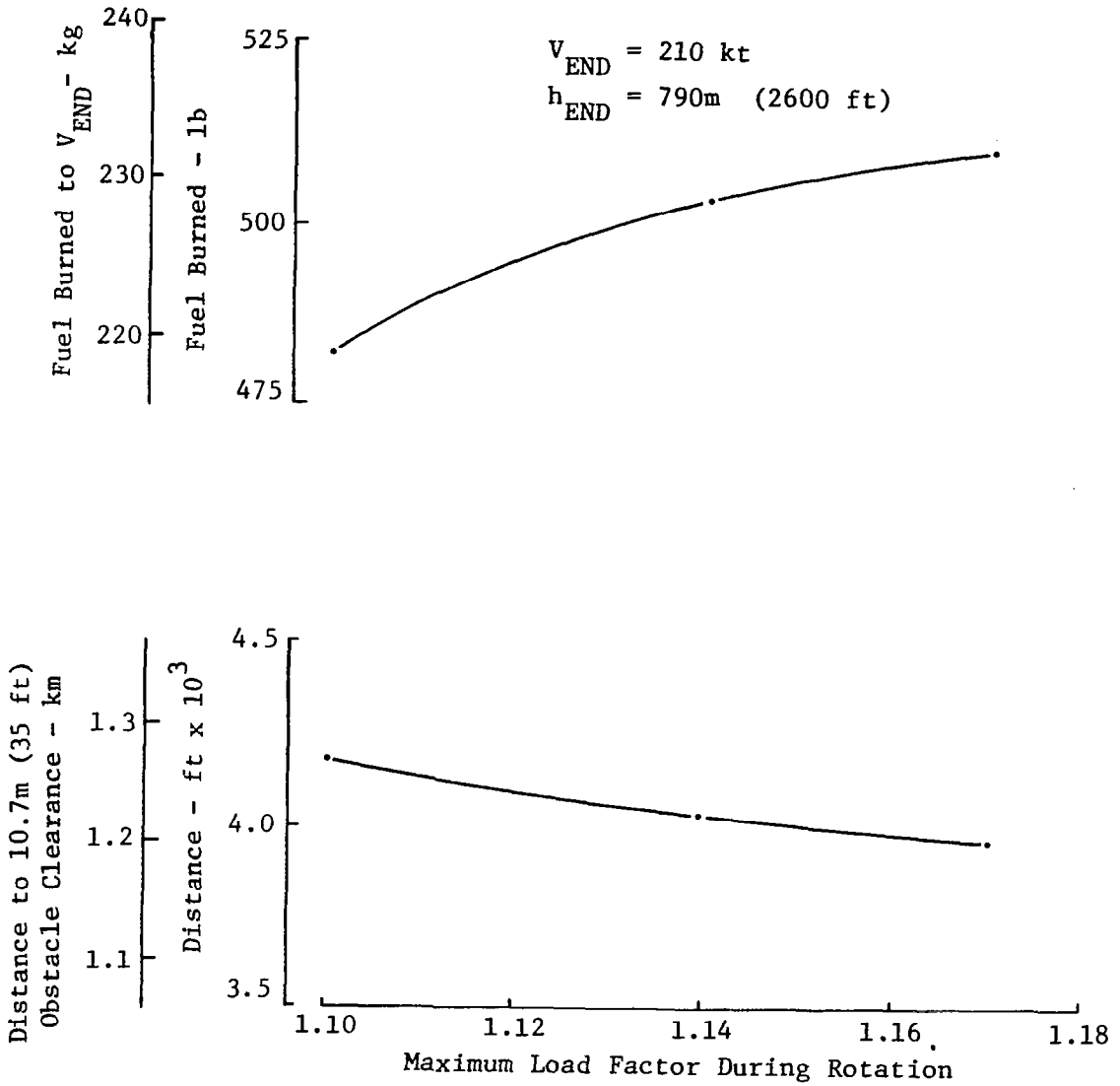

Figure B.7. Performance as a Function of Maximum Rotation Load Factor

Airport and Atmospheric Considerations Any procedures that might be developed to reduce fuel burn would have to adapt to changes in the atmospheric temperatures or the airport altitude. Also, take-off heading changes are required in almost all cases, which offers the opportunity for further optimization. Heading change parameters include the altitude for heading change and the bank angle (and associated turn radius). The following results are examples of these effects which indicate the magnitude of the performance penalty for increase in the ambient temperature and airport altitude or changes in heading.

Figures B.8 and B.9 show the effect of airport altitude and ambient temperature variations, respectively. Increases in either will increase both field length and take-off fuel burn requirements. One factor which may mitigate the fuel penalty for higher altitude airports is the subsequent reduced amount of climb to cruise altitude. This can be investigated with the OPTIM program.

The effect of departure heading change requirements is shown in Fig. B.10. This figure shows (a) the increase in take-off fuel and fuel required for additional cruise range, and (b) the decrease in down-range distance resulting from having to make a heading change because of runway alignment. Actually, the fuel burn penalty to climb to V_{END}, even for the full 180 degree turn, is relatively small. However, if one adds on the fuel required for the increased cruise range required to reach the destination, then the total fuel burn required for the heading change is more significant. This penality was computed by estimating the specific range at the end of cruise and using this value to compute the increase in fuel burn over the longer range.

As can be seen from the results in Figs. B.4 - B.10, the take-off simulation represents another useful fuel performance analysis tool which complements the results of the OPTIM and TRAGEN programs. This program can be used to select realistic starting conditions (beginning of climb) to input to the OPTIM program. It also can be used for tradeoff and performance analysis studies of the take-off phase of flight.

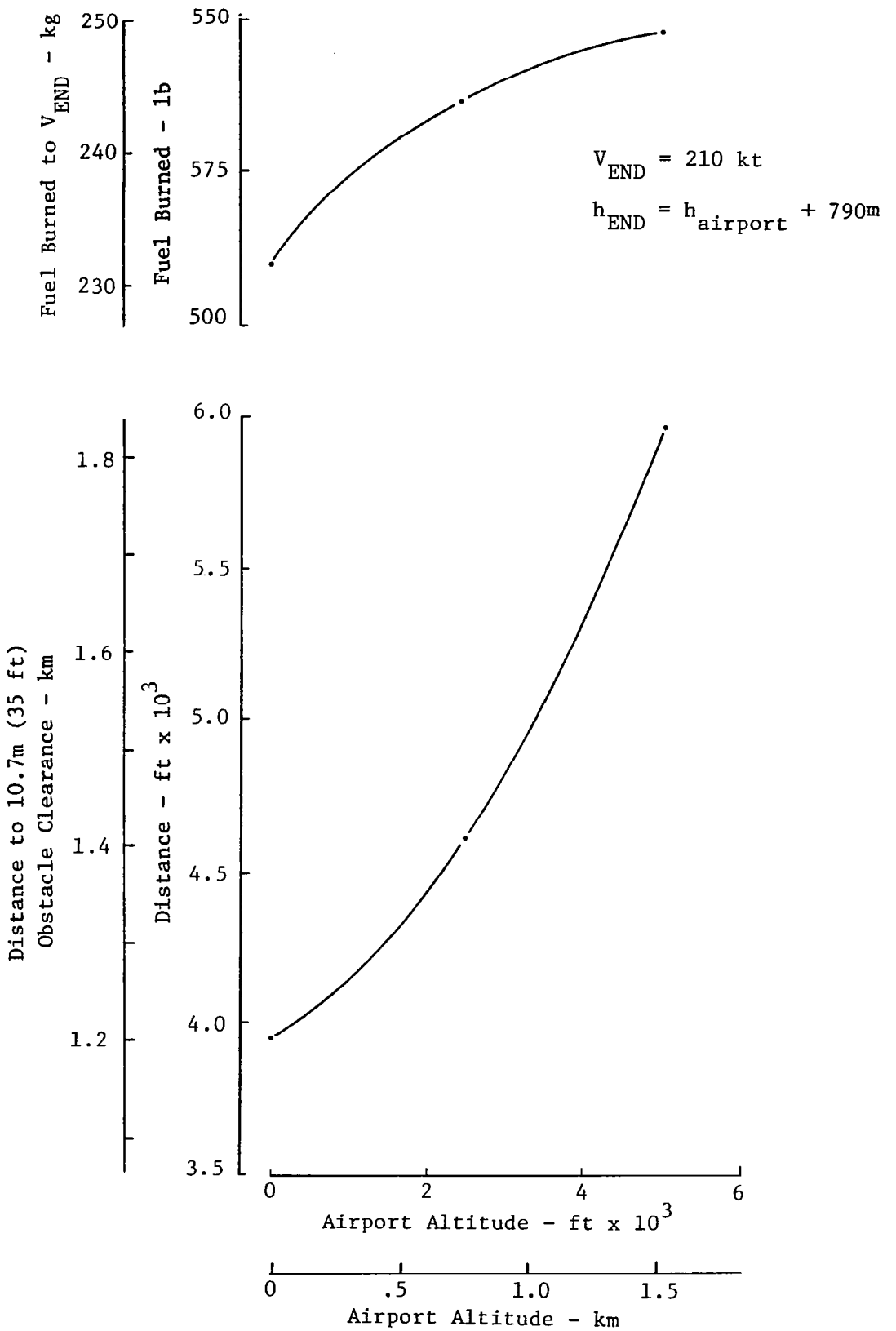

Figure B.8. Performance as a Function of Airport Altitude

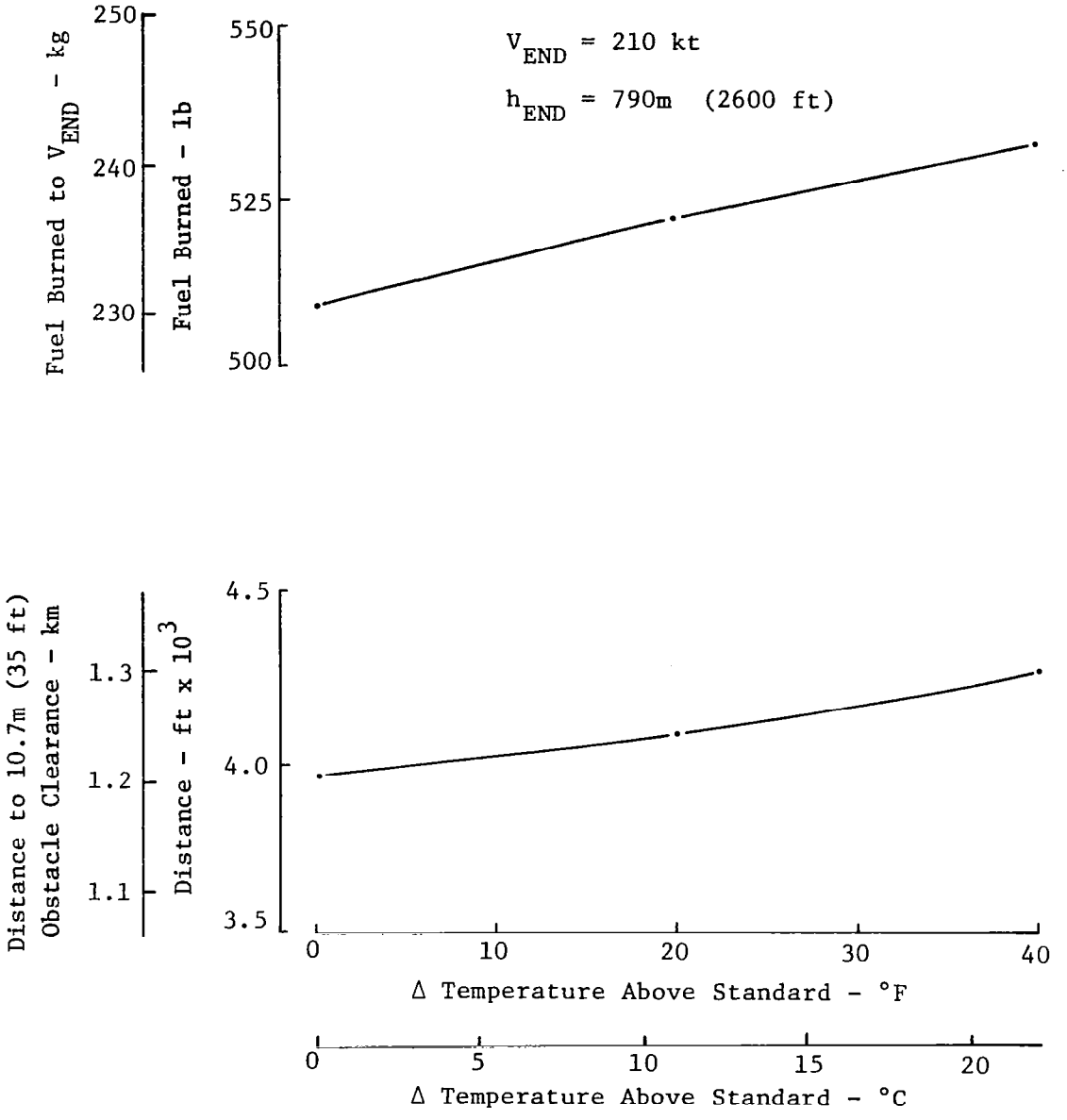

Figure B.9. Performance as a Function of Change in Ambient Temperature

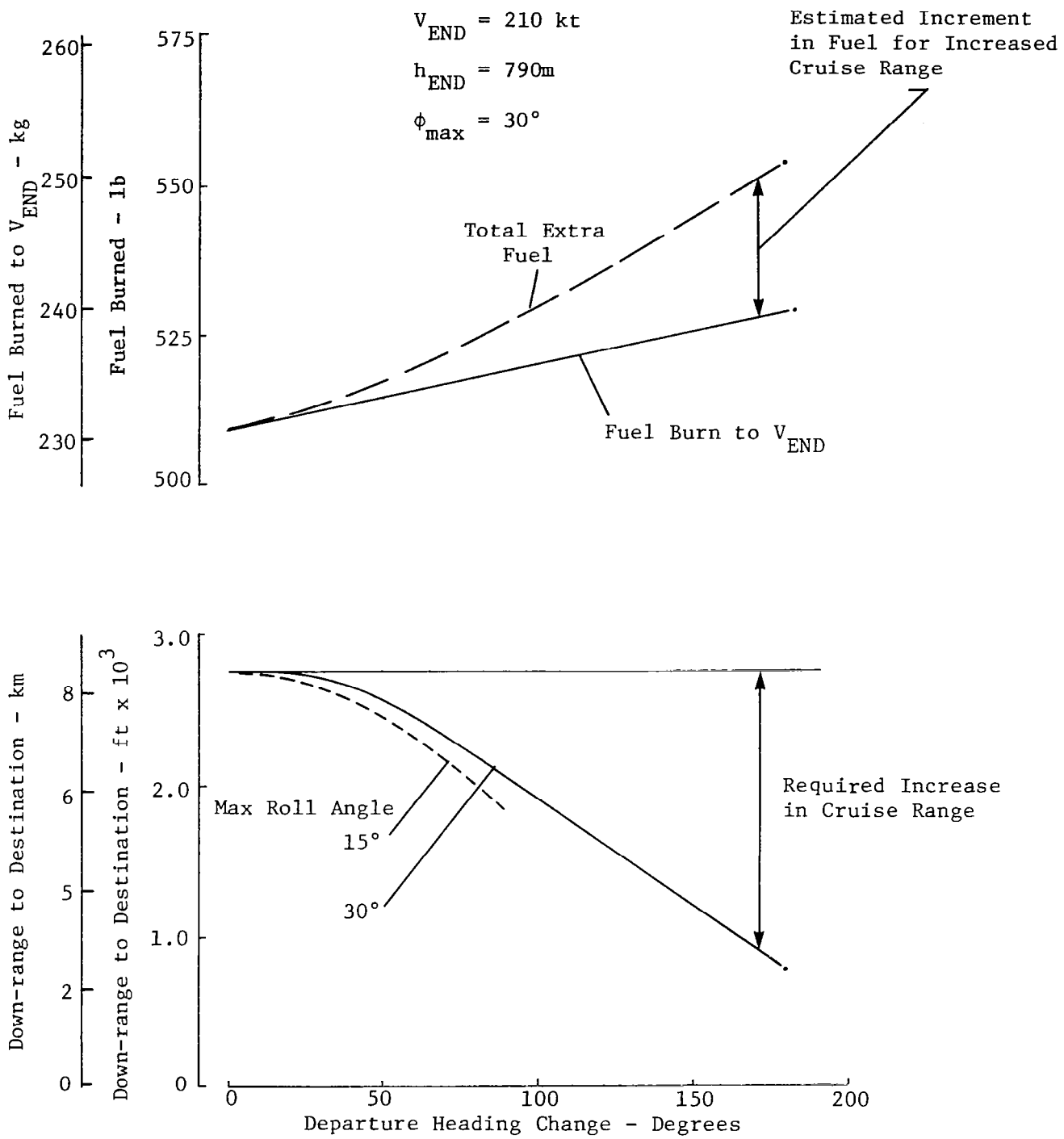

Figure B.10. Performance as a Function of Departure Heading Change

REFERENCES

1. Sorensen, J.A., "Concepts for Generating Optimum Vertical Profiles," NASA CR-159181, September 1979.

2. Sorensen, J.A., and Waters, M.H., "Generation of Optimum Vertical Profiles for an Advanced Flight Management System," NASA CR-165674, March 1981.

3. Erzberger, H., McLean, J.A., and Barman, J.R., "Fixed-Range Optimum Trajectories for Short Haul Aircraft," NASA TN D-8115, December 1975.

4. Erzberger, H., and Lee, H.O., "Characteristics of Constrained Optimum Trajectories with Specified Range," NASA TM-78519, September 1978.

5. Lee, H.Q., and Erzberger, H., "Algorithm for Fixed-Range Optimal Trajectories," NASA TN-1565, July 1980.

6. Anon., "OPTIM - Computer Program to Generate a Vertical Profile Which Minimizes Aircraft Fuel Burn or Direct Operating Cost. User's Guide," NASA CR-166061, March 1983.

7. Bochem, J.H., and Mossman, D.C., "Simulator Evaluation of Optimal Thrust Management/Fuel Conservation Strategies for Airbus Aircraft on Short Haul Routes," NASA CR-151966, January 1977.

8. Samms, K.H., and Morello, S.A., "Pilot Guidance and Display Considerations for Energy Efficient Flight Profiles," 1981 Joint Automatic Control Conference, Charlottesville, VA, June 1981.

9. DeJong, H.M., "Optimal Track Selection and 3-Dimensional Flight Planning," Koninklijk Netherlands Meteorologisch Institute No. 93, Gravenhage, Netherlands, 1974.

10. Hague, D.S., et al, "GASP - General Aviation Synthesis Program," NASA CR-152303, January 1978.

11. Anon., "TRAGEN - Computer Program to Simulate an Aircraft Steered to Follow a Specified Vertical Profile," NASA CR-166062, March 1983.

12. Coykendall, R.E., et al, "Study of Cost/Benefit Tradeoffs for Reducing the Energy Consumption of the Commercial Air Transportation System," NASA CR-137891, June 1976.

13. Wauer, J.C., Bruckner, J.M.H., and Humphrey, C.H., "Airplane Performance Sensitivities to Lateral and Vertical Profiles," J. Guidance and Control, Vol. 4, No. 6, Nov.-Dec. 1981.

1. Report No.	2. Government Accession No.	3. Recipient's Catalog No.
NASA CR-3688		

4. Title and Subtitle	5. Report Date
COMPUTER PROGRAMS FOR GENERATION AND EVALUATION OF NEAR-OPTIMUM VERTICAL FLIGHT PROFILES	May 1983
	6. Performing Organization Code
7. Author(s) John A. Sorensen, Mark H. Waters, and Leda C. Patmore	8. Performing Organization Report No. AMA 82-39
	10. Work Unit No.
9. Performing Organization Name and Address Analytical Mechanics Associates, Inc. 2483 Old Middlefield Way Mountain View, CA 94043	11. Contract or Grant No. NAS1-15497
	13. Type of Report and Period Covered Contractor report
12. Sponsoring Agency Name and Address National Aeronautics and Space Administration Washington, DC 20546	14. Sponsoring Agency Code

15. Supplementary Notes

Langley technical monitor: Kathy H. Samms
Final Report

16. Abstract

The objectives of this continuing effort are to develop and evaluate algorithms and flight management concepts for the minimization of fuel or direct operating costs. These concepts are to be used for on-board computation and steering of turbojet transport aircraft in the vertical plane between fixed origin and destination airports along a given horizontal path. The algorithms developed may be used either for flight planning purposes or incorporated in an on-board flight management system.

As part of these objectives, two extensive computer programs have been developed. The first, called OPTIM, generates a reference near-optimum vertical profile, and it contains control options so that the effects of various flight constraints on cost performance can be examined. The second, called TRAGEN, is used to simulate an aircraft flying along an optimum or any other vertical reference profile. TRAGEN is used to verify OPTIM's output, examine the effects of uncertainty in the values of parameters (such as prevailing wind) which govern the optimum profile, or compare the cost performance of profiles generated by different techniques. This report presents a general description of these programs, the efforts to add special features to them, and sample results of their usage.

17. Key Words (Suggested by Author(s))	18. Distribution Statement
Flight management Trajectory optimization	Unclassified - Unlimited Subject Category 05

19. Security Classif. (of this report)	20. Security Classif. (of this page)	21. No. of Pages	22. Price
Unclassified	Unclassified	152	A08

For sale by the National Technical Information Service, Springfield, Virginia 22161

NASA-Langley, 1983